Detection of Stripping in the Downtown Connector

Michael I. Hammons, Ph.D., P.E.
Harold Von Quintus, P.E.
James H. Greene, P.E.
Applied Research Associates, Inc.

Kenneth Maser, Ph.D.
Infrasense, Inc.

Soheil Nazarian, Ph.D., P.E.
Consultant

January 26, 2007

Prepared for:

Office of Materials and Research
Georgia Department of Transportation
Forest Park, GA 30297-2534

Project Number 17316

5000 NW 27th Court, Suite E | Gainesville, Florida 326096 | transportation@ara.com | p 352 336.5366 | f 352 381.0022

TECHNICAL REPORT STANDARD TITLE PAGE

1.Report No.: FHWA-GA-07-0601	2. Government Accession No.:	3. Recipient's Catalog No.:

4. Title and Subtitle: **Development of a GDOT Protocol for Pavement Structural Survey**	5. Report Date: January 2007 6. Performing Organization Code:
7. Author(s): Michael I. Hammons, Ph.D., P.E. James H. Greene, P.E.	8. Performing Organ. Report No.: 06-01
9. Performing Organization Name and Address: Applied Research Associates, Inc. 4300 San Mateo Blvd. NE, Suite A-220 Albuquerque, NM 87110	10. Work Unit No.: 11. Contract or Grant No.: PENHS-M001-00(533)
12. Sponsoring Agency Name and Address: Georgia Department of Transportation Office of Materials & Research 15 Kennedy Drive Forest Park, GA 30297-2534	13. Type of Report and Period Covered: Final; January 2006 – January 2007 14. Sponsoring Agency Code:

15. Supplementary Notes:
Prepared in cooperation with the U.S. Department of Transportation, Federal Highway Administration.

16. Abstract:

This report documents the survey of 13 centerline miles, or approximately 130 lane miles, of mainline HMA pavements on the Atlanta Downtown Connector roadway, from the junction of I-75 and I-285 in Clayton County near Hartsfield-Jackson Atlanta International Airport to the I-75/I-85 split (Brookwood Interchange) in Fulton County. On average, complete distress and GPR surveys were performed on five travel lanes in each direction (northbound and southbound). Seismic tests and cores were collected in selected areas. Also, a GPR survey was performed on the outside shoulder (northbound and southbound) in anticipation of future widening requirements. Based on the survey results, there was little evidence to suggest widespread moisture damage along the Connector. Recommendations were made for a rehabilitation strategy of the Downtown Connector using procedures identified by Applied Research Associates, Inc. in 2005 to detect the presence of moisture damage, in preparation for a 2006 bid letting.

17. Key Words: Pavement evaluation, GPR, seismic tests, moisture damage	18. Distribution Statement:

19. Security Classification (of this report): Unclassified	20. Security Classification (of this page): Unclassified	21. Number of Pages: 121	22. Price:

Form DOT 1700.7 (8-69)

TABLE OF CONTENTS

TABLE OF CONTENTS ii
LIST OF TABLES iii
LIST OF FIGURES iv
EXECUTIVE SUMMARY v
1 INTRODUCTION 1-1
1.1 Background 1-1
1.2 Objective 1-1
1.3 Scope 1-2
2 RESEARCH APPROACH 2-1
2.1 Project Hypotheses 2-1
2.2 Distress Survey 2-1
2.2.1 Premise 2-1
2.2.2 Equipment 2-1
2.2.3 Method 2-4
2.3 GPR Survey 2-5
2.3.1 Premise 2-5
2.3.2 Equipment 2-6
2.3.3 Method 2-7
2.4 Seismic Measurements 2-7
2.4.1 Premise 2-7
2.4.2 Equipment 2-12
2.4.3 Method 2-14
2.5 Core Retrieval and Laboratory Testing 2-14
2.5.1 Premise 2-14
2.5.2 Method 2-14
3 DOWNTOWN CORRIDOR PROJECT 3-1
3.1 Procedure 3-1
3.2 Project Description 3-1
3.2.1 Location 3-1
3.2.2 Construction History 3-2
3.2.3 Expected Moduli 3-3
3.3 Test Results 3-4
3.3.1 Surface Distress 3-4
3.3.2 Ground Penetrating Radar 3-10
3.3.3 Seismic 3-11
3.3.4 Cores 3-13
3.3.5 Laboratory Tests 3-17
4 CONCLUSIONS AND RECOMMENDATIONS 4-1
4.1 Downtown Corridor Conclusions 4-1
4.2 Rehabilitation Recommendations 4-1
5 REFERENCES 5-1
APPENDIX A. LOCAL UNIFORMITY INDEX PROFILES A-1
APPENDIX B. GLOBAL UNIFORMITY INDEX PROFILES B-1
APPENDIX C. PHOTOGRAPHS OF CORES C-1
APPENDIX D. STRESS-STRAIN CURVES D-1

LIST OF TABLES

Table 2-1. Digital vehicle survey systems. 2-3
Table 3-1. Seismic test sections. 3-11
Table 3-2. Core locations. 3-14
Table 3-3. Project core observations. 3-15
Table 3-4. Previous core observations. 3-16
Table 3-5. Indirect tensile dynamic modulus summary. 3-17

LIST OF FIGURES

Figure 2-1. Rear view of digital survey vehicle. 2-2
Figure 2-2. Front view of digital survey vehicle. 2-3
Figure 2-3. Typical digital image workstation. 2-5
Figure 2-4. GPR survey vehicle. 2-7
Figure 2-5. Schematic of USW method. 2-9
Figure 2-6. Typical time records from an HMA site. 2-10
Figure 2-7. Phase spectra obtained from time records in Figure 2-6. 2-10
Figure 2-8. Typical dispersion curve. 2-11
Figure 2-9. Schematic of Impact Echo method. 2-12
Figure 2-10. Portable Seismic Properties Analyzer. 2-13
Figure 3-1. Extent of Downtown Connector project. 3-2
Figure 3-2. Expected high and low resilient modulus values. 3-4
Figure 3-3. Northbound lane 4 PACES rutting summary plot. 3-5
Figure 3-4. Southbound lane 4 PACES rutting summary plot. 3-5
Figure 3-5. Northbound lane 4 FHWA rutting summary plot. 3-6
Figure 3-6. Southbound lane 4 FHWA rutting summary plot. 3-6
Figure 3-7. Northbound lane 4 roughness summary plot. 3-7
Figure 3-8. Southbound lane 4 roughness summary plot. 3-7
Figure 3-9. Northbound lane 4 load cracking summary plot. 3-8
Figure 3-10. Southbound lane 4 load cracking summary plot. 3-8
Figure 3-11. Northbound lane 4 block and transverse cracking summary plot. 3-9
Figure 3-12. Southbound lane 4 block and transverse cracking summary plot. 3-9
Figure 3-13. GPR estimated HMA thickness for northbound lane 4. 3-10
Figure 3-14. Northbound seismic tests. 3-12
Figure 3-15. Southbound seismic tests. 3-12
Figure 3-16. Plot of UI and seismic modulus showing no relationsip. 3-13
Figure 3-17. Relationship between IDT strength and dynamic modulus. 3-18
Figure 3-18. Comparison of the IDT dynamic modulus and strain at failure. 3-18
Figure 4-1. Maximum vertical HMA strain for different milling depths. 4-2
Figure 4-2. Distortion strain ratio for different milling depths. 4-3
Figure 4-3. Northbound rehabilitation recommendation. 4-4
Figure 4-4. Southbound rehabilitation recommendation. 4-4

EXECUTIVE SUMMARY

In early 2005, Applied Research Associates, Inc. (ARA) completed a study for the Georgia Department of Transportation (GDOT) that recommended procedures to survey potential mill and overlay projects for the presence of moisture damage. This method includes the documentation of observable surface distresses, a complete ground penetrating radar (GPR) survey, seismic testing of selected areas, limited coring, and laboratory testing of selected cores. By following the procedures identified by this research, areas with various levels of damage can be discriminated so that effective rehabilitation strategies can be developed.

A survey of the Atlanta Downtown Connector, from the junction of I-75 and I-285 in Clayton County near Hartsfield-Jackson Atlanta International Airport to the I-75/I-85 split (Brookwood Interchange) in Fulton County, was completed in 2006 using the same guidelines. Based on the survey results, there was little evidence to suggest widespread moisture damage along the Downtown Corridor. The following field and laboratory tests were completed that support this conclusion:

- A distress survey showed minor surface distresses with the exception of increased rut depths from mileposts 248 to 250 in both directions, particularly the southbound direction.
- GPR data collected in the travel lanes and shoulders indicated that moisture damage should not be widespread.
- Seismic testing showed 10 percent of the northbound tests and 20 percent of the southbound tests had seismic moduli less than the expected lower modulus values. The majority of northbound tests with less than anticipated modulus values were found in the northernmost tested portion of lane 2, while southbound seismic tests with less than expected values were found primarily in lanes 4 and 5 at the southernmost tested section, lane 4 in the middle test section, and lanes 2 and 3 in the northernmost tested section.
- The lack of correlation between UI and seismic modulus reinforced the conclusion that the observed electromagnetic variability (as measured by UI) was not caused by moisture damage but was most likely due to local changes in moisture, air voids, mix design, or aggregates.
- Approximately 60 percent of the cores were retrieved intact. The remaining cores broke primarily along layer interfaces during extraction, suggesting weak interlayer bonds. The HMA mixture generally stayed intact and did not disintegrate near the fracture, indicating moisture was confined primarily to the layer interface where it reduced the bond between layers but had not significantly affected the integrity of the mixture itself.
- Laboratory tests showed little evidence of moisture damage but indicated inferior fatigue properties for most of the samples tested.

Overall, information collected on the Downtown Connector suggests that a typical milling depth of 4 inches is adequate for the majority of the roadway. A milling depth of 8 inches is recommended for the northbound and southbound sections in which seismic tests indicate moduli with less than expected values or where rut depths were considerably greater. Following is a summary of the milling depth recommendations:

- Milling depth of 8 inches in northbound lane 2 from milepost 244 to Georgia Avenue Overpass (approximately 31,460 feet north of MP 238 to 40,400 feet north of MP 238).
- Milling depth of 8 inches in northbound lanes 1 through 7 from Williams Street Entrance (just north of US 78 Overpass) to the Brookwood Interchange (approximately 56,205 feet north of MP 238 to 63,000 feet north of MP 238).
- Milling depth of 8 inches in southbound lanes 2 through lane 7 from the University Avenue Overpass to Exit 243 (approximately 34,900 feet north of MP 238 to 27,780 feet north of MP 238).
- Milling depth of 8 inches in southbound lane 4 from MP 242 to Mount Zion Overpass (approximately 20,805 feet north of MP 238 to 16,200 feet north of MP 238).
- Milling depth of 8 inches in southbound Lanes 4 and 5 from Mount Zion Overpass to MP 240 (approximately 15,970 feet north of MP 238 to 10,520 feet north of MP 238).
- Milling depth of 8 inches in southbound lanes 1 through 7 from the Brookwood Interchange to Williams Street Exit (just south of US 78 Overpass) (approximately 63,140 feet north of MP 238 to 53,250 feet north of MP 238).
- Milling depth of 4 inches for the remaining Downtown Connector.

1 INTRODUCTION

1.1 Background

Stripping in hot mix asphalt (HMA) refers to the loss of adhesion between the asphalt cement and the aggregate surface, and it is caused primarily by the action of moisture and moisture vapor (Kandhal and Rickards 2001). When advanced stripping is present, cores recovered from the roadway often will disintegrate during the coring operation. The damage mechanisms that lead to stripping significantly affect the dynamic modulus and tensile strength of HMA.

Stripping is causing problems in some pavement sections for the Georgia Department of Transportation (GDOT). In Georgia, routine mill and overlay rehabilitation projects typically consist of milling 2¾ inches followed by an HMA inlay of equal or near equal thickness. When stripped material is encountered below the planned milling depth, it must be removed and replaced, causing significant cost overruns and time delays.

In current GDOT practice, coring and visual examination is the preferred method for detecting the presence of stripped asphalt. A number of cores are extracted and visually examined and/or tested in the laboratory to identify the presence of stripping. However, coring is time-consuming, and because it is a point sampling method, it limits the area and extent of pavement that can be investigated. American Association of State Highway and Transportation Officials (AASHTO) T283 (Resistance of Compacted Bituminous Mixture to Moisture Induced Damage) is commonly used to determine moisture damage in HMA mixtures, but many agencies do not have a high level of confidence in this test method for identifying mixes susceptible to stripping. Most agencies use hydrated lime or some anti-stripping additive in HMA mixtures that are known to be susceptible to moisture damage, simply because the reliability of AASHTO T283 and other test procedures are considered low at best.

In early 2005, Applied Research Associates, Inc. (ARA) completed a study for GDOT that recommended procedures to survey potential mill and overlay projects for the presence of moisture damage. This method includes the documentation of observable surface distresses, a complete ground penetrating radar (GPR) survey, seismic testing of selected areas, limited coring, and laboratory testing of selected cores. By following the procedures identified by this research, areas with various levels of damage can be discriminated so that effective rehabilitation strategies can be developed.

1.2 Objective

The objective of this project was to develop recommendations for a rehabilitation strategy of the Atlanta Downtown Connector using procedures identified by ARA in 2005 to detect the presence of moisture damage, in preparation for a 2006 bid letting.

1.3 Scope

The project scope consisted of a survey of 13 centerline miles, or approximately 130 lane miles, of mainline HMA pavements on the Atlanta Downtown Connector roadway, from the junction of I-75 and I-285 in Clayton County near Hartsfield-Jackson Atlanta International Airport to the I-75/I-85 split (Brookwood Interchange) in Fulton County. On average, complete distress and GPR surveys were performed on five travel lanes in each direction (northbound and southbound). Seismic tests and cores were collected in selected areas. In addition, a GPR survey was performed on the outside shoulder (both northbound and southbound) in anticipation of future widening requirements.

2 RESEARCH APPROACH

2.1 Project Hypotheses

The hypotheses used for the Downtown Corridor project are as follows:

1. The modulus, strength, and tensile strain at failure of an HMA mixture are affected significantly by the level of moisture damage. In other words, these properties of an HMA mixture with moisture damage are significantly less than those measured for the same HMA mixture without moisture damage. In addition, these properties will continue to decrease with increasing levels of moisture damage, progressing from a loss of cohesion in the asphalt to advanced stripping.
2. Non-uniformity in electromagnetic properties, as indicated by the GPR Uniformity Index (UI), may indicate changes in the physical properties of the HMA.
3. Seismic tests can be used to determine the modulus of HMA mixtures. The adjusted seismic modulus is affected significantly by the level of moisture damage in the HMA mixture.

ARA used the protocol developed in the 2005 study to identify areas with moisture damage along the project corridor. The following subsections outline the survey plan.

2.2 Distress Survey

2.2.1 Premise

HMA that is prone to stripping would be categorized as having poor durability. Mixes with poor durability often show other symptoms, such as localized areas of increased surface distress, including severe fatigue cracking, potholing, raveling, or a greater frequency of transverse and block cracking. Kandhal and Rickards (2001) observed that stripping in overlays also resulted in “flushing” of stripped asphalt binder to the surface and white staining where fines in the asphalt concrete have been pumped to the surface. The presence of stripping can also result in more variability that might increase the potential for rutting and/or localized longitudinal profile distortions. Shoving is possible when stripping begins to occur in layers near the surface, but not in the wearing surface.

2.2.2 Equipment

The automated video distress survey was conducted using a state-of-the-art vehicle that simultaneously records the surface condition, rutting, and roughness of the pavement surface. It also records digital images of the roadway ahead and right-of-way. The vehicle contains the following synchronized survey systems:

- Digital Pavement Imaging System
- Pavement Illumination System
- Road Profiler System (roughness & rut data)

- Applanix POS-LV System (global positioning system, inertial navigation, and geometric data)
- Asset Management Imaging System (right-of-way and sign images)

The van-mounted camera and profiler system was manufactured by International Cybernetics Corporation (ICC). The digital survey vehicle is shown in Figures 2-1 and 2-2, and the survey system characteristics are summarized in Table 2-1.

Figure 2-1. Rear view of digital survey vehicle.

The digital pavement imaging system consisted of a Bassler 2000-pixel line-scanning digital video camera. The imaging system was mounted on the rear of the vehicle and recorded continuous images with a width of survey of 14.5 ft. The line scans are accumulated to form an image representing a 20-ft length of pavement. The images are of sufficient resolution that 1-mm defects are readily visible. The pavement beneath the digital line-scanning camera was illuminated by ten 150 W metal halide stage lights mounted on a custom framework on the rear of the vehicle. These lights have special lenses that allow their light to be focused into a narrow band of intense illumination directly under the digital line scan camera.

The Applanix POS-LV system is a differential global positioning system (GPS), inertial navigation, and geometric system for land vehicles. It provides the system with GPS coordinates for locations such as survey start, survey stop, section event, and image location. These coordinates have sub-meter accuracy.

Figure 2-2. Front view of digital survey vehicle.

Table 2-1. Digital vehicle survey systems.

Survey System	Manufacturer	Camera or Sensor Type	No. of Sensors	Resolution or Accuracy	Survey Speed, Max
Digital Pavement Imaging System	International Cybernetics Corporation	Bassler Line-Scan Monochrome	1	2,000 pixels per scan line	50 MPH @ 20-ft image Intervals
Road Profiler	International Cybernetics Corporation	Selcom, 16 kHz, Laser	9	0.002 inches	60 + MPH
GPS Receiver	Trimble	AG 320	1	Sub-meter	60 + MPH
Differential GPS	Applanix	DGPS	2	Sub-meter	60 + MPH
POS LV – X,Y Position	Applanix	N/A	1	0.20 m	15 sec signal outage
POS LV – Z Vert. Position	Applanix	N/A	1	0.20 m	15 sec signal outage
Roll & Pitch	Applanix	N/A	1	0.07 degrees	15 sec signal outage
True Heading	Applanix	N/A	1	0.07 degrees	15 sec signal outage
Asset Management – Windshield & Shoulder Images	International Cybernetics Corporation	Color, Digital Video Camera	2	1300 by 1024 pixels, each	60 + MPH @ 25-ft intervals
Distance Measuring Instrument	International Cybernetics Corporation	N/A	1	1 ft per mile	60 + MPH

Two 1300 by 1024 pixel color digital cameras were used to collect right-of-way (ROW) images. One camera was oriented straight ahead for identifying number of lanes, overhead signs, etc. The side camera was oriented to the right side of the road for identifying traffic signs, mile markers, and other roadway assets.

An ICC-manufactured ASTM E950 Class I South Dakota-type Road Profiler was used for road roughness data collection. Profile data were collected in each wheel path using three 16-kHz Selcom lasers in combination with accelerometers and a distance measuring instrument (DMI). The profiler is capable of collecting profile data points at intervals of 1 inch or less and storing average profile measurements at intervals of approximately 3 inches at speeds up to 60 mph. The laser sensors have a height resolution of 0.002 inches or better. The system uses the continuous 16-khz output of the lasers to determine the height points, eliminating narrow cracks and openings from roughness calculations. During the surveying operation, the data are stored in the onboard computer's memory until the end of the portion of roadway is reached. At that point, the data are saved to a computer file on the profiler's hard drive. The system uses industry standard analysis software to convert the sensor and accelerometer readings into longitudinal profiles and International Roughness Index (IRI) in accordance with ASTM E1926-98. Quarter-car simulation (QCS) and half-car simulation (HRI) are used to produce IRI values for the left and right wheel paths and the average IRI value, respectively.

The profiler was validated at sites maintained by the Pennsylvania Department of Transportation (PennDOT) near Harrisburg. PennDOT selected the sites to cover the range of roughness applicable to most highway systems. Each site is 528 feet long with a 1,056-ft lead-in to the test section. The Face Technologies Dipstick or AARB Profiling Unit is used to measure the profile of each wheel path between the reference bumps. Both units are ASTM E950 Class I profiling devices. Standard software, as described in World Bank Technical Paper No. 46, is used to generate the reference IRI from the profile data. These data are produced and maintained by PennDOT.

For rutting data collection, the South Dakota-type Road Profiler was operated in the five-sensor configuration, which used two 32-kHz Selcom lasers, accelerometers, four additional acoustic sensors, and a DMI. This configuration allowed a 9-ft-wide five-point transverse profile to be measured.

2.2.3 Method

A detailed pavement distress survey was conducted using a digital image workstation (Figure 2-3). The downward digital photographs of the pavement surface were organized into sample units 20 ft long by one lane wide. The photographs were analyzed, and the distress types, severity, and extent were observed and recorded. The distresses observed included weathering and raveling, alligator cracking, longitudinal and transverse cracking, and patching. Using the workstation, the distress data were linked with the corresponding images and the associated pavement management sample unit.

Figure 2-3. Typical digital image workstation.

The surface distresses were identified in accordance with the GDOT's Road Surface Pavement Condition Evaluation System (PACES) and the *Distress Identification Manual for the Long-Term Pavement Performance Program* (FHWA 2003). An exception to the LTPP protocol was made for weathering and raveling: the severity of weathering and raveling was set at the maximum level observed within the sample unit, and that value was assigned to the entire area of the sample unit. All longitudinal cracking in the wheel path was identified as alligator (fatigue) cracking and assigned an appropriate area extent for purposes of this research. The profile data was used to calculate rutting and the HRI.

All of the data obtained in the distress survey was compiled and used in the selection of the areas to be tested with the seismic technique and coring.

2.3 GPR Survey

2.3.1 Premise

GPR operates by transmitting short pulses of electromagnetic energy into the pavement using an antenna attached to a survey vehicle traveling at normal driving speed. These pulses are reflected back to the antenna with an arrival time and amplitude that are related to the location and nature of discontinuities in the material (air/asphalt or asphalt/concrete, reinforcing steel, etc). The reflected energy is received in the form a series of pulses that are referred to as the radar waveform. The waveform contains a record of the properties and thickness of the layers within the deck.

GPR measures changes in the dielectric properties of pavement layers and the velocity of wave propagation within those layers. In a study on Texas highways, Scullion and Rmeili (1997) found that GPR technology was effective for detecting stripping in HMA layers

where the deterioration was at a moderate or advanced stage. Stripped HMA typically has higher moisture contents or higher air voids, or both. The dielectric constant of the material is affected by both moisture content and air voids, as is the velocity of wave propagation.

In the 2005 ARA study for GDOT, a GPR indicator defined as the GPR Uniformity Index was developed to identify areas of potential moisture damage. Moisture damage is a deterioration process characterized by local changes in the asphalt physical properties associated with increased porosity and higher moisture content. These changes are accompanied by corresponding changes in the electromagnetic properties. Increased reflections from affected layers produce localized reflection anomalies within otherwise homogeneous layers. Because these deterioration processes tend to occur non-uniformly in the pavement, a measure of the uniformity of the electromagnetic properties was found to be useful in segmenting the roadway into features which can subsequently be used to plan seismic testing and coring. As a GPR indicator, the UI can be defined as the normalized average absolute amplitude of the GPR scan as follows:

$$UI(x) = \frac{\overline{A}(x)}{\overline{A}\left(x \pm \frac{L}{2}\right)} \qquad \textbf{Equation 1}$$

where $\bar{A}$ is the average reflection amplitude, x is the current station, and L is the normalization length. When compared to the values from neighboring locations, the index shows changes in reflection activity, which, if sufficient, may be related to moisture damage or stripping.

Normalization allows for a UI that varies around 1.0, and thus permits lane to lane and site to site comparison without concern for the absolute values. For the initial site screening and segmentation, the normalization length can be selected as the entire project length. For detailed mapping of areas with potential moisture damage, a smaller normalization length may be appropriate to highlight local variability.

Another key parameter in the UI computation is the depth range over which this scan amplitude is calculated. The depth range should be selected to highlight the depth in which stripping is believed to be occurring. If this is not known, then a larger range can be used. Once cores are obtained and other data are available, this range can be reduced, and the index recalculated.

2.3.2 Equipment

Dr. Ken Maser of Infrasense performed the GPR surveys using dual vehicle-mounted GSSI model 4108 air-coupled 1 GHz horn antennas controlled by a SIR-20 data acquisition and control unit. A photo of the survey vehicle and equipment is shown in Figure 2-4. The vehicle was set up with a movable antenna mounting so that the antennas could be positioned over the left wheel path, right wheel path, or centerline of the vehicle. This permitted the vehicle to collect data for all of the passes without having to straddle lanes.

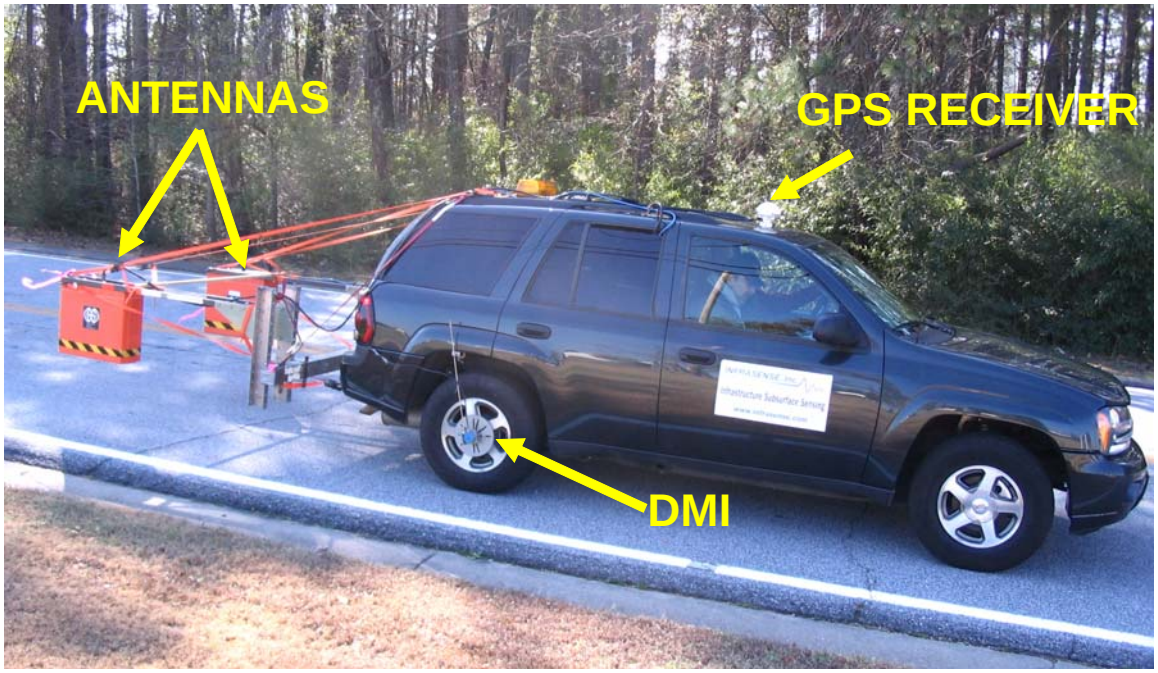

Figure 2-4. GPR survey vehicle.

2.3.3 Method

GPR survey lines were collected in the wheel paths, centerline, and lane boundaries of each lane. The data was continuously digitized and stored at a controlled rate of two scans per foot. The acquisition rate was controlled by a wheel-mounted DMI, which was calibrated prior to the survey. The DMI produces 1000 pulses per vehicle wheel revolution. Using the calibration factor, the GPR system is triggered to record a scan every N pulses, where N is determined from the calibration factor and the scan rate setting. In addition to recording the GPR data, the SIR-20 also records the GPS station data and associated GPR scan numbers every second. The GPS station data were provided by a Trimble Ag114 differential GPS system with sub-meter accuracy.

During the survey, manual markers were placed in the data at mileposts and other reference locations for ground control of the radar distance measurements.

Data obtained in the GPR survey were compiled and used in the selection of the areas to be tested with the seismic technique and additional coring.

2.4 Seismic Measurements

2.4.1 Premise

Moisture damage (with or without stripping) typically will result in a significant decrease in the modulus of the HMA mixture. Seismic methods generate a stress wave at one point on the pavement surface and measure the time required for the waves to propagate to other points on the pavement surface. A shear modulus profile is obtained by measuring the dispersion of the shear waves using Fourier-transformed time records and spectral analysis to obtain phase information.

This study utilized the Portable Seismic Properties Analyzer (PSPA) for assessing the impact of stripping on the variation of HMA modulus with depth. The PSPA uses two methodologies to evaluate the bound layer properties:

- Ultrasonic Surface Waves (USW) – measures the stiffness of the bound layer
- Impact Echo – measures the thickness of the bound layer or identifies delaminated areas

When the surface of the HMA is impacted with a point source, body and surface waves propagate in the material. The focus of this study is primarily on the use of the surface waves. Surface waves contain about two-thirds of the seismic energy generated within a layer; thus, the analysis is more robust. Because surface waves propagate along a cylindrical front, the depth of inspection can be controlled easily.

The goal with seismic methods is to measure the propagation velocity of waves within a medium. The propagation velocity is theoretically related to the linear elastic modulus of a material. The relationship between velocity (V), travel time (Δt), and receiver spacing (ΔX) can be written in the following form:

$$V = \frac{\Delta X}{\Delta t} \qquad \textbf{Equation 2}$$

In this equation, V can be the propagation velocity of any of seismic waves, i.e., compression wave (V_P), shear wave (V_S), or surface (Rayleigh) wave, (V_R). Knowing any one wave velocity, the modulus can be determined using appropriate transformations. V_S can be used to determine shear modulus, G, using

$$G = \rho V_s^2 \qquad \textbf{Equation 3}$$

where ρ is mass density. Young's modulus, E, which is the primary parameter of interest to pavement engineers, can be determined from shear modulus, through the Poisson's ratio, ν, using

$$E = 2(1+\nu)G \qquad \textbf{Equation 4}$$

To obtain the modulus from V_R, it must first be converted to shear wave velocity using

$$V_s = V_R(1.13 - 0.16\nu) \qquad \textbf{Equation 5}$$

Young's modulus is then determined by using Equations 3 and 4.

USW Method. The USW method, an offshoot of the Spectral Analysis of Surface Waves (SASW) method (Nazarian et al., 1997) is used to obtain the modulus of the HMA. As sketched in Figure 2-5, at wavelengths less than or equal to the thickness of the uppermost layer, the velocity of propagation is independent of wavelength. Therefore, if one simply generates high-frequency (short-wavelength) waves, and if one assumes that the properties of the uppermost layer are uniform, the shear wave velocity of the upper layer can be determined from

$$V_s = (1.13 - 0.16\nu)V_{ph} \qquad \textbf{Equation 6}$$

where V_{ph} is the phase velocity of surface waves. The modulus of the top layer, E_{field}, can be determined from

$$E_{field} = 2\rho V_s^2 (1+\nu)$$ **Equation 7**

The wavelength at which the velocity of individual frequency component (phase velocity) is no longer constant and is closely related to the thickness of the top layer (NCHRP, 1996).

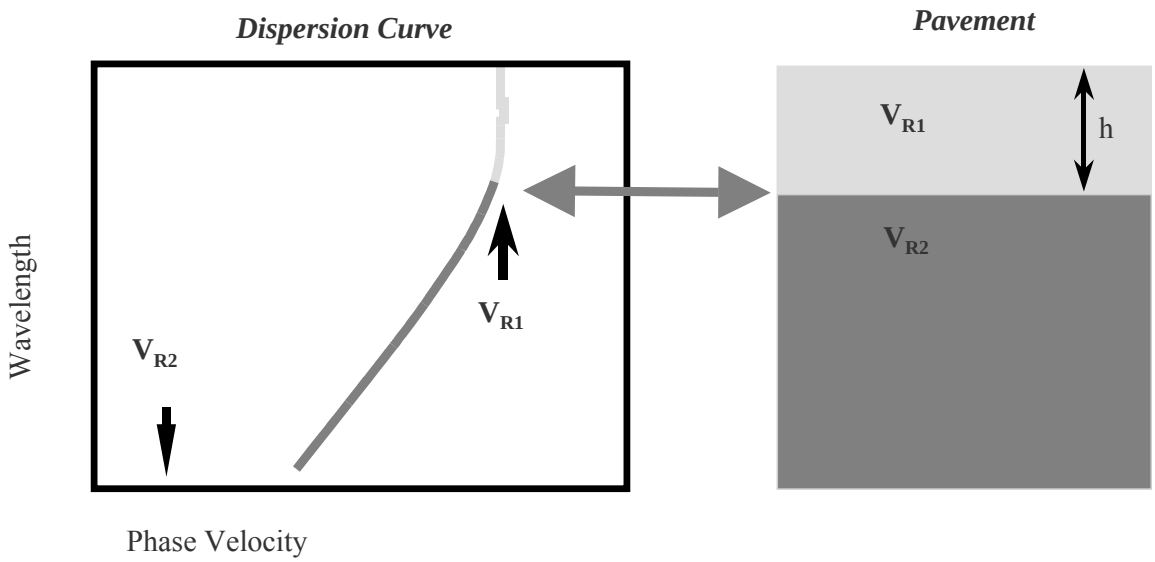

Figure 2-5. Schematic of USW method.

Figure 2-6 shows typical time-history records from an HMA site. From these records, phase spectra, shown in Figure 2-7, are calculated by conducting Fourier transform and spectral analysis on the time records from the two sensors. Two phase spectra are shown: one measured from the time records and the other that represents the best estimation of the phase when the effects of the body waves are removed. The latter is used to compute the dispersion curves shown in Figure 2-8 (Nazarian and Desai, 1993). The actual dispersion curve (variation in velocity with wavelength) is presented in Figure 2-8a. As approximated by the solid line, the phase velocity is reasonably constant for the first 3 inches, below which the phase velocity tends towards lower values with depth. One can conclude that the average phase velocity is about 4200 fps and the approximate thickness is about 3 inches. The second dispersion curve (Figure 2-8b) shows the calculated modulus obtained from the phase velocity using Equations 5 and 6.

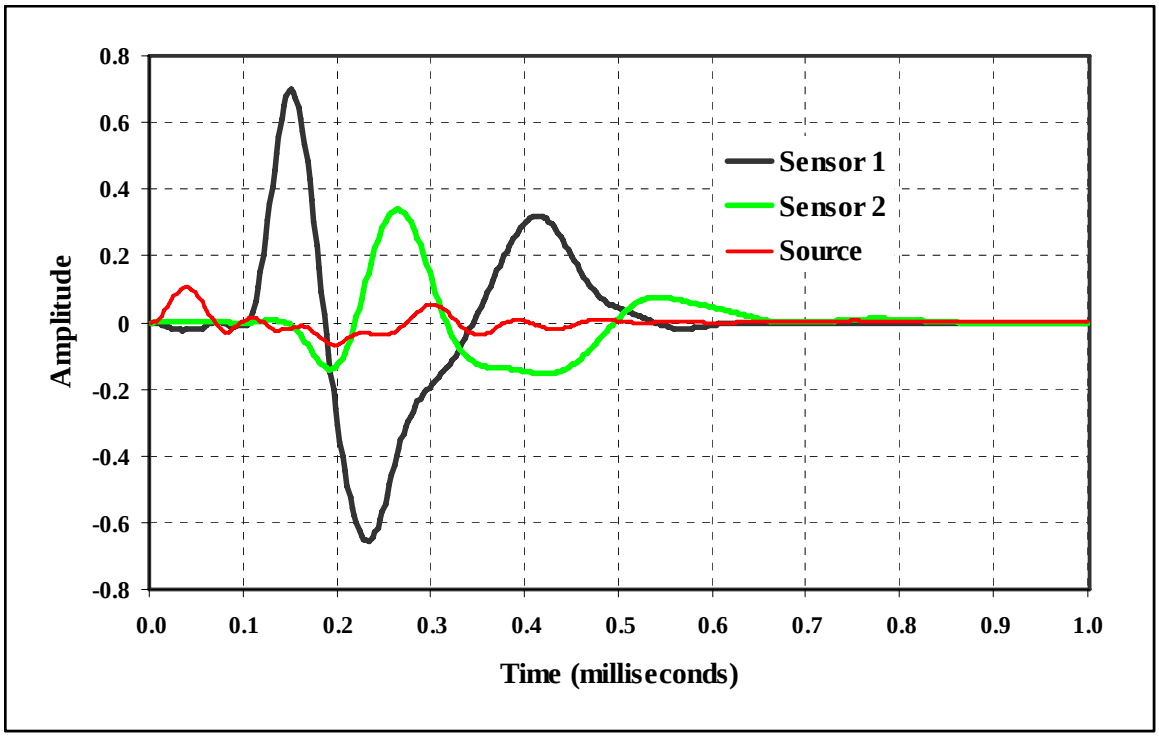

Figure 2-6. Typical time records from an HMA site.

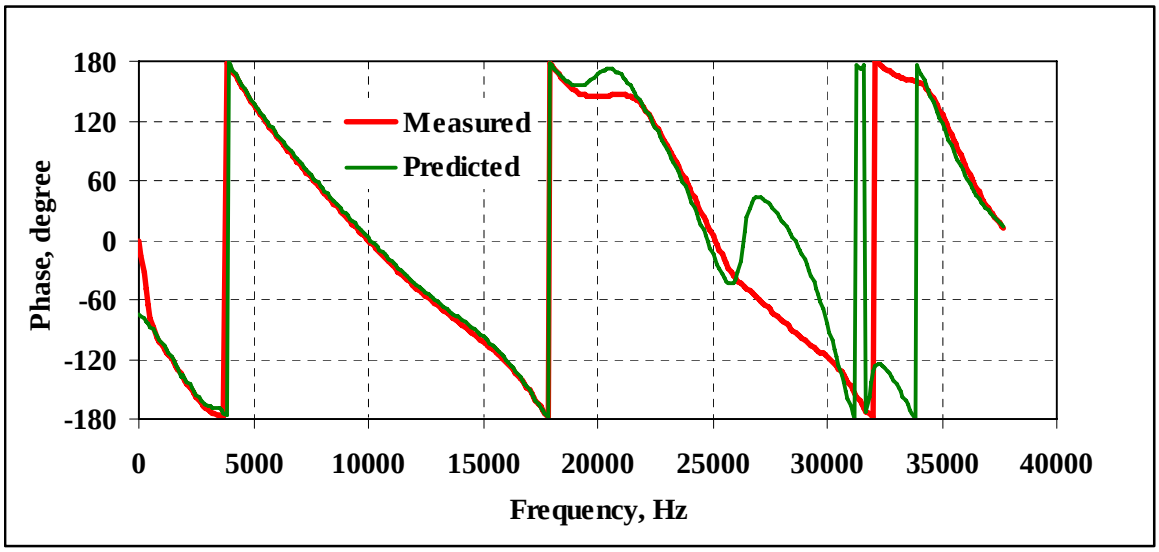

Figure 2-7. Phase spectra obtained from time records in Figure 2-6.

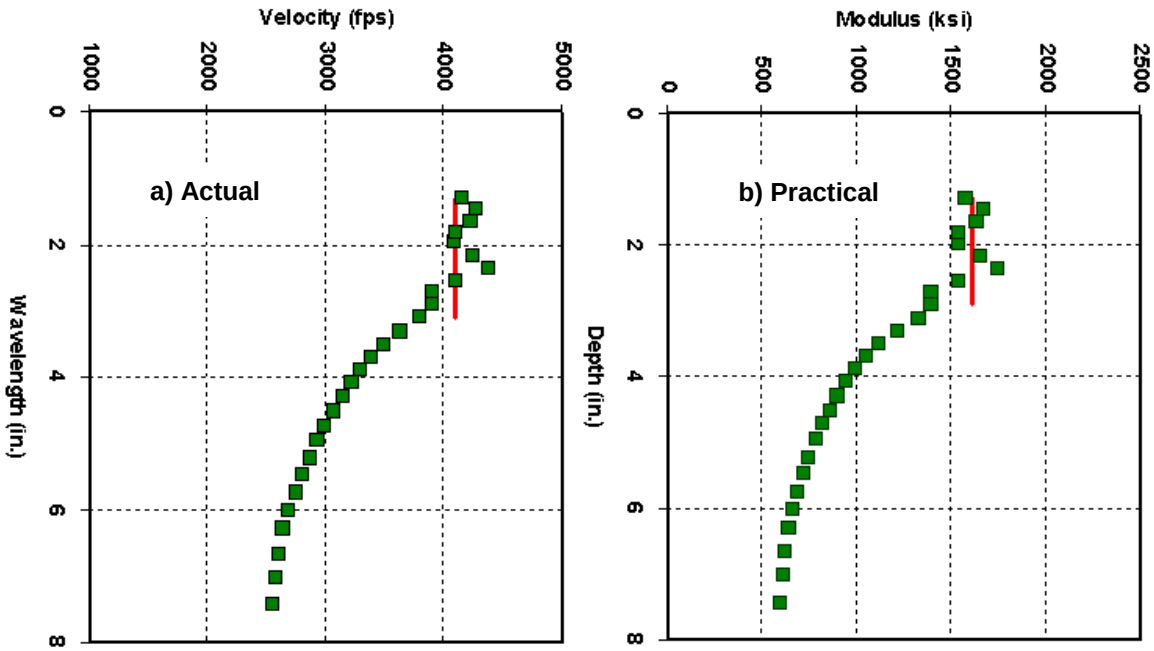

Figure 2-8. Typical dispersion curve.

Impact Echo Method. The Impact Echo method primarily provides information about the thickness of a layer. Sansalone and Carino (1986) also used the method to locate defects, voids, cracks, and zones of deterioration within concrete. As detailed in Nazarian et al. (1997), the method is not applicable to relatively thin layers or layers where the difference in moduli of adjacent layers is small.

The Impact Echo method, as sketched in Figure 2-9, is based on detecting the frequency of the standing wave reflecting from the bottom and the top of the top pavement layer. Upon impact, some of the source energy is reflected from the bottom of the layer, and some is transmitted into the base and subgrade. Since the top of the layer is in contact with air, almost all of the energy is reflected from that interface. The receiver senses the reflected energy at periodic time intervals. The period depends on the thickness and compression wave velocity of the layer. To determine the frequency associated with the periodic arrival of the signal, one can utilize a fast Fourier transform algorithm. The frequency associated with the reflected wave appears as a peak in the amplitude spectrum. Using the compression wave velocity of the layer (V_p) the depth-to-reflector, h, can be determined from

$$h = \frac{V_p}{2f} \qquad \textbf{Equation 8}$$

where f is the resonant frequency obtained by transforming the time record into the frequency domain. The compression wave velocity can be determined if the surface wave velocity is known as follows:

$$V_p = \frac{V_R \sqrt{\frac{1-\nu}{1/2 - \nu}}}{0.13 - 0.16\nu}$$ **Equation 9**

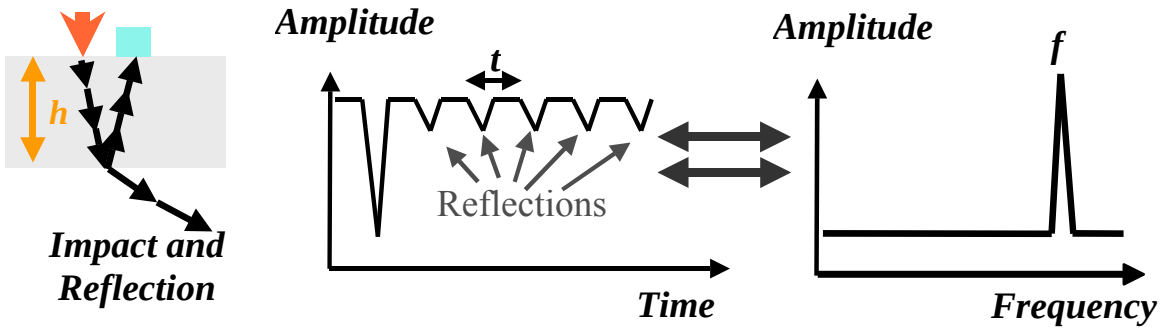

Figure 2-9. Schematic of Impact Echo method.

2.4.2 Equipment

The PSPA was used in this study to implement the methodologies described above. With the PSPA, the average modulus of the exposed surface layers can be estimated within a few seconds in the field. In addition, the variation in modulus with depth can be qualitatively investigated. The PSPA, shown in Figure 2-10, consists of two transducers (accelerometers, in this case) and a source packaged into a hand-portable system. The source package is also equipped with a transducer for consistency in triggering and for some advanced analysis of the signals. The device is operable from a computer connected to the hand-carried transducer unit by a cable that carries operational commands to the PSPA and returns the measured signals to the computer.

The operating principle of the PSPA is based on generating and detecting stress waves in a medium. The USW interpretation method, which is implemented in the Spa Manager software in the PSPA computer, is used to determine the modulus of the material.

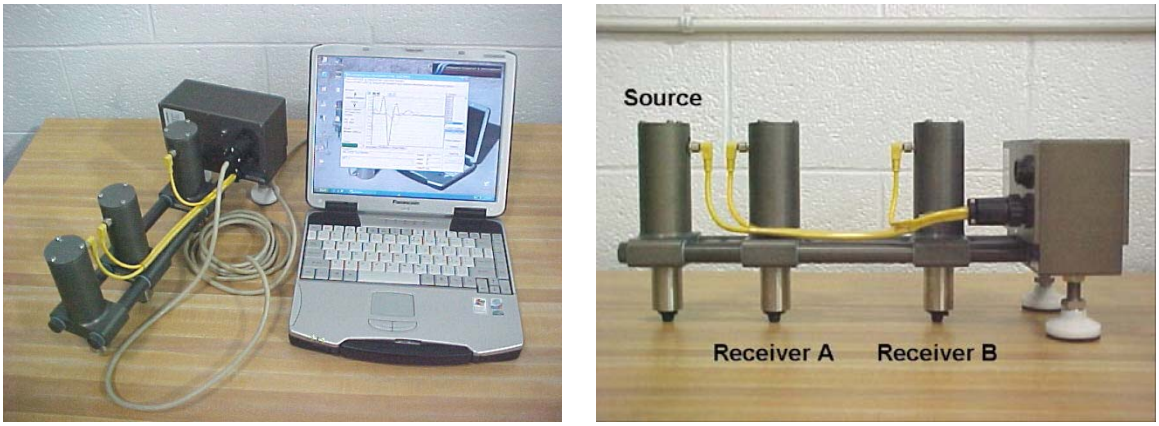

Figure 2-10. Portable Seismic Properties Analyzer.

Moduli obtained with seismic measurements are low-magnitude, high-strain-rate values. Vehicular traffic causes relatively high magnitude deformation at low strain rates. Because of the difference, there has been concern in the pavement community regarding how to implement seismic moduli in the design. This concern has been resolved by implementing a master curve concept, which tracks modulus over wide frequency range.

The most desirable way of calculating the design modulus is to develop the master curve based on the recommendations of Andrei,Witczak, and Mirza (1999). The response of a viscoelastic material, such as HMA, is dependent on the loading frequency and temperature. The general practice has been to perform the testing at various temperatures with similar loading frequencies. A master curve is generated at a reference temperature by using time-temperature shift factors. The following sigmoid function proposed by Ferry (1970) can be used to generate a master curve:

$$\log(E^*) = \delta + \frac{\alpha}{1 + e^{\beta + \gamma \times \log t_r}} \qquad \textbf{Equation 10}$$

where E^* is dynamic modulus, t_r is the loading period, δ is the minimum value of dynamic modulus, $\delta + \alpha$ is the maximum value of dynamic modulus, and β and γ are sigmoid function shape parameters. Once the master curve is established, the design modulus can be determined from the design vehicular speed and the design temperature. Parameters α, β, γ, and δ ideally should be obtained from complex modulus tests. However, in the absence of laboratory testing, Mirza and Witczak (1995) proposed relationships for obtaining values of α, β, γ, and δ from volumetric information about a mixture. Tandon, Nazarian and Bai (2004) showed that the seismic modulus and the master curve from complex modulus correlate well.

Since laboratory testing was not in the scope of this study, an approximate procedure was used to obtain the design modulus (Aouad, Stokoe, and Briggs, 1993; Li and Nazarian, 1994). The relationship suggested by Li and Nazarian (1994) for adjusting the modulus of asphalt concrete to a reference temperature of 77° F is used here. That relationship is in the form of

$$E_{77} = \frac{E_t}{1.35 - 0.0078(t - 32)} \qquad \textbf{Equation 11}$$

where E_{77} and E_t are the moduli at 77° F and temperature t (in Fahrenheit). Aouad, Stokoe, and Briggs (1993) developed an empirical relationship between seismic modulus and design modulus. For a temperature of 77° F (25° C), the design modulus is obtained by dividing the seismic modulus by a factor of 3.2.

2.4.3 Method

To collect data with the PSPA, the technician simply initiates the testing sequence through the computer. All other data acquisition tasks are handled automatically. The high-frequency source is activated four to six times. Pre-recording impacts of the source are used to adjust the gains of the amplifiers in a manner that optimizes the dynamic range of the electronics. The outputs of the three transducers from the final three impacts are saved and averaged.

Based upon the results of the distress and GPR survey, a field testing plan for seismic tests and coring was devised. Seismic testing required lane closures, and therefore, nighttime testing. Four sections in the northbound direction and five in the southbound direction were selected based on survey data and location along the corridor. Caution was taken to select sections with minimal impact on entrance and exit ramps, and GDOT traffic control supervisors were consulted to ensure lane closure feasibility.

Dr. Sohiel Nazarian was in charge of the seismic testing. Tests were conducted at a frequency that allowed completion within lane closure limits and, therefore, were different for each section. With the PSPA, the average seismic modulus of the exposed surface layers can be estimated within a few seconds in the field. In addition, the variation in modulus with depth can be investigated qualitatively.

Seismic data was analyzed to estimate the seismic modulus for each test point at a loading frequency of 15 Hz. Seismic modulus values were compared to an estimated lower baseline value. Values less than the lower baseline indicate a certain level of moisture-related damage or compromised structural integrity.

2.5 Core Retrieval and Laboratory Testing

2.5.1 Premise

Stripping is visually evident in cores; however, lesser degrees of moisture damage may not be. As mentioned previously, moisture damage and/or actual stripping typically will result in a significant decrease in the strength, modulus, and tensile strain at failure of an HMA mixture. Therefore, HMA with no moisture damage should exhibit better mechanical properties than HMA with moisture damage. Laboratory testing should confirm the presence of moisture damage and verify seismic modulus values.

2.5.2 Method

While the lane closures were in place for seismic testing, a GDOT core rig and operator obtained approximately five roadway cores throughout each section. The number of cores was limited so that they could be obtained while the lanes were closed for the seismic tests. Core locations were selected based primarily upon the GPR survey and seismic measurements.

Cores were visually examined for indications of moisture damage, and a limited number of cores were selected for laboratory testing based upon the visual examination. Two to three tests were conducted on each core to measure the modulus and indirect tensile strain at failure for each area sampled. Tests were performed on cores recovered from areas with and without visible indications of moisture damage.

3 DOWNTOWN CORRIDOR PROJECT

3.1 Procedure

The following process was established and recommended by ARA in a 2005 GDOT study to develop effective rehabilitation design strategies where HMA moisture damage is suspected:

4. Review the construction history of the roadway to determine the pavement cross section and volumetric and physical properties of the different HMA layers (if possible).
5. Review the surface condition as an aid in developing the field sampling plan and, later, the rehabilitation design strategy.
6. Estimate the lower baseline HMA dynamic modulus value. The lower baseline value is the modulus at the nondestructive testing (NDT) temperature that would represent an HMA mixture without any moisture damage.
7. Perform a complete GPR survey on the roadway. From the GPR data, determine the UI along the project.
8. Segment the roadway based on the UI values.
9. Conduct at least three seismic tests in each segmented area.
10. Develop a field sampling plan to take cores within each of the different segmented areas.
11. Correlate the GPR UI, seismic modulus, and core condition index to confirm the initial criteria used.
12. Validate by performing laboratory tests on a few cores recovered from areas.
13. Designate the areas with various levels of moisture damage for use in rehabilitation design.

3.2 Project Description

3.2.1 Location

The Downtown Corridor project consists of approximately 13 centerline miles, or 130 lane miles of mainline HMA, from the junction of I-75 and I-285 in Clayton County near Hartsfield-Jackson Atlanta International Airport to the I-75/I-85 split (Brookwood Interchange) in Fulton County. The approximate location of the project is indicated by the box in Figure 3-1. An average of five travel lanes were surveyed in each direction (northbound and southbound). GPR, rutting, roughness, and cracking surveys were performed on all lanes. Nine sections between 1 and 2 miles long were selected to perform seismic testing and core collection.

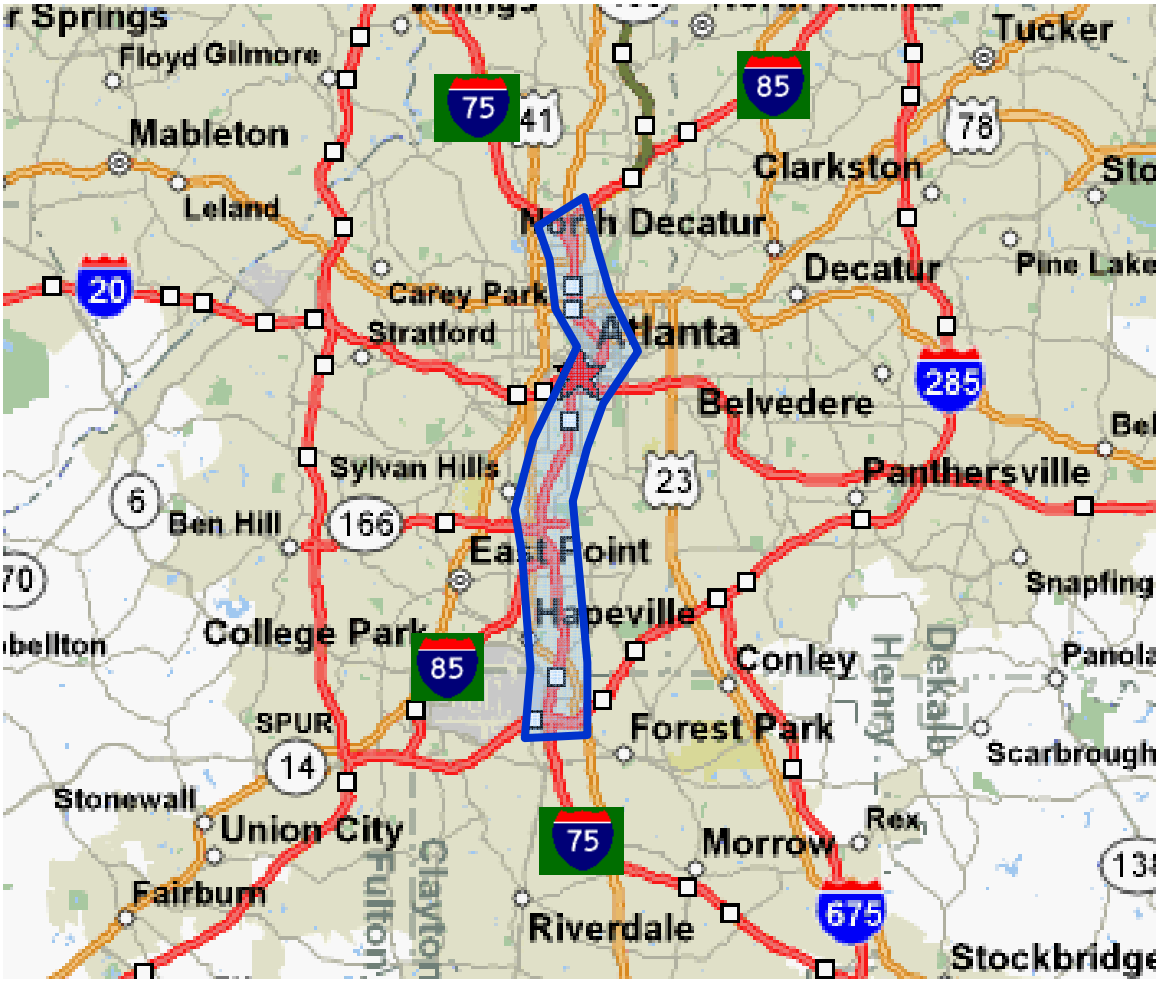

Figure 3-1. Extent of Downtown Connector project.

3.2.2 Construction History

This section of I-75 originally was constructed as a four-lane roadway with 12-ft-wide lanes. Portions of the Downtown Connector were constructed in the early 1950's as a six-lane roadway. Throughout the years, additional lanes have been added in both directions to accommodate the increasing traffic demand. *Freeing the Freeways*, a $1.4 billion widening program undertaken by GDOT, began in 1980 and was completed in 1989. Under this program, four-lane facilities were widened to between six and twelve lanes. Construction history available from this time indicates additional lanes were constructed and existing lanes were reconstructed full-depth using asphalt or overlaid. Typical profiles from this era include $1^1/_2$ inches of asphalt concrete "E," 2 to 4 inches of asphalt concrete "B," 8 to 11 inches of asphalt concrete base, and more than 8 inches of graded aggregate base. An additional 12 inches of graded aggregate base was provided where directed by the supervising engineer. Asphalt mixtures for Interstate roadways during this time were based on 75-blow Marshall mix designs and used AC-20 binder. Concrete barriers separating travel directions and perforated underdrains conforming to Georgia Standard 9029B also were constructed. The last major resurfacing performed preceded the 1996 Olympics and consisted of milling and inlaying a stone matrix asphalt

(SMA) layer and an open graded friction course (OGFC) to assist in drainage. Core data retrieved for this project indicate approximately $2^1/_2$ to $4^1/_2$ inches of the existing asphalt concrete was milled and replaced with $1^1/_2$ inches of SMA and $^3/_4$ inches of OGFC. A leveling course was used where required for cross-slope correction. Lane widths were narrowed to 11 feet to allow the addition of a high-occupancy vehicle (HOV) lane.

3.2.3 Expected Moduli

The dynamic modulus regression equation commonly referred to as the Witczak equation (Andrei, Witczak, and Mirza 1999) was used to estimate the modulus at different temperatures and depths within the pavement structure:

$$\log E^* = -1.249937 + 0.02932\rho_{200} - 0.001767(\rho_{200})^2 - 0.002841\rho_4 - 0.058097V_a$$
$$- 0.802208\left(\frac{V_{beff}}{V_{beff} + V_a}\right) + \frac{3.871977 - 0.0021\rho_4 + 0.003958\rho_{38} - 0.000017(\rho_{38})^2 + 0.005470\rho_{34}}{1 + e^{(-0.603313 - 0.313351\log(f) - 0.393532\log(\eta))}}$$

Equation 12

where:

E^*	=	dynamic modulus, 10^5 psi.
η	=	bitumen viscosity, 10^6 Poise.
f	=	loading frequency, Hz.
V_a	=	air void content, %.
V_{beff}	=	effective bitumen content, % by volume.
ρ_{34}	=	cumulative % retained on the ¾ in sieve.
ρ_{38}	=	cumulative % retained on the 3/8 in sieve.
ρ_4	=	cumulative % retained on the No. 4 sieve.
ρ_{200}	=	% passing the No. 200 sieve.

Little information regarding the mechanical properties of the Downtown Connector HMA was available prior to this study. Broad assumptions were required to estimate the baseline moduli and anticipated ranges shown in Figure 3-2.

In summary, the expected low modulus value at 77°F for the Downtown Connector was 400 ksi, while the expected high modulus value was 700 ksi. Values greater than 700 ksi were thought to be the result of oxidized asphalt cement, while values lower than 400 ksi were suspected to have been damaged by means of moisture or some other mechanism.

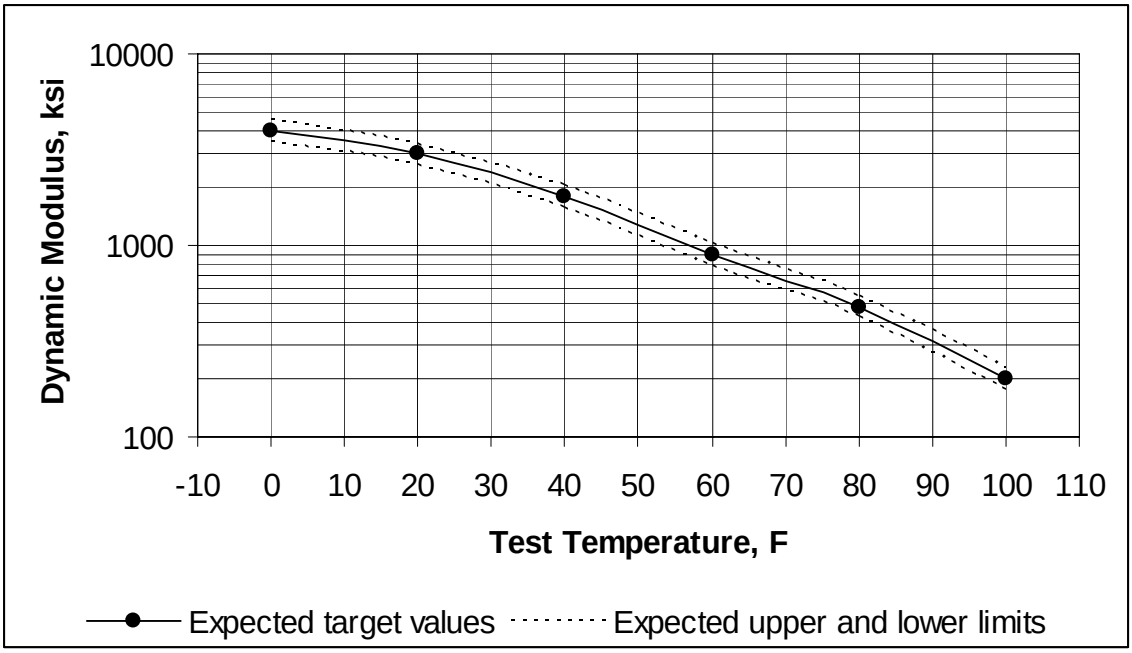

Figure 3-2. Expected high and low resilient modulus values.

3.3 Test Results

3.3.1 Surface Distress

Surface distresses were measured for each mile and lane of roadway. Distresses were identified and measured according to GDOT's PACES. Distress measurements for Lane 4 are shown and should be considered typical.

Transverse profile measurements were used to measure the rut depths. The PACES rut profiles are shown in Figures 3-3 and 3-4, while profiles measured in accordance with Federal Highway Administration (FHWA) criteria are represented in Figures 3-5 and 3-6. All rut profiles show an increase in longitudinal depressions from mileposts 248 to 250, particularly in the southbound direction.

Longitudinal profile measurements were used to determine the HRI for 0.1-mile roadway segments in the left wheel path (LWP), the right wheel path (RWP) and the average of the LWP and RWP. These data are plotted in Figures 3-7 and 3-8. No discernable pattern can be found from these graphs, with the possible exception of increased roughness near bridges. Other distresses were sampled as 100-ft segments, and only the segment with the highest level of distress in a mile-long section was recorded. Level 1 load cracking, shown in Figures 3-9 and 3-10, and level 1 block and transverse cracking, shown in Figures 3-11 and Figure 3-12, were observed in both directions. Raveling was visually observed but not measured. Other distresses, such as bleeding or flushing, corrugations or pushing, edge distresses, and loss of pavement section were not observed.

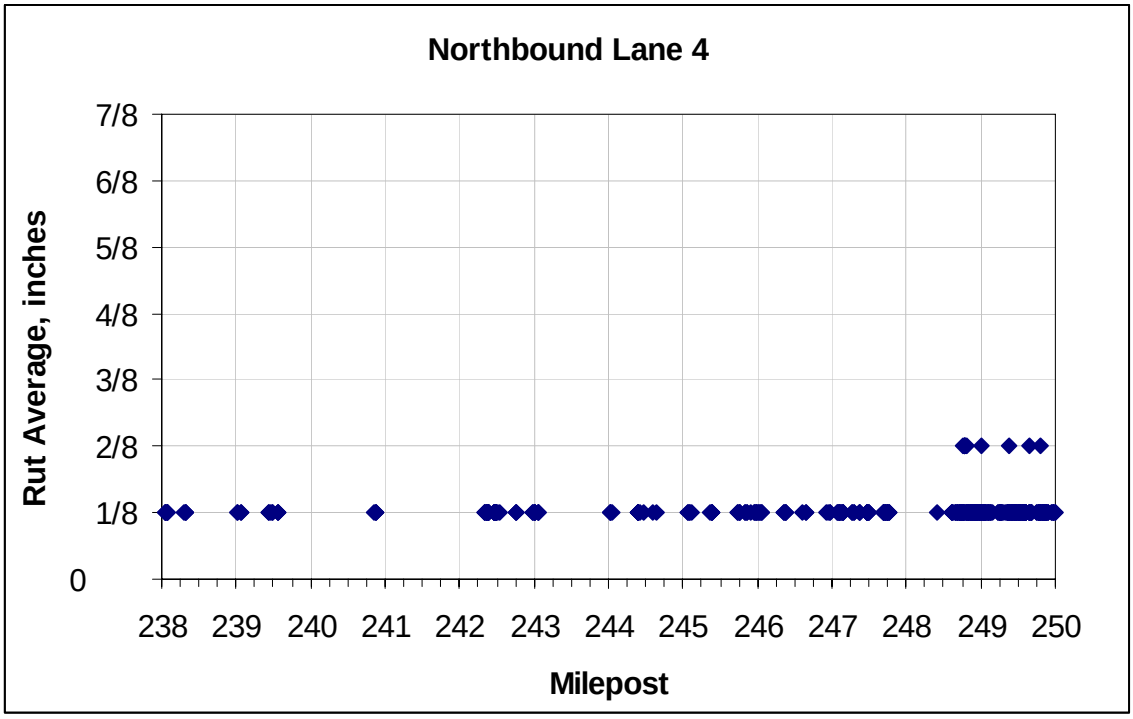

Figure 3-3. Northbound lane 4 PACES rutting summary plot.

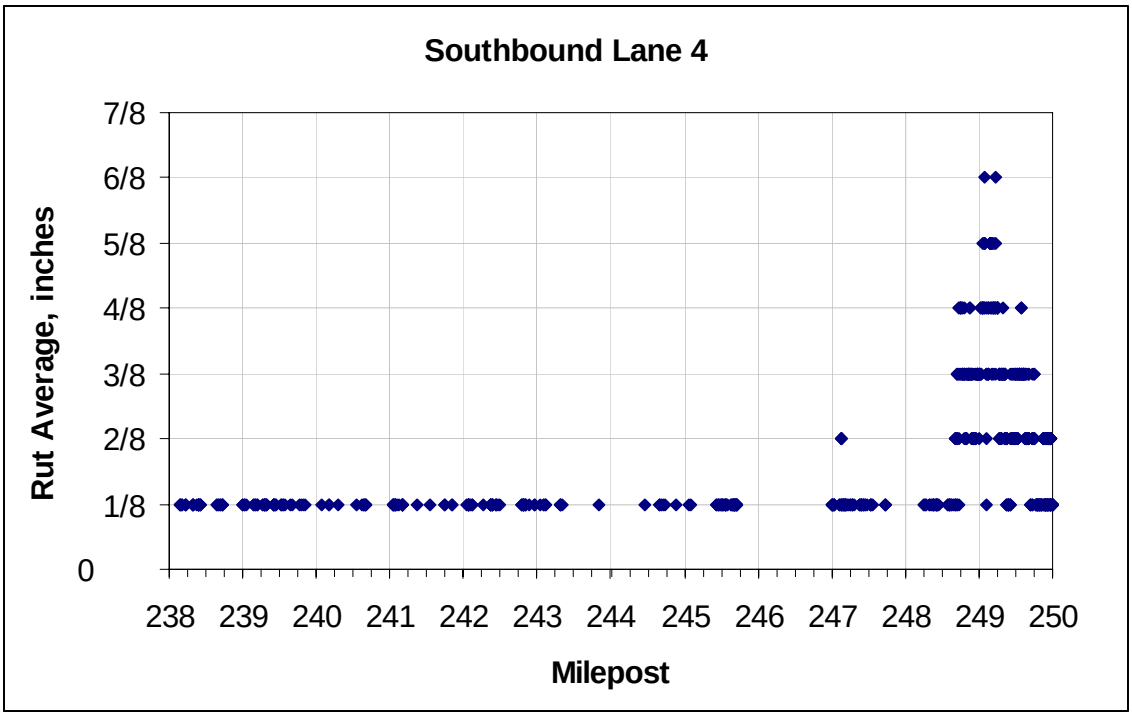

Figure 3-4. Southbound lane 4 PACES rutting summary plot.

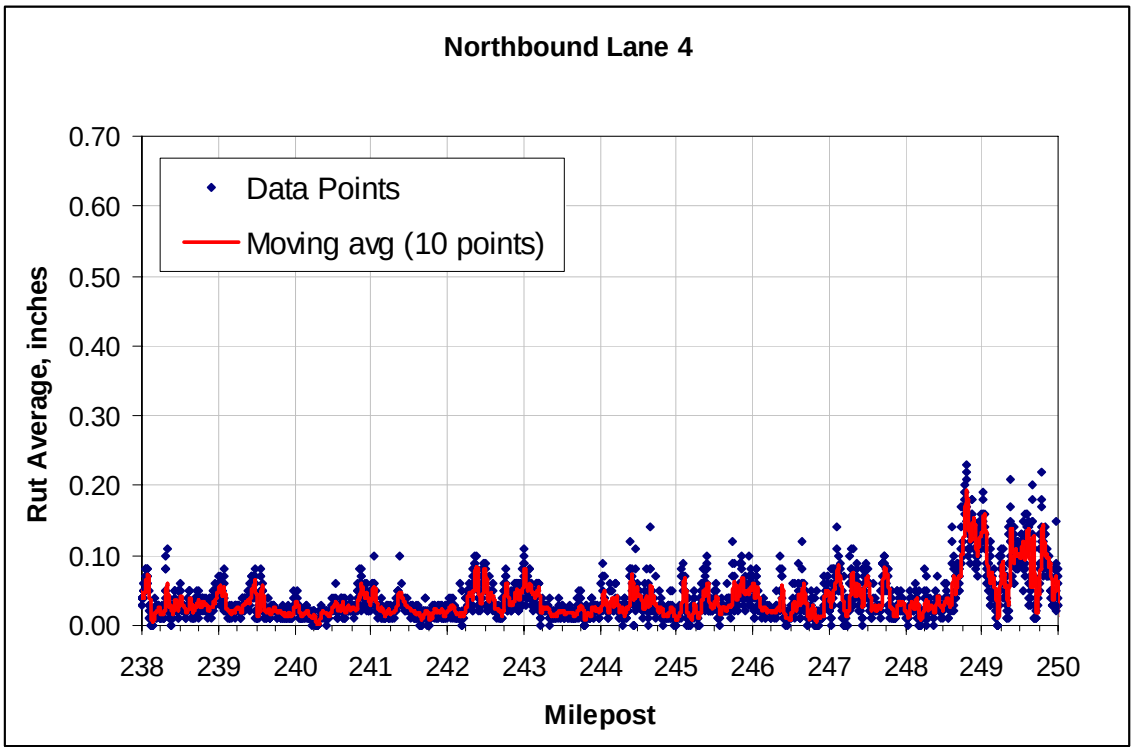

Figure 3-5. Northbound lane 4 FHWA rutting summary plot.

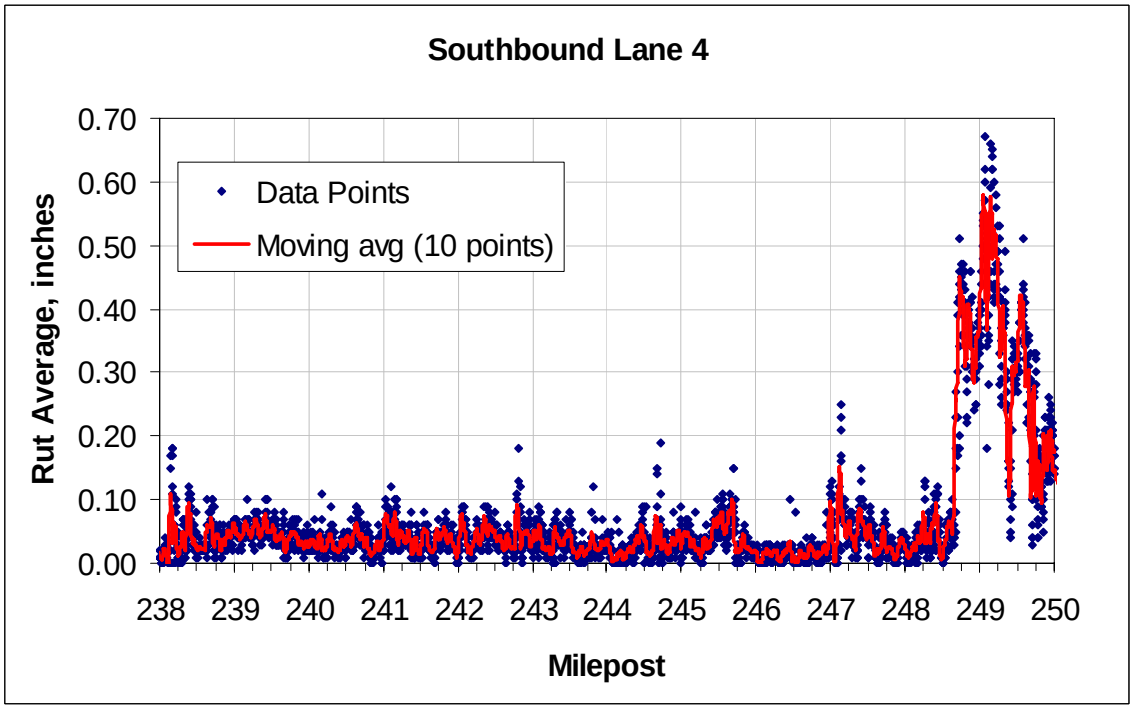

Figure 3-6. Southbound lane 4 FHWA rutting summary plot.

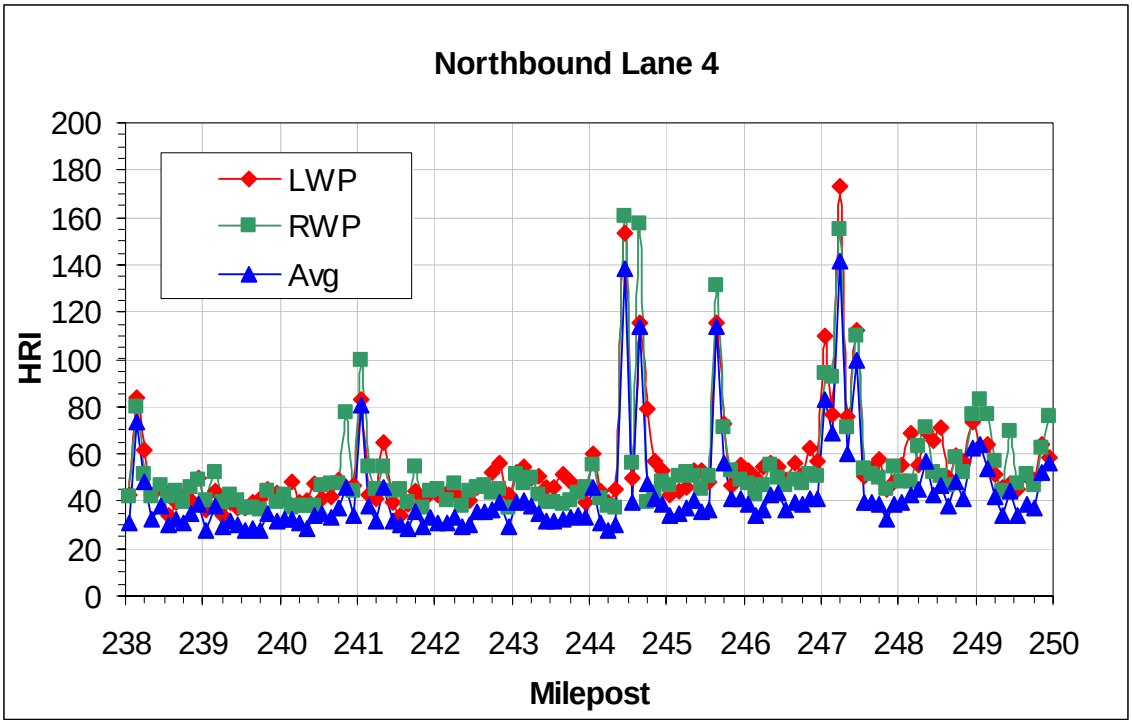

Figure 3-7. Northbound lane 4 roughness summary plot.

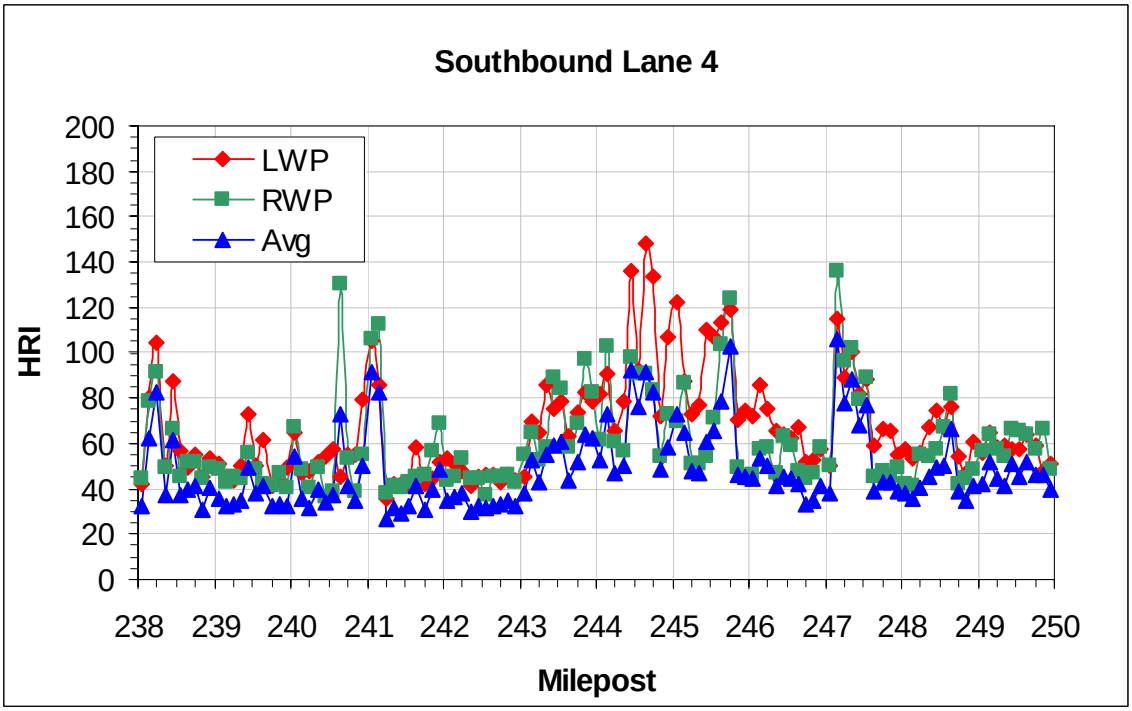

Figure 3-8. Southbound lane 4 roughness summary plot.

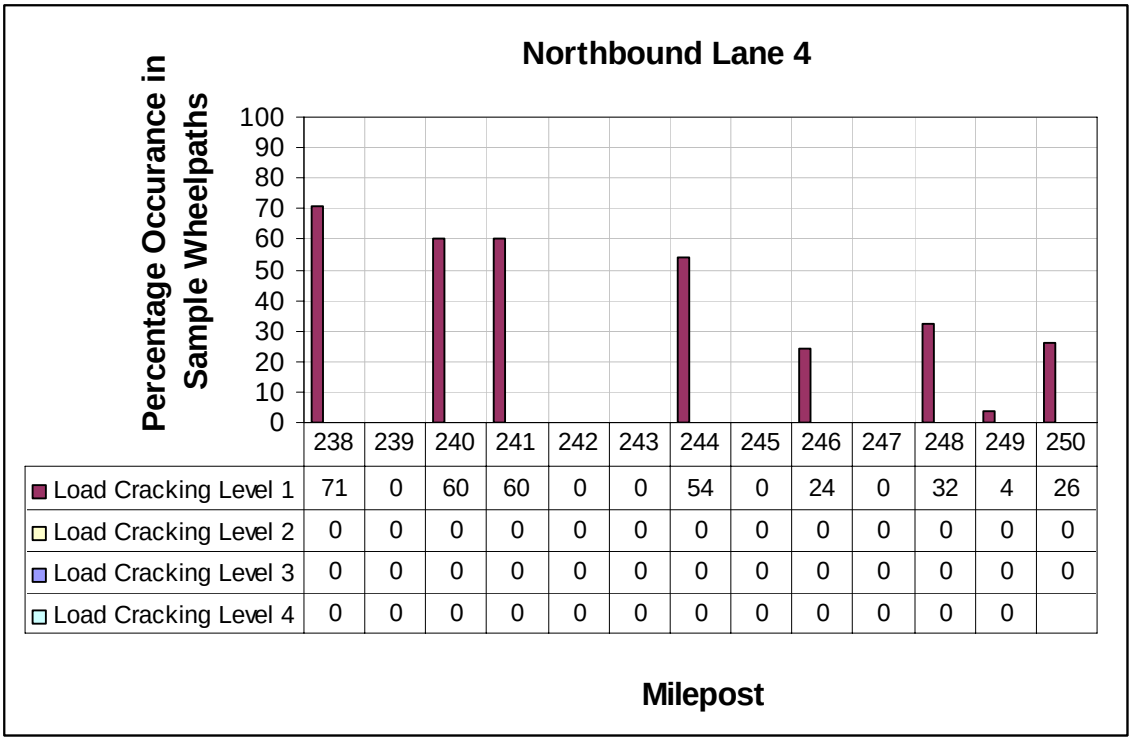

	238	239	240	241	242	243	244	245	246	247	248	249	250
Load Cracking Level 1	71	0	60	60	0	0	54	0	24	0	32	4	26
Load Cracking Level 2	0	0	0	0	0	0	0	0	0	0	0	0	0
Load Cracking Level 3	0	0	0	0	0	0	0	0	0	0	0	0	0
Load Cracking Level 4	0	0	0	0	0	0	0	0	0	0	0	0	

Figure 3-9. Northbound lane 4 load cracking summary plot.

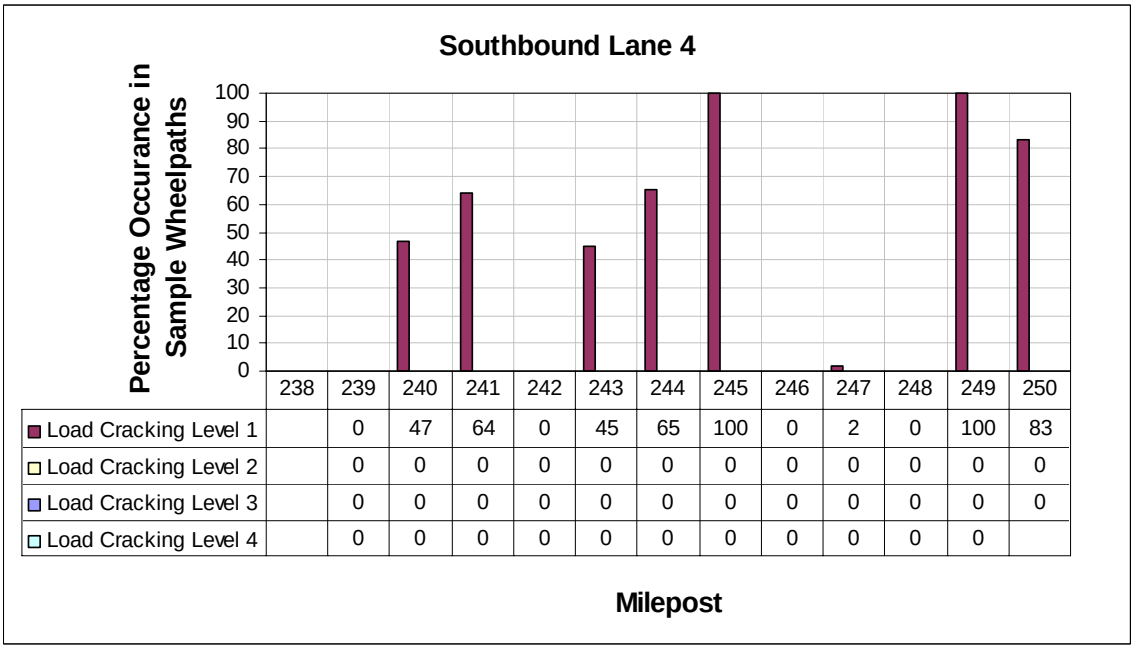

	238	239	240	241	242	243	244	245	246	247	248	249	250
Load Cracking Level 1		0	47	64	0	45	65	100	0	2	0	100	83
Load Cracking Level 2		0	0	0	0	0	0	0	0	0	0	0	0
Load Cracking Level 3		0	0	0	0	0	0	0	0	0	0	0	0
Load Cracking Level 4		0	0	0	0	0	0	0	0	0	0	0	

Figure 3-10. Southbound lane 4 load cracking summary plot.

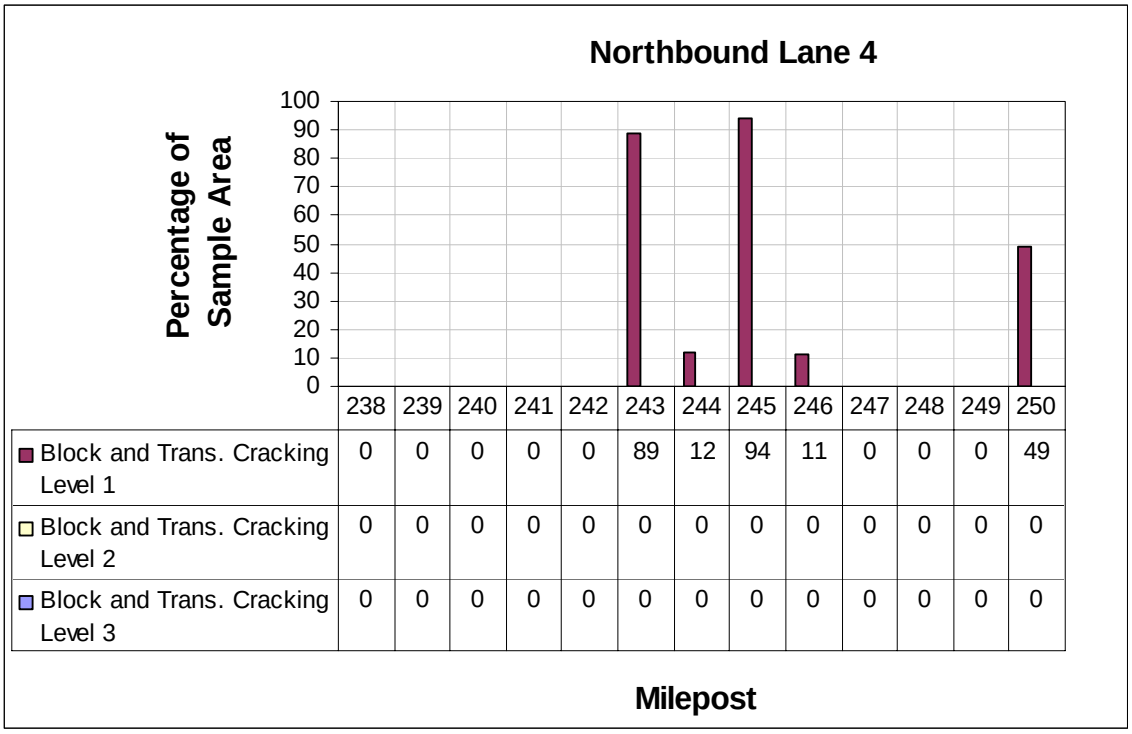

	238	239	240	241	242	243	244	245	246	247	248	249	250
Block and Trans. Cracking Level 1	0	0	0	0	0	89	12	94	11	0	0	0	49
Block and Trans. Cracking Level 2	0	0	0	0	0	0	0	0	0	0	0	0	0
Block and Trans. Cracking Level 3	0	0	0	0	0	0	0	0	0	0	0	0	0

Figure 3-11. Northbound lane 4 block and transverse cracking summary plot.

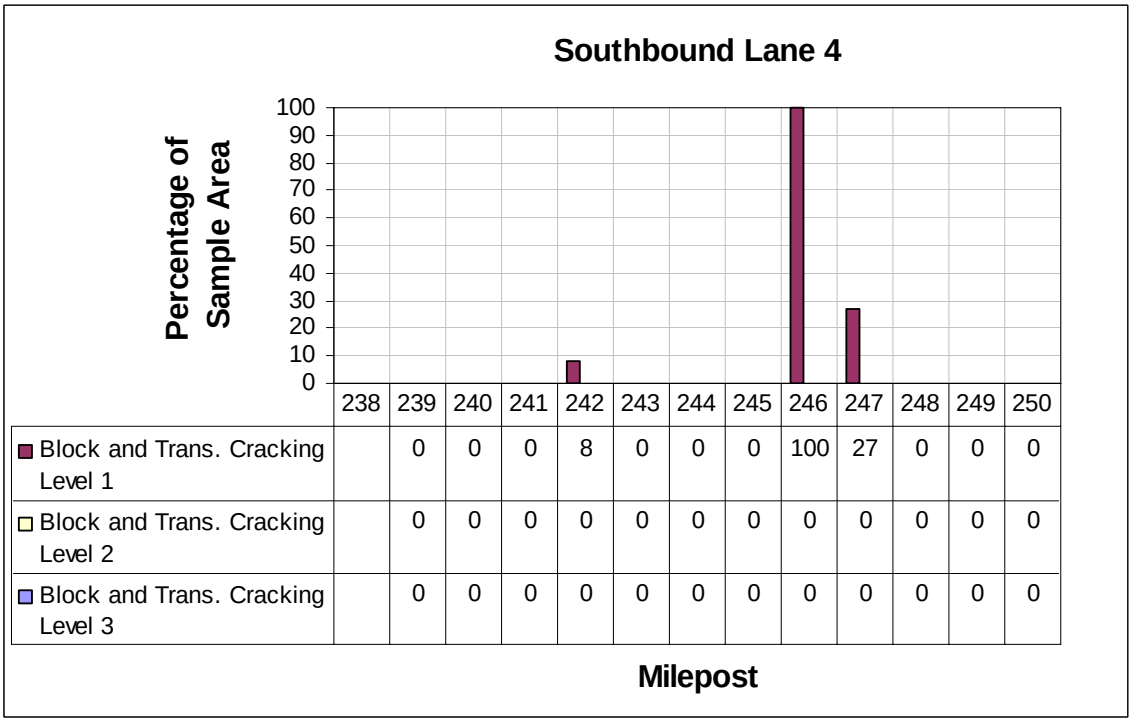

	238	239	240	241	242	243	244	245	246	247	248	249	250
Block and Trans. Cracking Level 1		0	0	0	8	0	0	0	100	27	0	0	0
Block and Trans. Cracking Level 2		0	0	0	0	0	0	0	0	0	0	0	0
Block and Trans. Cracking Level 3		0	0	0	0	0	0	0	0	0	0	0	0

Figure 3-12. Southbound lane 4 block and transverse cracking summary plot.

3.3.2 Ground Penetrating Radar

Collection of GPR data began at MP 238 and ended at MP 250 in both travel directions. Data was collected along each wheel path, the centerline of all lanes, and along lane boundaries of lanes 5 and 6, lanes 6 and 7, and lanes 7 and 8. Traffic control limitations prevented the surveying of other lane boundaries. The center of the shoulder was also surveyed.

The GPR data for the northbound full-depth HMA shows three major layers with interfaces at approximately 3.5, 9, and 15 inches below the surface. Interpreted HMA thicknesses for northbound lane 4 are shown in Figure 3-13. The core data shown in Figure 3-13 are from cores retrieved by GDOT prior to the current study.

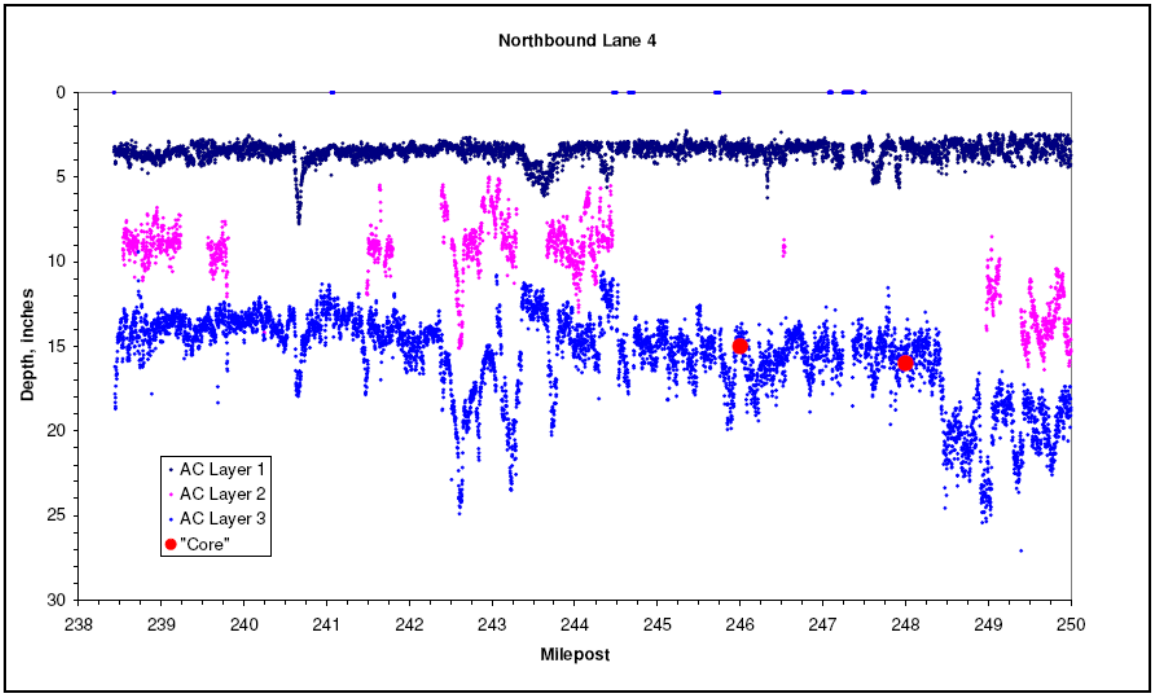

Figure 3-13. GPR estimated HMA thickness for northbound lane 4.

The GPR survey was used to determine the UI, a value that represents areas of potential moisture damage. This index can be calculated to represent specific vertical pavement profiles and, in this case, was used to model the pavement's potential for moisture damage at depths from approximately 4 inches to 10 inches. A Local UI was standardized to a survey length of 1,000 feet, while a Global UI was standardized using the entire project length. The Local UI indicated random areas of electromagnetic variability in the travel lanes and shoulders. The Global UI indicated a greater amount of variability but was also interpreted to be random and not characteristic of extensive moisture damage. Typically, moisture damage is expected to be found in significant continuous stretches, not randomly as predicted by each UI. Other factors that could influence the UI include changes in moisture and air void content and mix and aggregate type. Therefore, based on the UI values, it was postulated that moisture damage should not be widespread.

Appendix A shows the Local UI with each test section highlighted and core locations represented, while Appendix B shows the Global UI. Numbers to the right of each figure indicate the lane number while shoulder are not marked but still represented adjacent to the outside lane.

3.3.3 Seismic

Nine sections approximately 1 to 2 miles long were chosen for seismic testing and are summarized in Table 3-1. These sections were selected based upon the UI and lane closure restrictions. Seismic data was reduced into seismic modulus values and adjusted to a standard loading frequency of 15 Hz and a temperature of 77° F. The range of the instrument was a depth of approximately 10 inches.

Approximately 10 percent of the northbound tests had seismic moduli less than the expected lower modulus value of 400 ksi, while approximately 20 percent of the southbound tests were found to be less than the lower modulus value. As illustrated in Figure 3-14, the majority of northbound tests with less than anticipated modulus values were found in the northernmost tested portion of lane 2. Figure 3-15 shows southbound seismic tests with less than expected values spread out all over the tested lanes but primarily in lanes 4 and 5 at the southernmost tested section, lane 4 in the middle test section, and lanes 2 and 3 in the northernmost tested section.

Seismic moduli were compared with GPR UI values in Figure 3-16 to determine if a relationship could be found. Trend lines indicate a very weak positive correlation, indicating that as electromagnetic variability, as measured by UI, the seismic modulus also tends to increase. This, of course, is opposite of what one would expect in a pavement where moisture damage was the cause of the increased UI. The lack of a correlation between UI and seismic modulus reinforces the conclusion that electromagnetic variability, as measured by the UI, in the Downtown Connector is not necessarily due to moisture damage but most likely due to local changes in moisture, air voids, mix design, or aggregates and not necessarily moisture damage.

Table 3-1. Seismic test sections.

Section	Travel Direction	Beginning	End	Lanes Tested
NB-1	Northbound	Exit 239	MP 240	4, 5
NB-2	Northbound	MP 242	MP 244	2, 3
NB-3	Northbound	Langford Parkway Entrance	Bridge at University Avenue	2, 3, 4
NB-4	Northbound	Exit 244	Pryor Street Overpass	2, 3
SB-1	Southbound	University Ave Entrance	North of Exit 243	2, 3
SB-2	Southbound	University Ave Entrance	North of Exit 243	5, 6, 7
SB-3	Southbound	Exit 241	Bridge at Mt. Zion Road	4, 5
SB-4	Southbound	South of MP 241	North of Exit 239	4, 5, 6
SB-5	Southbound	MP 242	MP 241	2, 3

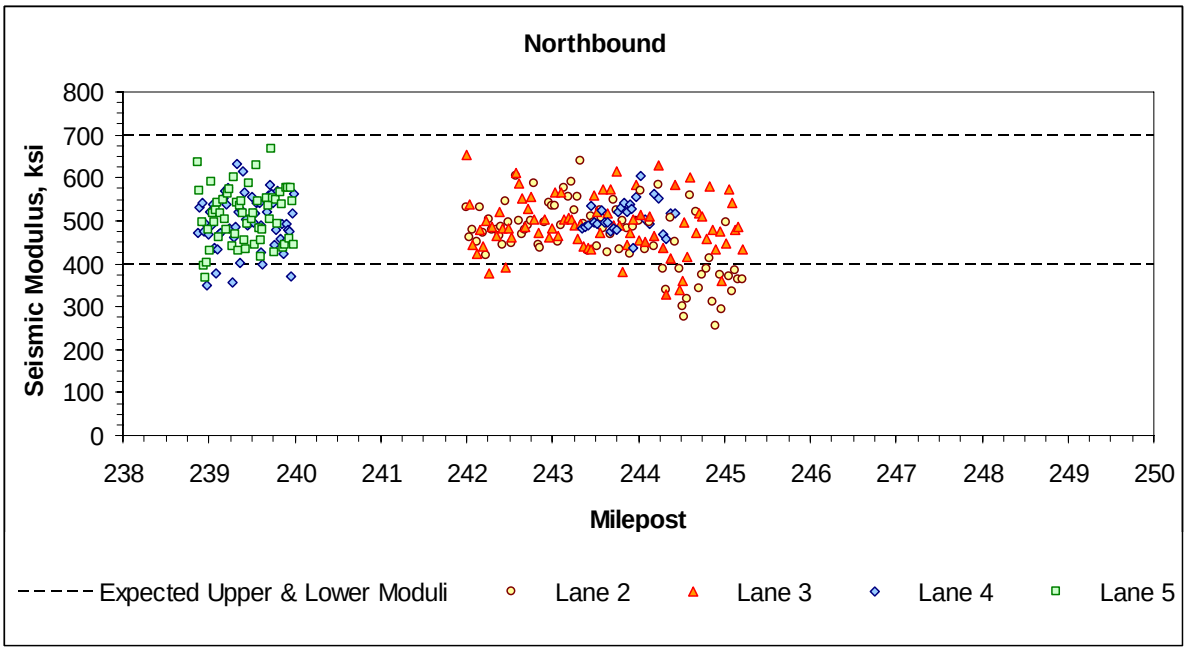

Figure 3-14. Northbound seismic tests.

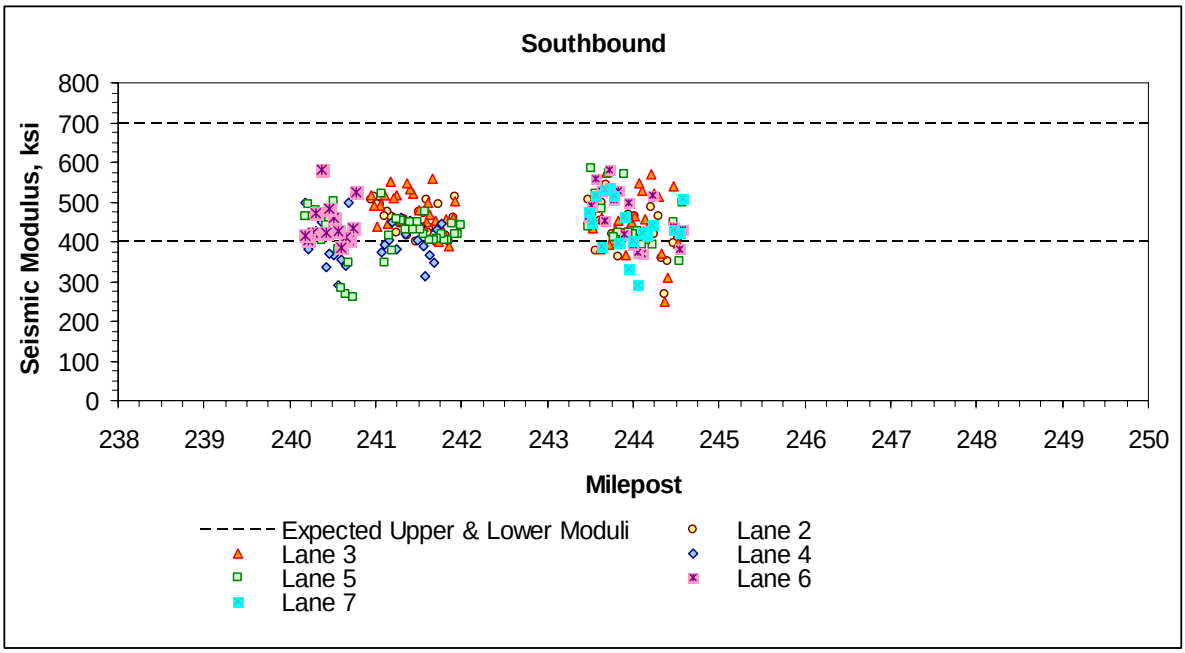

Figure 3-15. Southbound seismic tests.

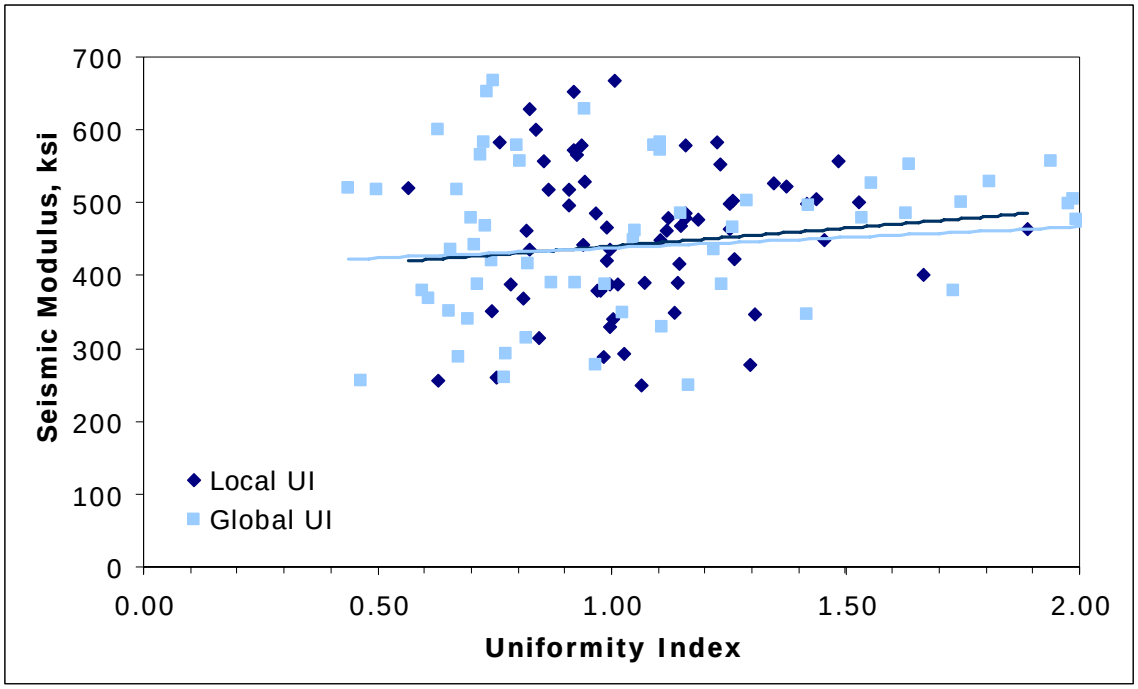

Figure 3-16. Plot of UI and seismic modulus showing no relationsip.

3.3.4 Cores

Fifty-two cores were extracted under the lane closures that were set up for the seismic testing. Core locations were chosen based on the Global UI and seismic tests. All cores were 4 inches in diameter. Core locations are provided in Table 3-2.

A photograph of each core is presented in Appendix C. Evidence of moisture damage was apparent in some cores but not in the advanced levels typically characterized as stripping. Approximately 60 percent of the cores were retrieved intact; however, not all of these were full depth. The remaining cores broke during extraction, either along layer interfaces or within layers. Breaks at interfaces suggest weak interlay bonds. Many times the core barrel was not quite long enough to cut full depth, and retrieval often required breaking the core at one or more locations. The HMA mixture generally stayed intact and did not disintegrate near the fracture. This condition is evidence that moisture may be confined primarily to the layer interface where it reduces the bond between layers, but has not affected the integrity of the mixture itself. Table 3-3 summarizes the observations made from the cores. Additional cores were extracted by GDOT prior to this study. The conditions of these cores, summarized in Table 3-4, were assessed using digital photographs provided by GDOT. Overall, the cores appeared similar to the ones retrieved for the study.

Table 3-2. Core locations.

Core ID	Distance North of MP 238, feet	MP	GPS Coordinate		Lane of GPS Measurement	Lane of Core Extraction	Location in Lane
			Latitude (N)	Longitude (W)			
NB 1-1	5540	239.049	33.644503	84.398629	5	5	Center
NB 1-2	6395	239.211	33.646758	84.397859	5	5	Center
NB 1-3	6895	239.306	33.648074	84.397399	5	5	Center
NB 1-4	7493	239.419	33.649654	84.396865	5	4	Center
NB 1-5	9039	239.712	33.653608	84.395517	5	4	Center
NB 2-1	23008	242.358	33.690989	84.401677	2	2	Center
NB 2-2	24797	242.696	33.695452	84.404685	2	2	Center
NB 2-3	25385	242.808	33.696764	84.404382	2	2	Center
NB 2-4	27643	243.235	33.702978	84.403920	2	2	Center
NB 2-5	29231	243.536	33.706979	84.403130	2	2	Center
NB 2-6	31225	243.914	33.712484	84.400756	2	2	Center
NB 3-1	29834	243.650	33.709107	84.402278	3	4	Center
NB 3-2	30480	243.773	33.710796	84.401629	3	4	Center
NB 3-3	31262	243.921	33.712719	84.400502	3	4	Center
NB 3-4	32926	244.236	33.716814	84.398184	3	4	Center
NB 3-5	33173	244.283	33.717449	84.397899	3	2	Center
NB 4-1A	34538	244.541	33.720777	84.395648	2/3	2	Center
NB 4-1B	34538	244.541	33.720777	84.395648	2/3	2	Center
NB 4-2	34842	244.599	33.721488	84.395120	2/3	3	Center
NB 4-3	35441	244.712	33.722926	84.394168	2/3	2	Center
NB 4-4	36042	244.826	33.724523	84.393711	2/3	3	Center
NB 4-5	36442	244.902	33.725618	84.393604	2/3	2	Center
NB 4-6	36838	244.977	33.726700	84.393496	2/3	2	Center
NB 4-7	37834	245.166	33.729351	84.392737	2/3	3	Center
SB 1-1	33807	244.403	33.719228	84.397075	2	2	Center
SB 1-2	32189	244.096	33.715132	84.399075	2	3	Center
SB 1-3	31806	244.024	33.714189	84.399628	2	3	Center
SB 1-4	29767	243.638	33.709194	84.402522	2	2	Center
SB 1-5	29406	243.569	33.708258	84.402916	2	2	Center
SB 1-6	29071	243.506	33.707371	84.403201	2	2	Center
SB 2-1	32550	244.165	33.715213	84.399181	6	7	Center
SB 2-2	32200	244.099	33.714347	84.399678	6	6	Center
SB 2-3	31702	244.004	33.713206	84.400585	6	6	Center
SB 2-4	29710	243.627	33.708170	84.403043	6	7	Center
SB 2-5	29407	243.570	33.707375	84.403335	6	7	Center
SB 3-1	21093	241.995	33.686737	84.399196	5	5	Center
SB 3-2	20892	241.957	33.686197	84.399062	5	5	Center
SB 3-3	18746	241.550	33.680334	84.398611	5	4	Center
SB 3-4	17974	241.404	33.678236	84.398262	5	5	Center
SB 3-5	16196	241.067	33.673382	84.397822	5	5	Center
SB 4-1	14484	240.743	33.668598	84.397869	5	5	Center
SB 4-2	14217	240.693	33.667890	84.397642	5	5	Center
SB 4-3	13279	240.515	33.665438	84.396706	5	5	Center
SB 4-4	12158	240.303	33.662506	84.395593	5	4	Center
SB 4-5	11991	240.271	33.662064	84.395449	5	4	Center
SB 4-6	11821	240.24	33.685450	84.398862	5	5/6	5/6 Joint
SB 5-1	20631	241.907	33.685450	84.398862	2	2	IWP
SB 5-2	20389	241.862	33.684788	84.398874	2	2	IWP
SB 5-3	19104	241.618	33.681274	84.398640	2	2	IWP
SB 5-4	16944	241.209	33.675398	84.397750	2	2	IWP
SB 5-5	16777	241.177	33.674939	84.397713	2	2	IWP
SB 5-6	16609	241.146	33.674479	84.397707	2	2	IWP

Table 3-3. Project core observations.

Core ID	Thickness, inches	Condition of Core	Moisture Damage
NB 1-1	13.3	Intact, full depth core.	None
NB 1-2	14.3	Intact, full depth core.	None
NB 1-3	12.6	Intact, full depth core.	None
NB 1-4	13.6	Intact, full depth core.	None
NB 1-5	12.2	Intact, full depth core.	None
NB 2-1	17.1	Broke at approximately 11 inches along interface. Dark color near break.	Likely
NB 2-2	16.7	Broke at approximately 11 inches along interface.	Low
NB 2-3	16.5	Intact core but not full depth.	Low
NB 2-4	16.1	Broke at approximately 11.5 inches along interface. Dark color near break.	Likely
NB 2-5	15.5	Broke at approximately 6.5 inches along interface.	Low
NB 2-6	17.2	Broke at approximately 8.5 inches while along interface	Low
NB 3-1	16.2	Broke at approximately 6.5 inches along interface.	Low
NB 3-2	15.6	Broke at approximately 9 inches along interface.	Low
NB 3-3	14.1	Intact, full depth core.	Low
NB 3-4	15.0	Intact, full depth core.	Low
NB 3-5	15.4	Broke at approximately 4 inches. Dark color near break.	Likely
NB 4-1A	NA	Broke in several pieces. Did not retrieve most of core.	Likely
NB 4-1B	16.1	Broke below SMA and at 9 inches. Dark color near first break.	Likely
NB 4-2	16.9	Intact, full depth core.	None
NB 4-3	NA	Broke below SMA while coring.	Likely
NB 4-4	13.9	Intact, full depth core.	None
NB 4-5	14.3	Broke below SMA. Dark color near break.	Likely
NB 4-6	13.6	Broke below SMA. Dark color near break.	Likely
NB 4-7	15.7	Intact, full depth core	None
SB 1-1	11.9	Broke at approximately 4 inches along interface. Dark color above break.	Likely
SB 1-2	15.2	Broke at approximately 11 inches along interface.	Likely
SB 1-3	15.0	Intact core but not full depth.	Likely
SB 1-4	16.6	Intact core but not full depth.	Likely
SB 1-5	14.9	Broke at approximately 7.5 inches along interface.	Likely
SB 1-6	14.9	Broke at approximately 8 inches along interface.	Likely
SB 2-1	13.9	Intact, full depth core.	None
SB 2-2	14.2	Intact, full depth core.	None
SB 2-3	15.0	Intact, full depth core.	None
SB 2-4	12.9	Intact, full depth core.	None
SB 2-5	11.1	Intact, full depth core.	None
SB 3-1	15.7	Intact, full depth core. Slight fracturing at 6 to 8 inches	None
SB 3-2	16.1	Broke at approximately 7 inches along interface.	Likely
SB 3-3	13.4	Broke at approximately 4.5 inches along interface. Dark color above break.	Likely
SB 3-4	12.0	Intact, full depth core.	None
SB 3-5	13.2	Intact, full depth core.	None
SB 4-1	11.5	Intact, full depth core.	Low
SB 4-2	12.0	Intact, full depth core.	Low
SB 4-3	13.3	Intact, full depth core.	Low
SB 4-4	12.2	Intact, full depth core.	Low
SB 4-5	12.3	Intact, full depth core.	Low
SB 4-6	11.8	Intact, full depth core.	Low
SB 5-1	14.1	Intact, full depth core.	Low
SB 5-2	14.2	Broke below SMA layer.	Low
SB 5-3	12.5	Intact, full depth core.	Low
SB 5-4	12.0	Intact, full depth core.	Low
SB 5-5	12.2	Intact, full depth core.	Low
SB 5-6	12.1	Intact, full depth core. Honeycombing at 6 to 9 inches.	Low

Table 3-4. Previous core observations.

Core ID	MP	Lane	Thickness, inches	Condition of Core
NB-59	244	7	12	Intact core.
NB-61	244	5	17	Intact core.
NB-62	244	6	12.75	Intact core.
NB-63	245	7	15.5	Intact core.
NB-64	245	6	16.5	Broke at approximately 8 inches.
NB-65	245	5	15.5	Intact core.
NB-66	246	4	15	Intact core.
NB-67	246	5	15	Intact core.
NB-68	247	4	12.5	Vertical fracture entire length. Honeycombing below 7 inches. Longitudinal crack.
NB-69	247	6	17	Broke at approximately 8 inches.
NB-70	248	4	17	Intact core, extracted along longitudinal crack.
NB-71	248	5	15	Broke at approximately 5 inches along interface. Longitudinal crack.
NB-72	248	6	15	Fracture or honeycombing at approximately 8 inches. Longitudinal crack.
NB-73	249	5	24	Broke at approximately 8 inches along interface.
NB-74	249	6	23.25	Broke at approximately 10 inches along interface.
NB-75	249	7	25	Possible stripping from 2 to 6 inches.
NB-76	250	7	17	Broke at approximately 2.5 inches along interface.
NB-77	250	5	18	Broke in several pieces. Extracted along longitudinal crack.
NB-78	250	6	15	Broke at approximately 4 inches, honeycombing present.
SB-4	250	6	17.25	Intact core.
SB-5	250	7	18	Intact core.
SB-6	250	8	17.75	Intact core.
SB-8	249	5	NA	Asphalt concrete/Portland cement concrete
SB-10	249	6	17.5	Broke at approximately 4 inches along interface.
SB-12	248	4	16.4	Intact core.
SB-13	248	5	15	Intact core.
SB-14	248	6	15.5	Intact core.
SB-15	248	7	16	Intact core.
SB-17	247	4	15.25	Intact core, honeycombing at approximately 10 inches.
SB-18	247	5	15.5	Broke at approximately 12 inches along interface.
SB-19	247	6	15.75	Fracture at approximately 8 inches.
SB-20	247	7	15.5	Intact core.
SB-21	246	4	15.75	Broke at approximately 8 inches along interface.
SB-23	246	4	15.5	Broke at approximately 6.5 inches along interface.
SB-24	245	4	16.75	Intact core.
SB-25	245	5	NA	Broke at approximately 6 inches along interface.
SB-26	245	6	17.25	Broke at approximately 6 inches along interface.
SB-27	245	7	17	Intact core.
SB-28	244	5	13.5	Intact core.
SB-29	244	6	13	Intact core.
SB-30	244	7	13.75	Intact core.
SB-32	243	4	14.5	Fracture at approximately 4 inches.
SB-36	250	2	17	Broke at approximately 4 inches along interface, fracture at 9 inches.
SB-37	250	3	NA	Broken into several pieces.
SB-43	248	1	15	Intact core.
SB-44	248	2	15	Intact core.
SB-45	248	3	15	Intact core.
SB-46	247	1	15.5	Intact core.
SB-47	247	2	14	Intact core.
SB-48	247	3	15	Intact core.
SB-51	246	3	16	Intact core.
SB-56	244	1	15	Broke at approximately 10 inches along interface.
SB-57	244	2	14	Intact core, honeycombing at approximately 10 inches.
SB-58	244	3	13	Broke at approximately 5 inches along interface.

3.3.5 Laboratory Tests

Two to three sections of 19 cores were selected for indirect tensile (IDT) tests. The average dynamic modulus for samples tested was 604 ksi. The lowest dynamic modulus values were found at a depth between 6 and 8 inches, where 31 percent of the samples tested had a dynamic modulus less than 400 ksi. Overall, 15 percent of the measurements were less than the expected modulus. Table 3-5 summarizes the IDT dynamic modulus values.

Table 3-5. Indirect tensile dynamic modulus summary.

Core ID	Indirect Tensile Dynamic Modulus, ksi				
	2 to 4 inches	4 to 6 inches	6 to 8 inches	8 to 10 inches	10 to 12 inches
NB 1-5		515	495		
NB 2-4			297	669	454
NB 2-5		505	672	894	
NB 3-1	865	711			
NB 3-2		665	292	783	
NB 3-5	401		737		
NB 4-4		889		725	
NB 4-5		318	317		
SB 1-1	550	537		587	
SB 1-2		629	699	479	
SB 1-4		515	242	419	
SB 2-1		652		948	
SB 2-4		572	969		
SB 3-1		663		300	
SB 3-4	789		876		
SB 4-1		452	575	868	
SB 4-2	305		718		
SB 5-2		605	795	455	
SB 5-5		759		618	

The lower modulus values shown in Table 3-5 could suggest moisture damage, but may also be the result of higher air voids, lower asphalt contents, or micro-fatigue cracks. If the lower modulus values are a result of moisture damage, the relationship between strength and modulus for the moisture-damaged layer should be different from those layers without moisture damage. Figure 3-16 shows the relationship between strength and dynamic modulus for the different layers tested. As shown, all three layers have a consistent relationship, with one exception from a sample at 6 to 8 inches where oxidization likely resulted in a very stiff appearing mixture.

Overall, the tensile strain at failure for the samples tested is lower than what would be expected for a good quality HMA mixture. Low tensile strains at failure suggest the adhesion between the asphalt and aggregate has been affected. However, based on visual examinations, high air voids were present in many of the cores. High air voids would significantly reduce the tensile strain at failure. Figure 3-17 graphically compares the fracture characteristics of the sections tested to a typical mix used at the AASHO Road Test and indicates the HMA along the Downtown Corridor exhibits behavior typical of marginal to brittle materials. Appendix D contains the stress-strain curves for each sample tested.

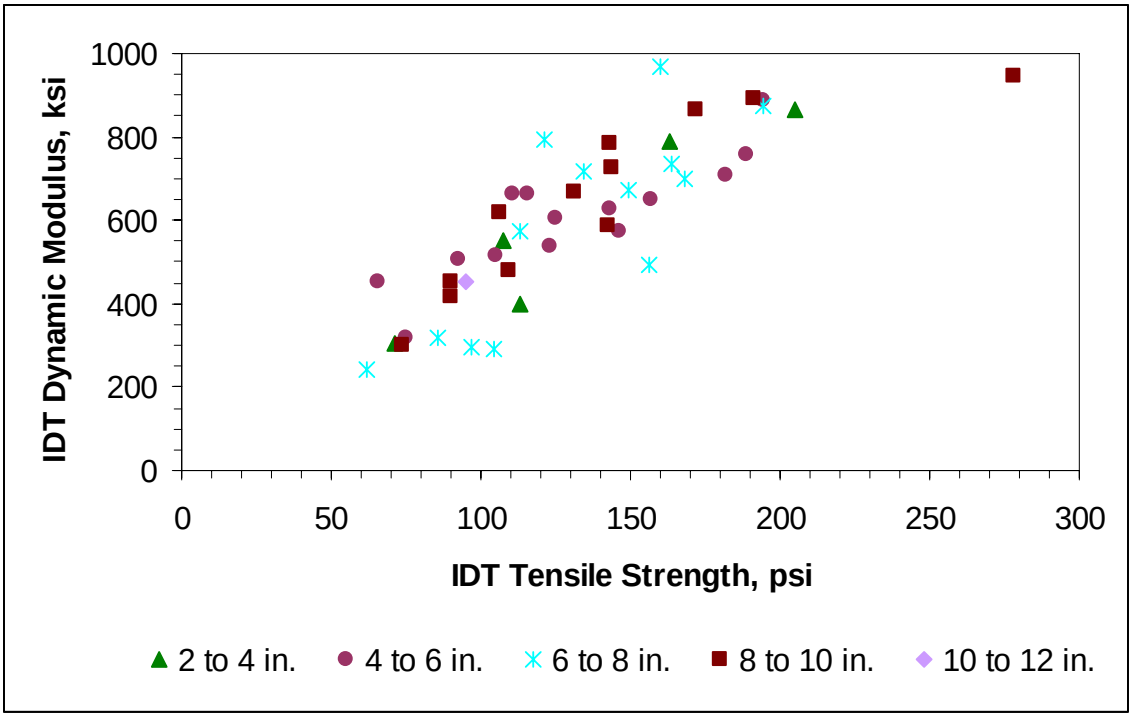

Figure 3-17. Relationship between IDT strength and dynamic modulus.

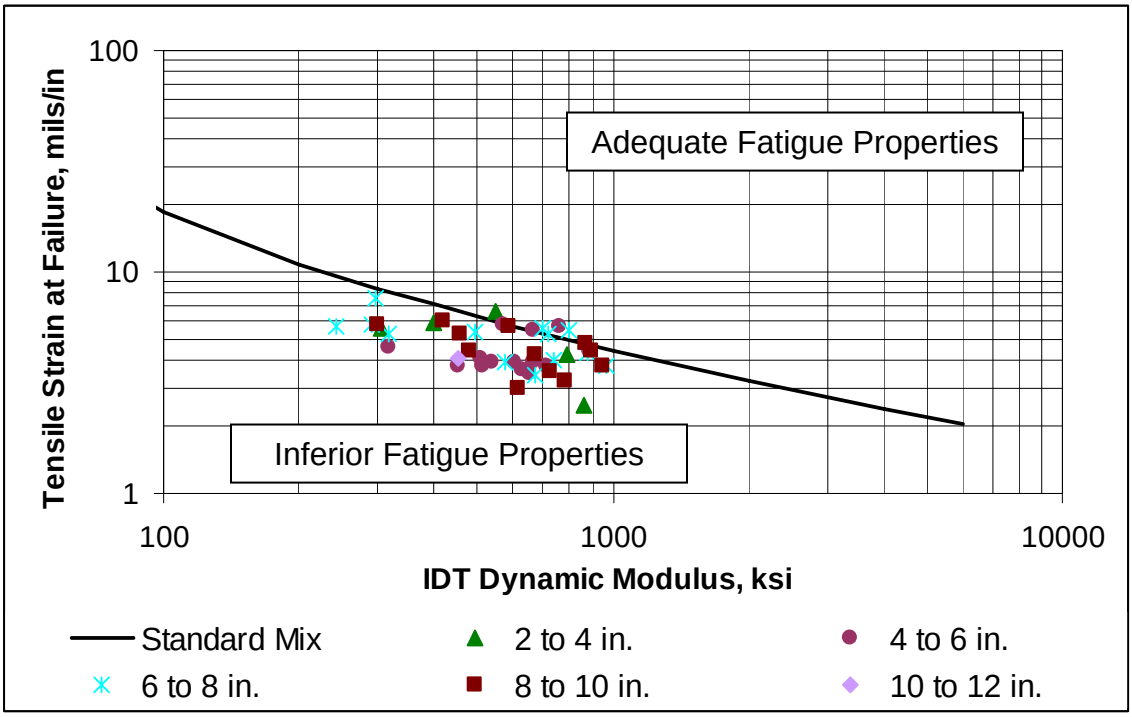

Figure 3-18. Comparison of the IDT dynamic modulus and strain at failure.

4 CONCLUSIONS AND RECOMMENDATIONS

4.1 Downtown Corridor Conclusions

There is little evidence to suggest any widespread moisture damage along the Downtown Corridor. The following field and laboratory tests were completed that support this conclusion:

- A distress survey showed minor surface distresses with the exception of increased rut depths from mileposts 248 to 250 in both directions, particularly the southbound direction.
- GPR data collected in the travel lanes and shoulders indicated that moisture damage should not be widespread.
- Seismic testing showed 10 percent of the northbound tests and 20 percent of the southbound tests had seismic moduli less than the expected lower modulus values. The majority of northbound tests with less than anticipated modulus values were found in the northernmost tested portion of lane 2, while southbound seismic tests with less than expected values were found primarily in lanes 4 and 5 at the southernmost tested section, lane 4 in the middle test section, and lanes 2 and 3 in the northernmost tested section.
- The lack of correlation between UI and seismic modulus reinforces the conclusion that the observed electromagnetic variability (as measured by UI) is not caused by moisture damage but is most likely due to local changes in moisture, air voids, mix design, or aggregates and not necessarily moisture damage.
- Approximately 60 percent of the cores were retrieved intact. The remaining cores broke primarily along layer interfaces during extraction, suggesting weak interlayer bonds. The HMA mixture generally stayed intact and did not disintegrate near the fracture, indicating moisture may be confined primarily to the layer interface where it reduces the bond between layers, but has not significantly affected the integrity of the mixture itself.
- Laboratory tests showed little evidence of moisture damage but indicated inferior fatigue properties for most of the samples tested.

4.2 Rehabilitation Recommendations

The elastic layer theory program EVERSTRS was used to calculate stresses and strains within the pavement structure. The layer modulus values used in the simulation were taken from the seismic test results but adjusted to account for the appropriate temperature and loading frequency. The baseline values were taken from the dynamic modulus regression equation (Equation 12) and adjusted for the values expected during construction or overlay placement.

The design criteria used in the rehabilitation design analyses were vertical strains in the HMA layers. The recommended depth of milling was determined based on limiting the vertical compressive strain in the HMA layer to values below those that would cause extensive damage or distortion during construction and with time under truck traffic.

EVERSTRS is limited to five layers, so the pavement model was divided into three HMA layers, base, and subgrade. For this example, the lower HMA modulus values were assumed to be between a depth of 5 and 8 inches, as indicated by the IDT tests. The results from these computations are shown in Figure 4-1. The loads used in the computations represent HMA delivery trucks.

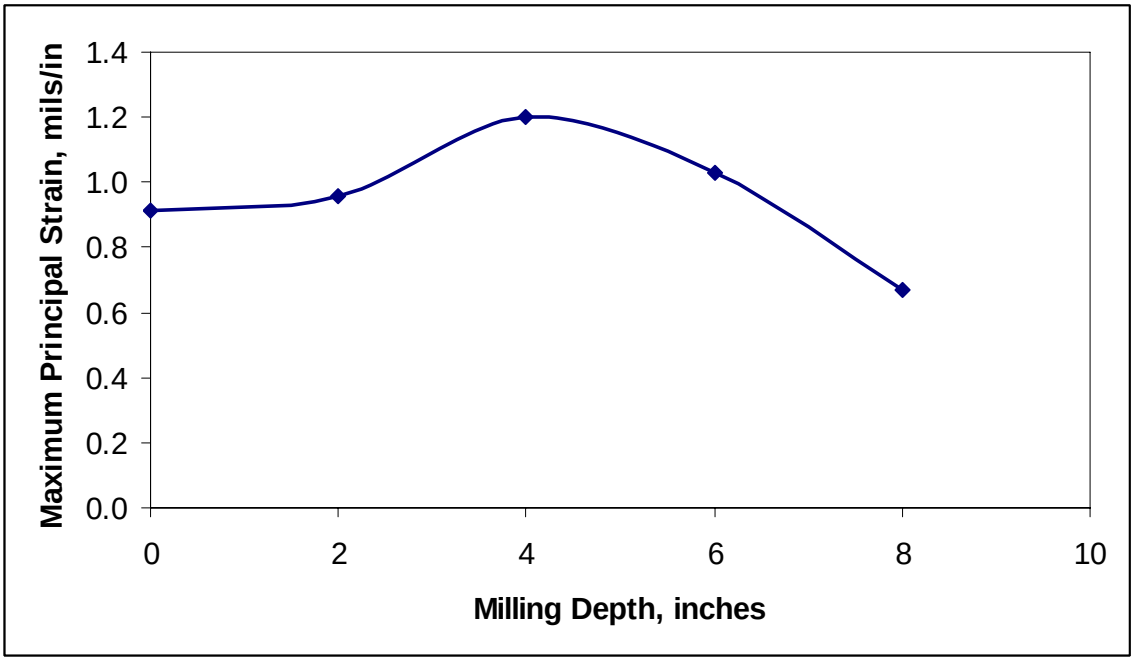

Figure 4-1. Maximum vertical HMA strain for different milling depths.

Figure 4-2 shows the distortion strain ratio expected for different milling depths. The distortion strain ratio is simply the ratio of the vertical compressive strain to the strain at failure and provides a quick check on the level of applied strain to the value that will result in excessive distortion. A distortion strain ratio criterion of 0.10, as shown in Figure 4-2, represents an acceptable value during construction or placement of the HMA overlay. The milling depth is selected to keep the distortion strain ratio less than 0.10. As a result, any milling should be restricted to less than 2 inches or greater than 7 inches for areas where seismic testing indicated lower than expected values.

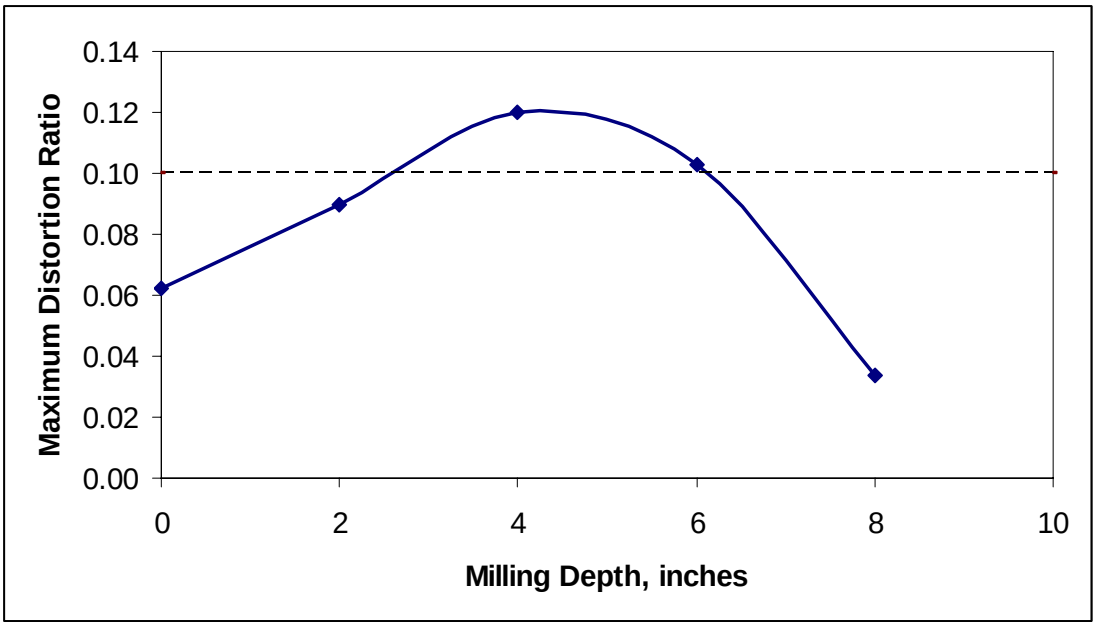

Figure 4-2. Distortion strain ratio for different milling depths.

Overall, information collected on the Downtown Connector suggests that a typical milling depth of 4 inches is adequate for the majority of the roadway. A milling depth of 8 inches is recommended for the northbound and southbound sections in which seismic tests indicate moduli with less than expected values or where rut depths were considerably greater. Areas of greater milling depth are illustrated in Figures 4-3 and 4-4 with annotated core locations. Following is a summary of the milling depth recommendations:

- Milling depth of 8 inches in northbound lane 2 from milepost 244 to Georgia Avenue Overpass (approximately 31,460 feet north of MP 238 to 40,400 feet north of MP 238).
- Milling depth of 8 inches in northbound lanes 1 through 7 from Williams Street Entrance (just north of US 78 Overpass) to the Brookwood Interchange (approximately 56,205 feet north of MP 238 to 63,000 feet north of MP 238).
- Milling depth of 8 inches in southbound lanes 2 through lane 7 from the University Avenue Overpass to Exit 243 (approximately 34,900 feet north of MP 238 to 27,780 feet north of MP 238).
- Milling depth of 8 inches in southbound lane 4 from MP 242 to Mount Zion Overpass (approximately 20,805 feet north of MP 238 to 16,200 feet north of MP 238).
- Milling depth of 8 inches in southbound Lanes 4 and 5 from Mount Zion Overpass to MP 240 (approximately 15,970 feet north of MP 238 to 10,520 feet north of MP 238).
- Milling depth of 8 inches in southbound lanes 1 through 7 from the Brookwood Interchange to Williams Street Exit (just south of US 78 Overpass) (approximately 63,140 feet north of MP 238 to 53,250 feet north of MP 238).
- Milling depth of 4 inches for the remaining Downtown Connector.

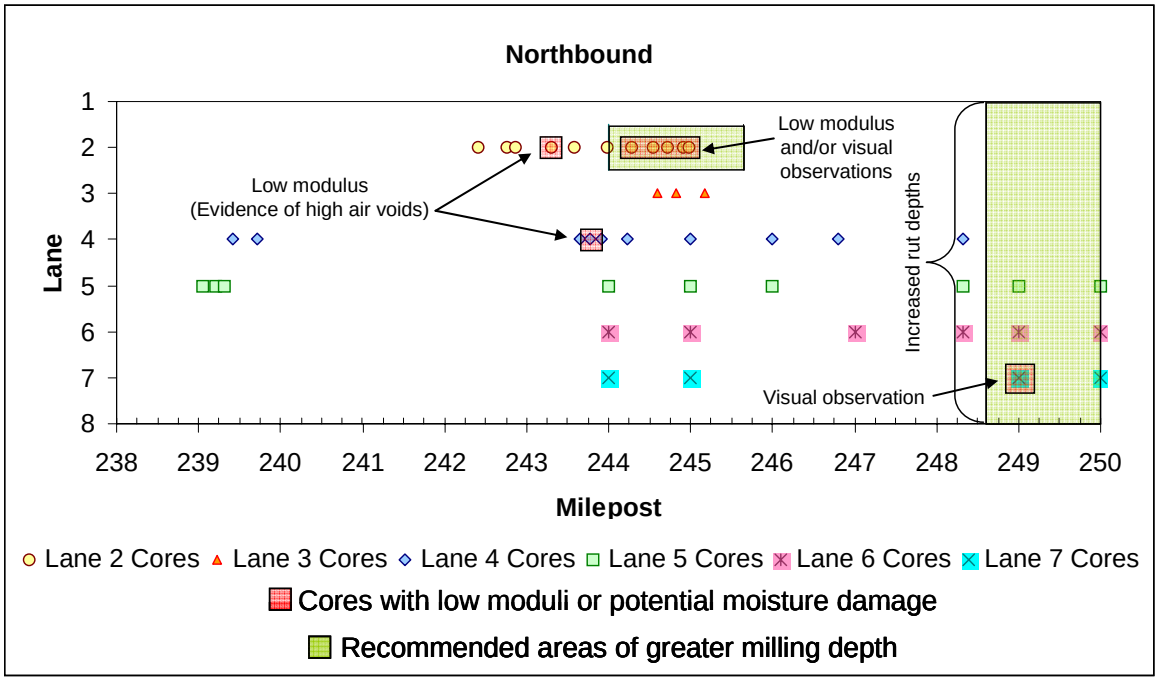

Figure 4-3. Northbound rehabilitation recommendation.

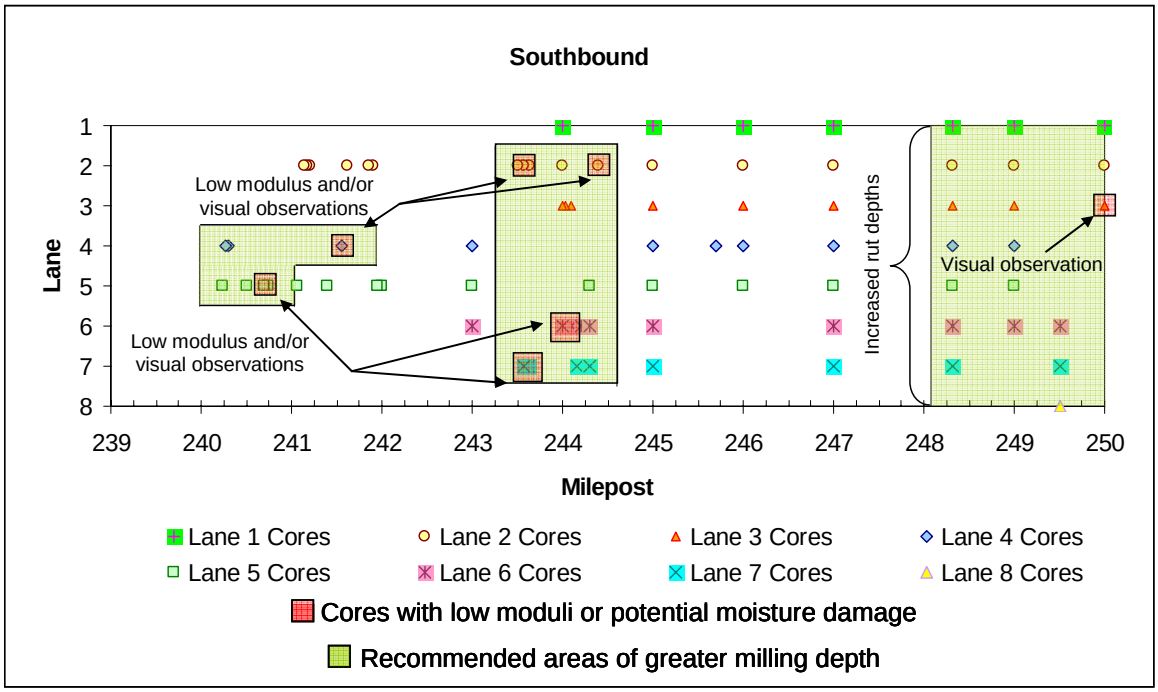

Figure 4-4. Southbound rehabilitation recommendation.

5 REFERENCES

Andrei, D., M.W. Witczak, and M.W. Mirza. 1999. “Development of a Revised Predictive Model for the Dynamic (Complex) Modulus of Asphalt Mixtures.” NCHRP 1-37A Inter Team Report, University of Maryland.

Witczak, M.W., and M.W. Mirza. 1995. “Development of a Global Aging System for Short and Long term Aging of Asphalt Cements,” *Journal of the Association of the Asphalt Paving Technologists*, Volume 64, St. Paul, Minnesota, pp. 393-430.

Aouad, M.F., K.H. Stokoe, and R.C. Briggs. 1993. "Stiffness of Asphalt Concrete Surface Layer from Stress Wave Measurements," *Transportation Research Record No. 1384*, Washington, DC, pp. 29-35.

Kandhal, P.S., and I.J. Rickards. April 2001. *Premature Failure of Asphalt Overlays from Stripping: Case Studies*, NCAT Report No. 01-01, National Center for Asphalt Technology, Auburn, AL.

Miller, J.S., and W.Y. Bellinger. June 2003. *Distress Identification Manual for the Long-Term Pavement Performance Program*. Report No. FHWA-RD-03-031, Federal Highway Administration, McLean, VA.

Georgia Department of Transportation. January 1990. *Road Surface Management Pavement Condition Evaluation System.*

Ferry, J.D. 1970. *Viscoelastic Properties of Polymers*. 2nd edition, John Willy, New York.

Li, Y., and S. Nazarian. 1994. “Evaluation of Aging of Hot-Mix Asphalt Using Wave Propagation Techniques,” *Engineering Properties of Asphalt Mixtures And the Relationship to Their Performance*, ASTM STP 1265, Philadelphia, pp.166-179.

National Cooperative Highway Research Program (NCHRP). 1996. “Nondestructive Testing to Determine Material Properties of Pavement Layers,” Interim Report, NCHRP 10-44, Washington, DC.

Nazarian, S., and M.R. Desai. 1993. “Automated Surface Wave Method: Field Testing,” *Journal of Geotechnical Engineering*, Volume: 119 Issue: 7, ASCE, New York, pp 1094-11.

Nazarian, S., M. Baker, and K. Crain. 1997. "Assessing Quality of Concrete with Wave Propagation Techniques," *Materials Journal*, American Concrete Institute, Farmington Hills, MI, Vol. 94, No. 4, pp. 296-306.

Sansalone, M., and N. J Carino. 1986. “Impact-Echo: A Method for Flaw Detection in Concrete Using Transient Stress Waves,” Report NBSIR 86-3452. National Bureau of Standards, Gaithersburg, MD.

Scullion, T., and E.H. Rmeili. October 1997. *Detecting Stripping in Asphalt Concrete Layers Using Ground-Penetrating Radar*, Research Report 2964-S. Texas Transportation Institute, College Station, TX.

Tandon, T., S. Nazarian, and X. Bai. 2004. "Assessment of Relationship between Seismic and Dynamic Modulus of Hot Mix Asphalt Concrete," *International Journal of Road Materials and Pavement Design*.

APPENDIX A. LOCAL UNIFORMITY INDEX PROFILES

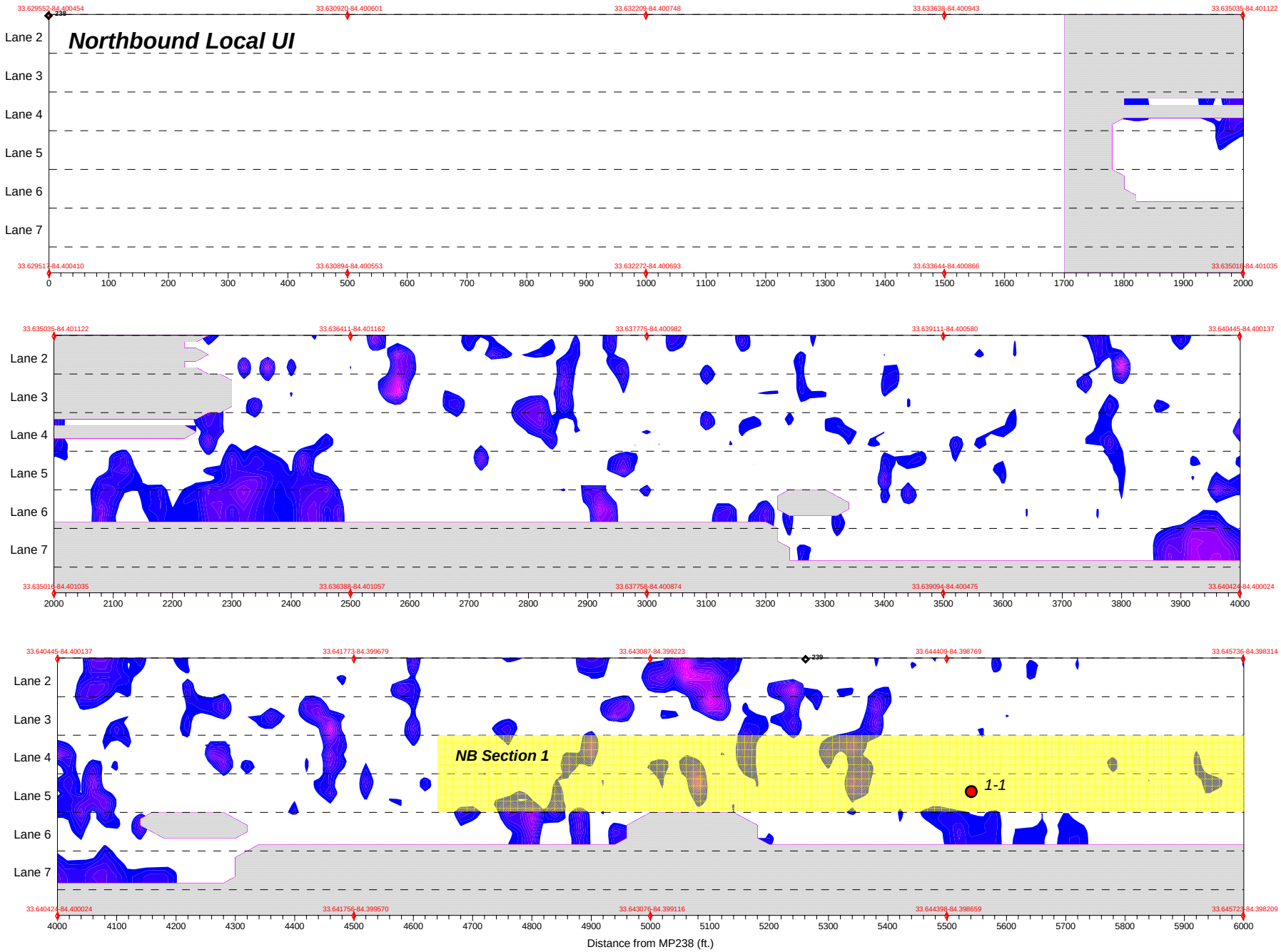
Northbound Local UI
Lane 2
Lane 3
Lane 4
Lane 5
Lane 6
Lane 7
NB Section 1
1-1
Distance from MP238 (ft.)

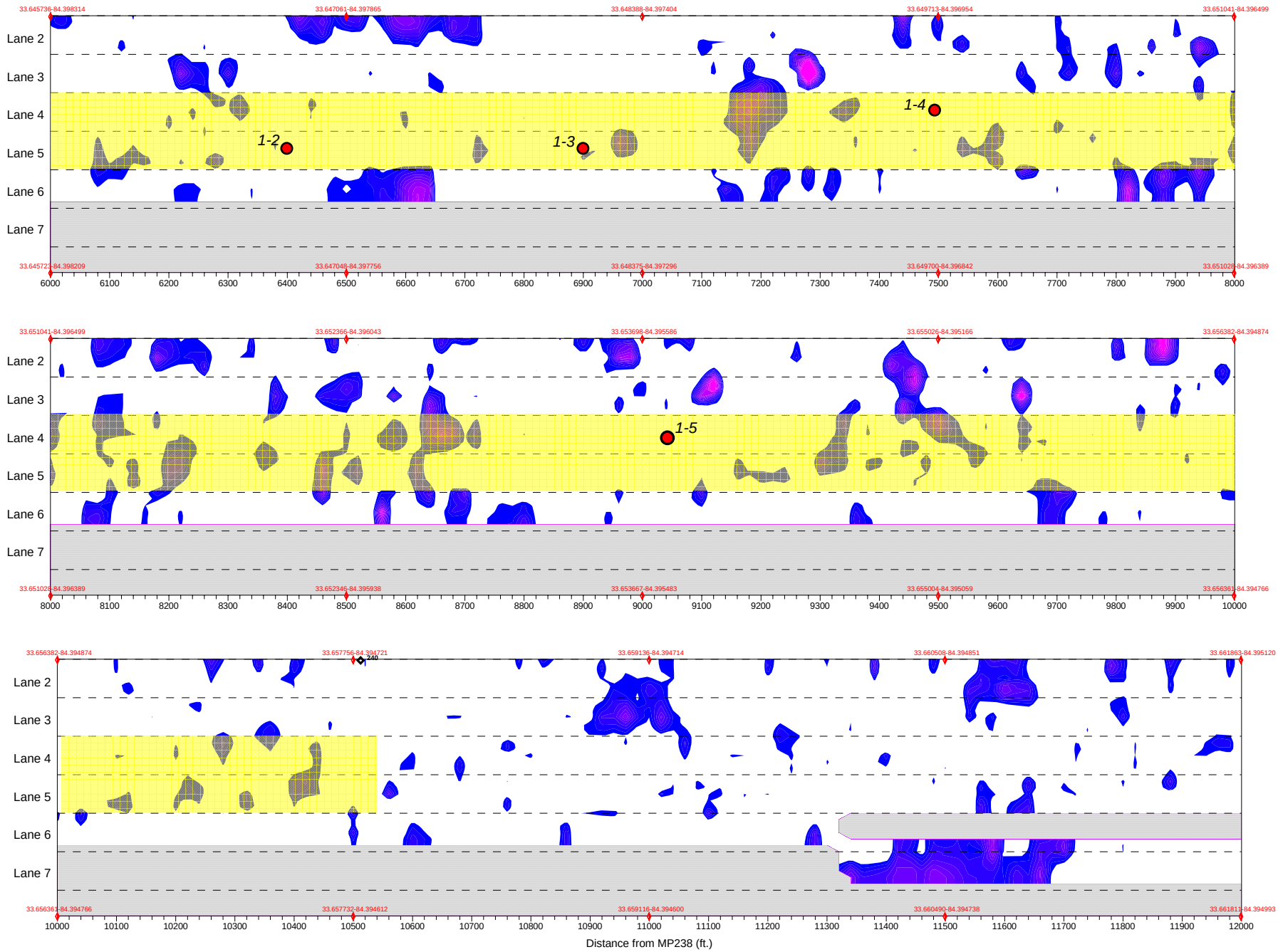
33.645736-84.398314
33.647061-84.397865
33.648388-84.397404
33.649713-84.396954
33.651041-84.396499
Lane 2
Lane 3
Lane 4
Lane 5
Lane 6
Lane 7
1-2
1-3
1-4
33.645723-84.398209
33.647048-84.397756
33.648375-84.397296
33.649700-84.396842
33.651028-84.396389
6000 6100 6200 6300 6400 6500 6600 6700 6800 6900 7000 7100 7200 7300 7400 7500 7600 7700 7800 7900 8000
33.651041-84.396499
33.652366-84.396043
33.653698-84.395586
33.655026-84.395166
33.656382-84.394874
1-5
33.651028-84.396389
33.652346-84.395938
33.653667-84.395483
33.655004-84.395059
33.656361-84.394766
8000 8100 8200 8300 8400 8500 8600 8700 8800 8900 9000 9100 9200 9300 9400 9500 9600 9700 9800 9900 10000
33.656382-84.394874
33.657756-84.394721
240
33.659136-84.394714
33.660508-84.394851
33.661863-84.395120
33.656361-84.394766
33.657732-84.394612
33.659116-84.394600
33.660490-84.394738
33.661811-84.394993
10000 10100 10200 10300 10400 10500 10600 10700 10800 10900 11000 11100 11200 11300 11400 11500 11600 11700 11800 11900 12000
Distance from MP238 (ft.)

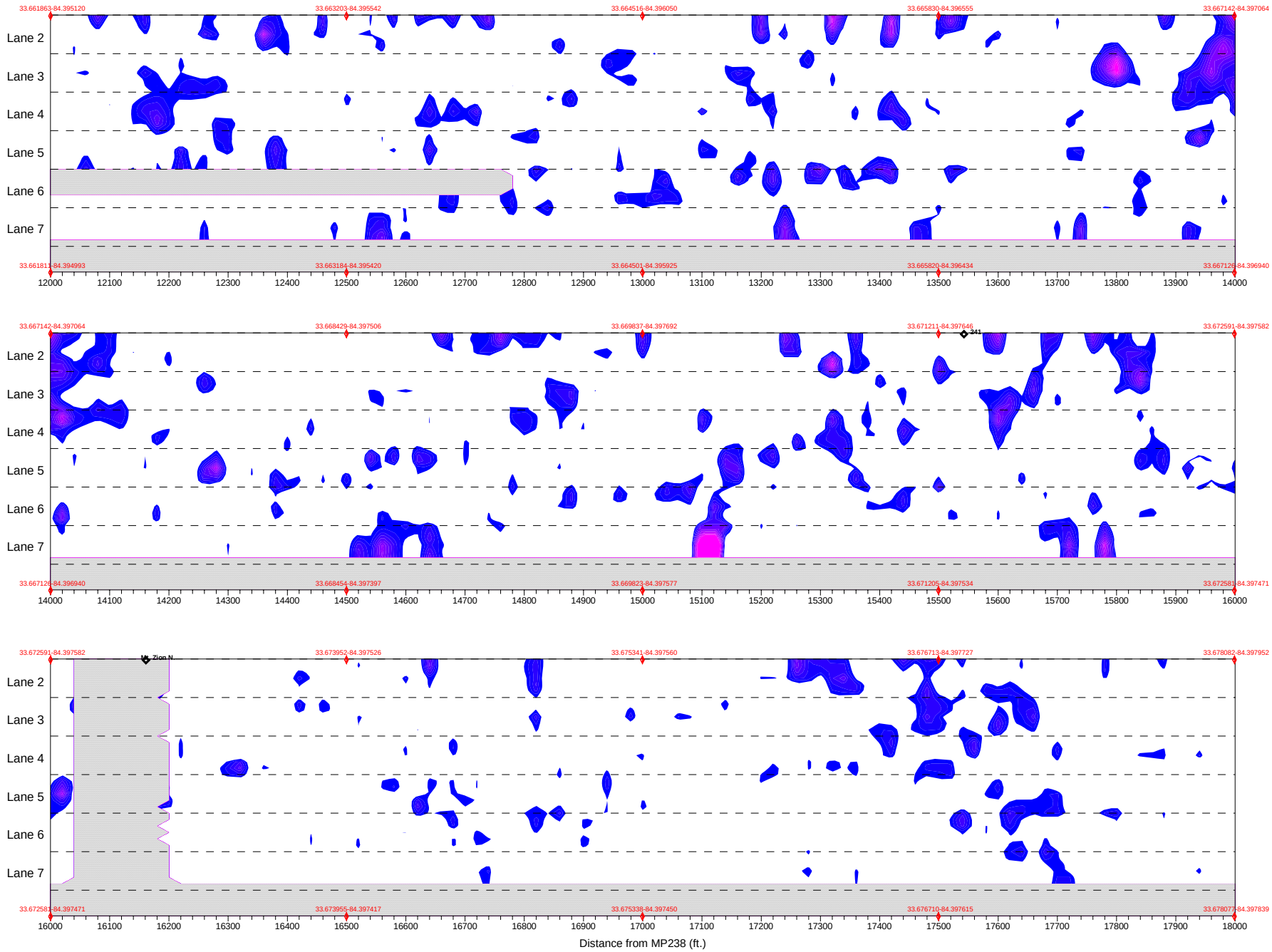
33.661863-84.395120
33.663203-84.395542
33.664516-84.396050
33.665830-84.396555
33.667142-84.397064
Lane 2
Lane 3
Lane 4
Lane 5
Lane 6
Lane 7
33.661811-84.394993
33.663184-84.395420
33.664501-84.395925
33.665820-84.396434
33.667126-84.396940
12000 12100 12200 12300 12400 12500 12600 12700 12800 12900 13000 13100 13200 13300 13400 13500 13600 13700 13800 13900 14000
33.667142-84.397064
33.668429-84.397506
33.669837-84.397692
33.671211-84.397646
241
33.672591-84.397582
33.667126-84.396940
33.668454-84.397397
33.669823-84.397577
33.671205-84.397534
33.672581-84.397471
14000 14100 14200 14300 14400 14500 14600 14700 14800 14900 15000 15100 15200 15300 15400 15500 15600 15700 15800 15900 16000
33.672591-84.397582
Mt. Zion N
33.673952-84.397526
33.675341-84.397560
33.676713-84.397727
33.678082-84.397952
33.672581-84.397471
33.673955-84.397417
33.675338-84.397450
33.676710-84.397615
33.678077-84.397839
16000 16100 16200 16300 16400 16500 16600 16700 16800 16900 17000 17100 17200 17300 17400 17500 17600 17700 17800 17900 18000
Distance from MP238 (ft.)

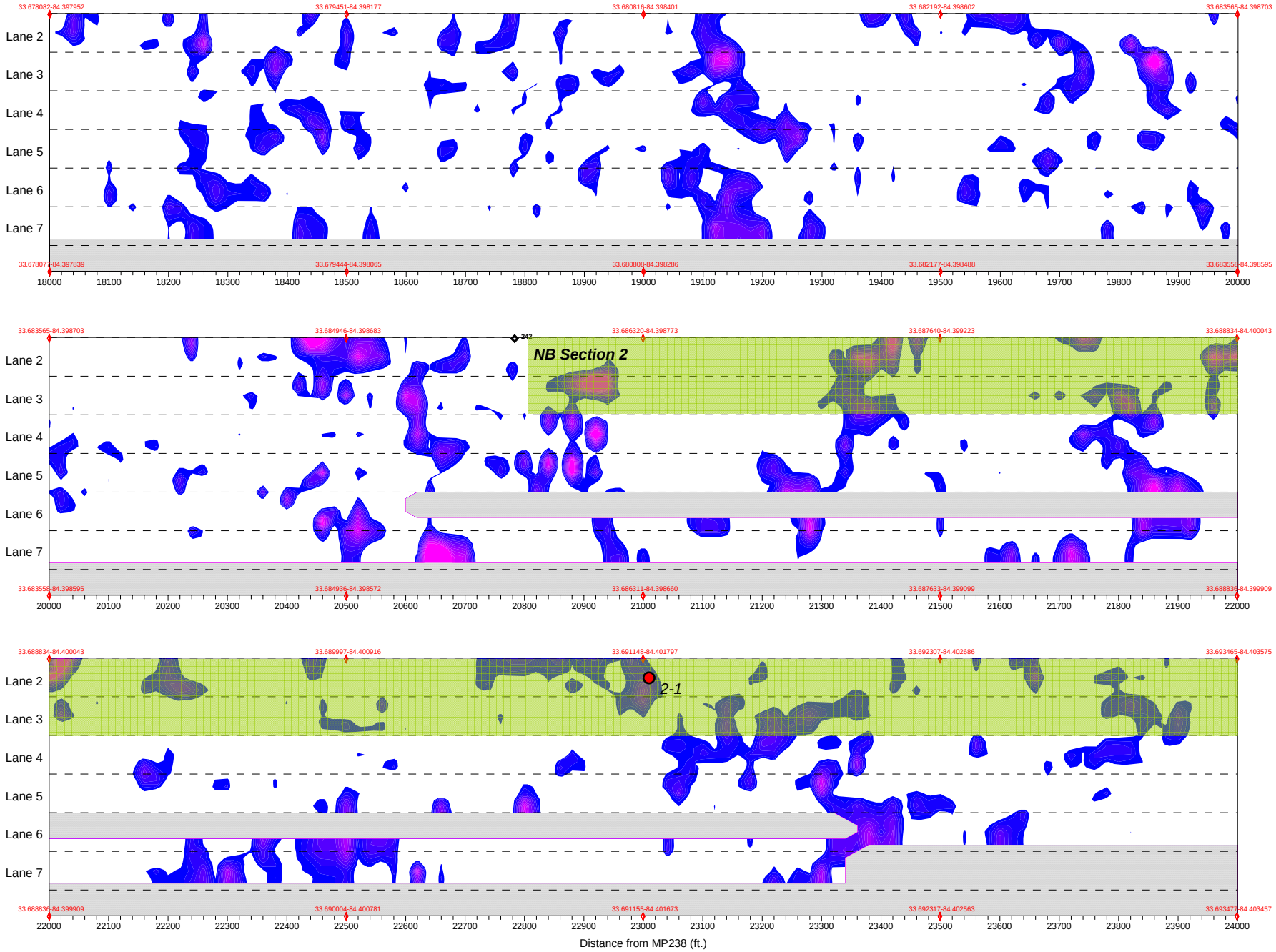
33.678082-84.397952
33.679451-84.398177
33.680816-84.398401
33.682192-84.398602
33.683565-84.398703
Lane 2
Lane 3
Lane 4
Lane 5
Lane 6
Lane 7
33.678077-84.397839
33.679444-84.398065
33.680808-84.398286
33.682177-84.398488
33.683558-84.398595
18000 18100 18200 18300 18400 18500 18600 18700 18800 18900 19000 19100 19200 19300 19400 19500 19600 19700 19800 19900 20000
33.683565-84.398703
33.684946-84.398683
33.686320-84.398773
33.687640-84.399223
33.688834-84.400043
NB Section 2
33.683558-84.398595
33.684936-84.398572
33.686311-84.398660
33.687633-84.399099
33.688836-84.399909
20000 20100 20200 20300 20400 20500 20600 20700 20800 20900 21000 21100 21200 21300 21400 21500 21600 21700 21800 21900 22000
33.688834-84.400043
33.689997-84.400916
33.691148-84.401797
33.692307-84.402686
33.693465-84.403575
2-1
33.688836-84.399909
33.690004-84.400781
33.691155-84.401673
33.692317-84.402563
33.693477-84.403457
22000 22100 22200 22300 22400 22500 22600 22700 22800 22900 23000 23100 23200 23300 23400 23500 23600 23700 23800 23900 24000
Distance from MP238 (ft.)

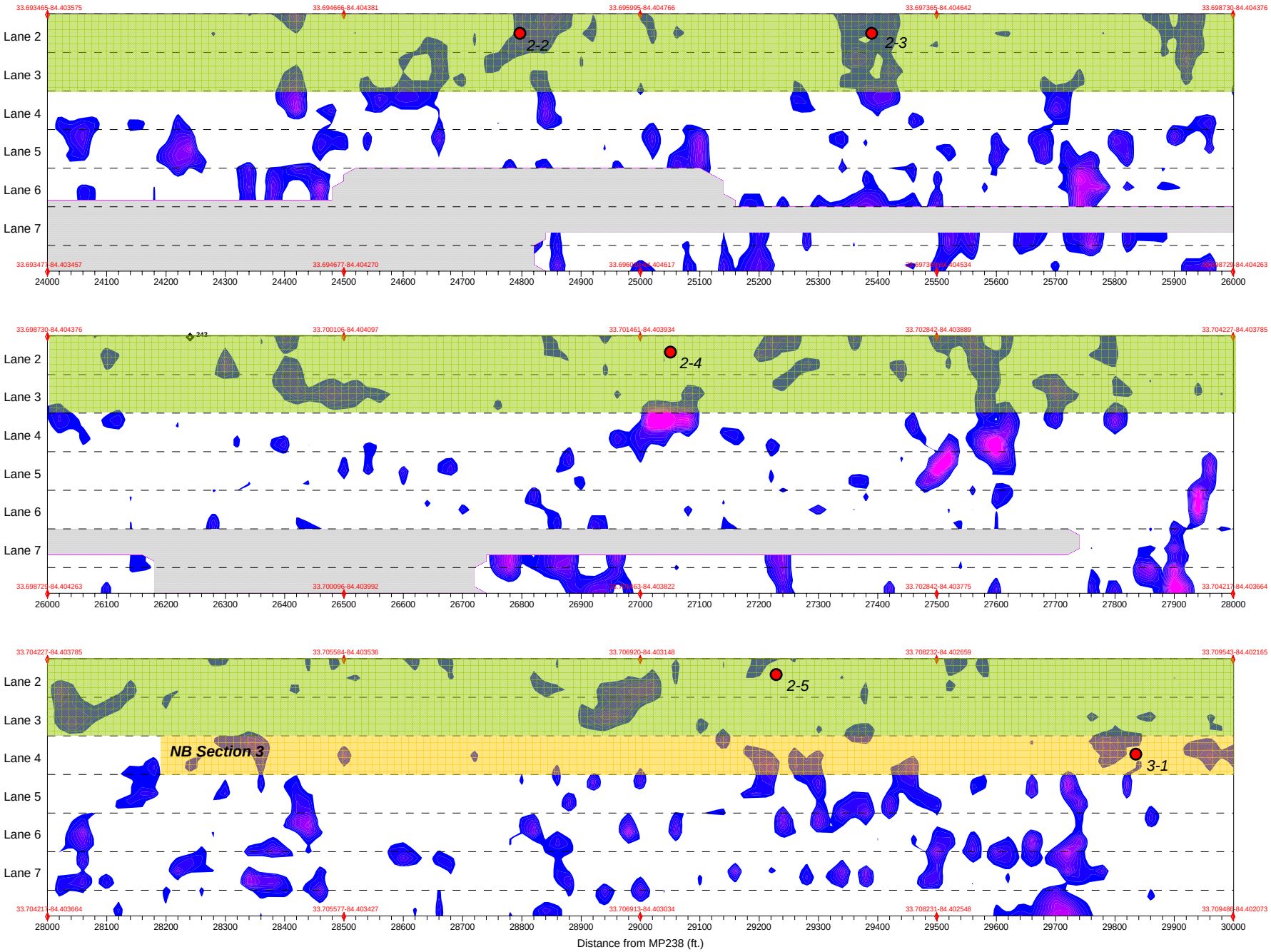
Lane 2
Lane 3
Lane 4
Lane 5
Lane 6
Lane 7
2-2
2-3
2-4
2-5
3-1
NB Section 3
Distance from MP238 (ft.)

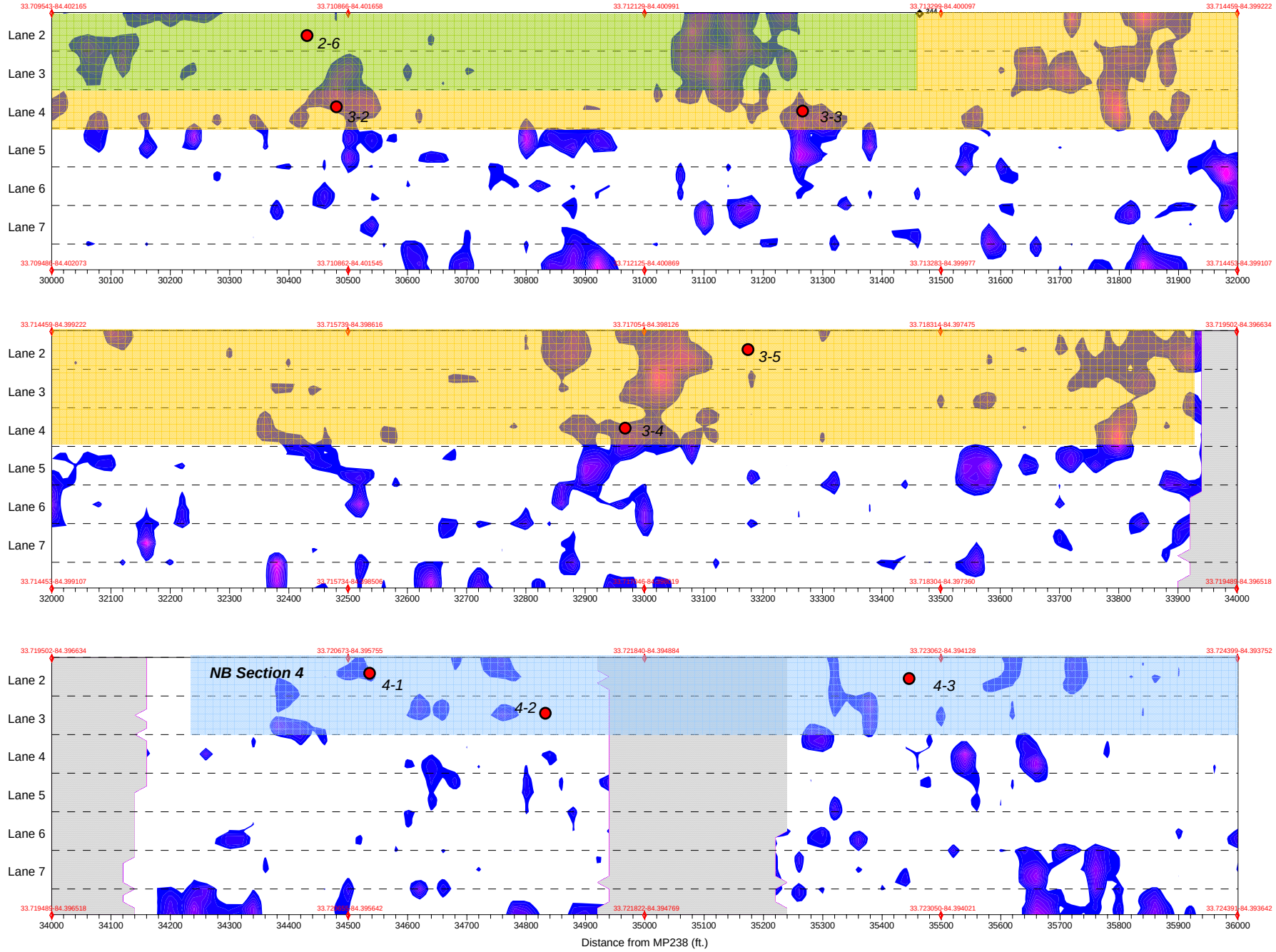
Lane 2
Lane 3
Lane 4
Lane 5
Lane 6
Lane 7
2-6
3-2
3-3
3-5
3-4
NB Section 4
4-1
4-2
4-3
Distance from MP238 (ft.)

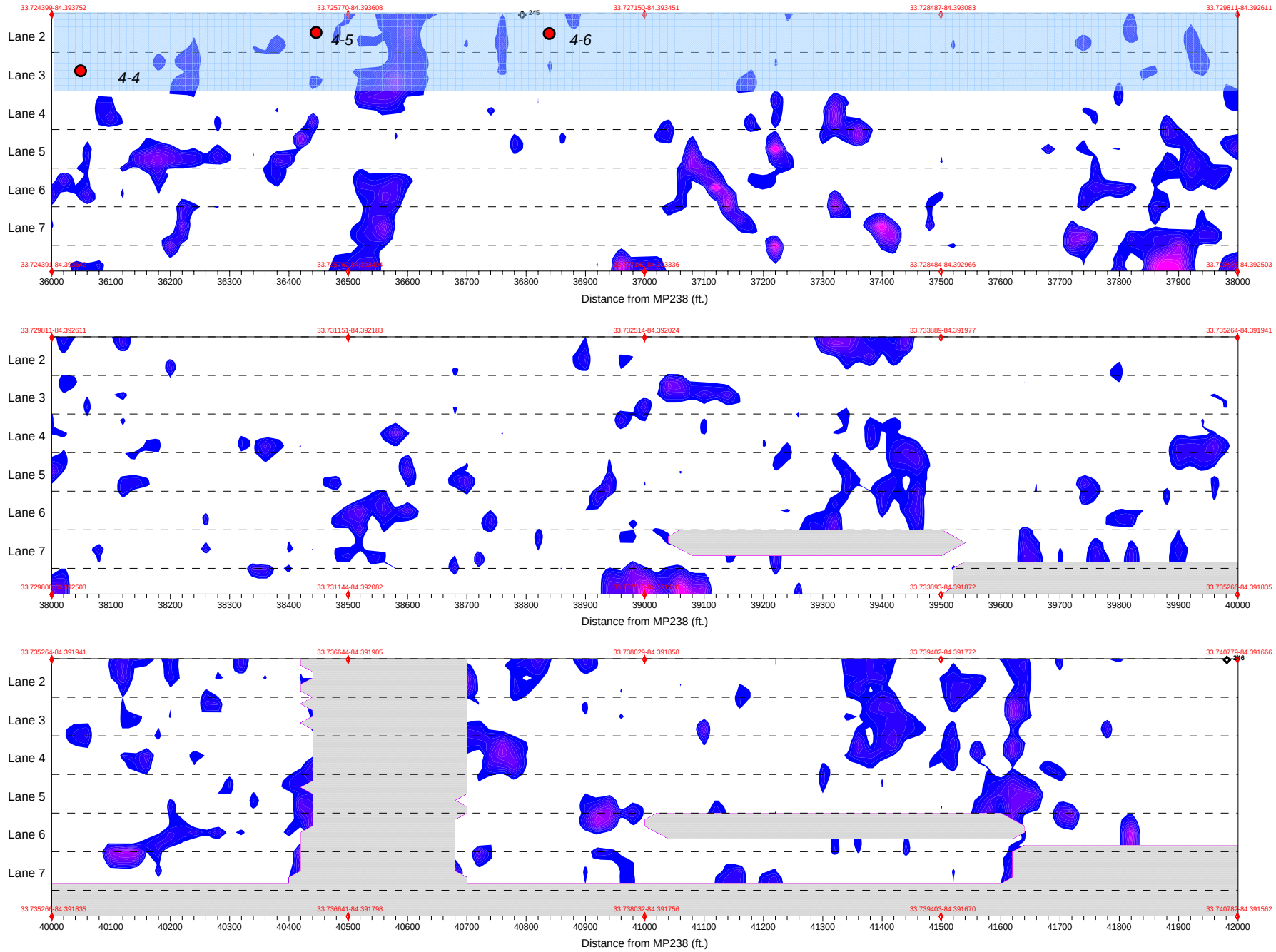
Lane 2
Lane 3
Lane 4
Lane 5
Lane 6
Lane 7
4-4
4-5
4-6
Distance from MP238 (ft.)
Distance from MP238 (ft.)
Distance from MP238 (ft.)

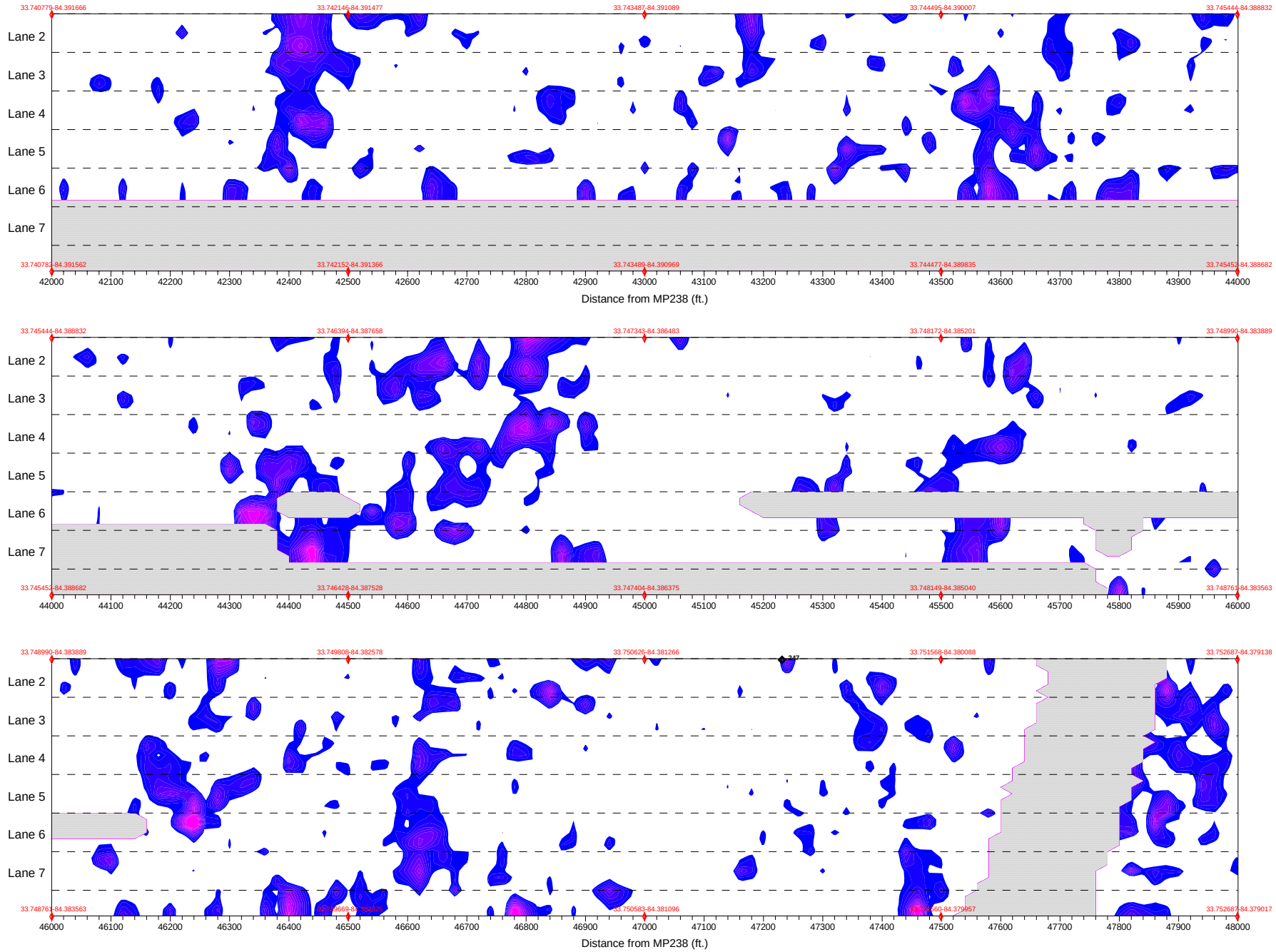
33.740779-84.391666
33.742146-84.391477
33.743487-84.391089
33.744495-84.390007
33.745444-84.388832
Lane 2
Lane 3
Lane 4
Lane 5
Lane 6
Lane 7
33.740782-84.391562
33.742152-84.391366
33.743488-84.390969
33.744477-84.389835
33.745452-84.388682
42000 42100 42200 42300 42400 42500 42600 42700 42800 42900 43000 43100 43200 43300 43400 43500 43600 43700 43800 43900 44000
Distance from MP238 (ft.)
33.745444-84.388832
33.746394-84.387658
33.747343-84.386483
33.748172-84.385201
33.748990-84.383889
Lane 2
Lane 3
Lane 4
Lane 5
Lane 6
Lane 7
33.745452-84.388682
33.746428-84.387528
33.747404-84.386375
33.748149-84.385040
33.748761-84.383563
44000 44100 44200 44300 44400 44500 44600 44700 44800 44900 45000 45100 45200 45300 45400 45500 45600 45700 45800 45900 46000
33.748990-84.383889
33.749808-84.382578
33.750626-84.381266
247
33.751568-84.380088
33.752687-84.379138
Lane 2
Lane 3
Lane 4
Lane 5
Lane 6
Lane 7
33.748761-84.383563
33.750583-84.381096
33.752687-84.379017
46000 46100 46200 46300 46400 46500 46600 46700 46800 46900 47000 47100 47200 47300 47400 47500 47600 47700 47800 47900 48000
Distance from MP238 (ft.)

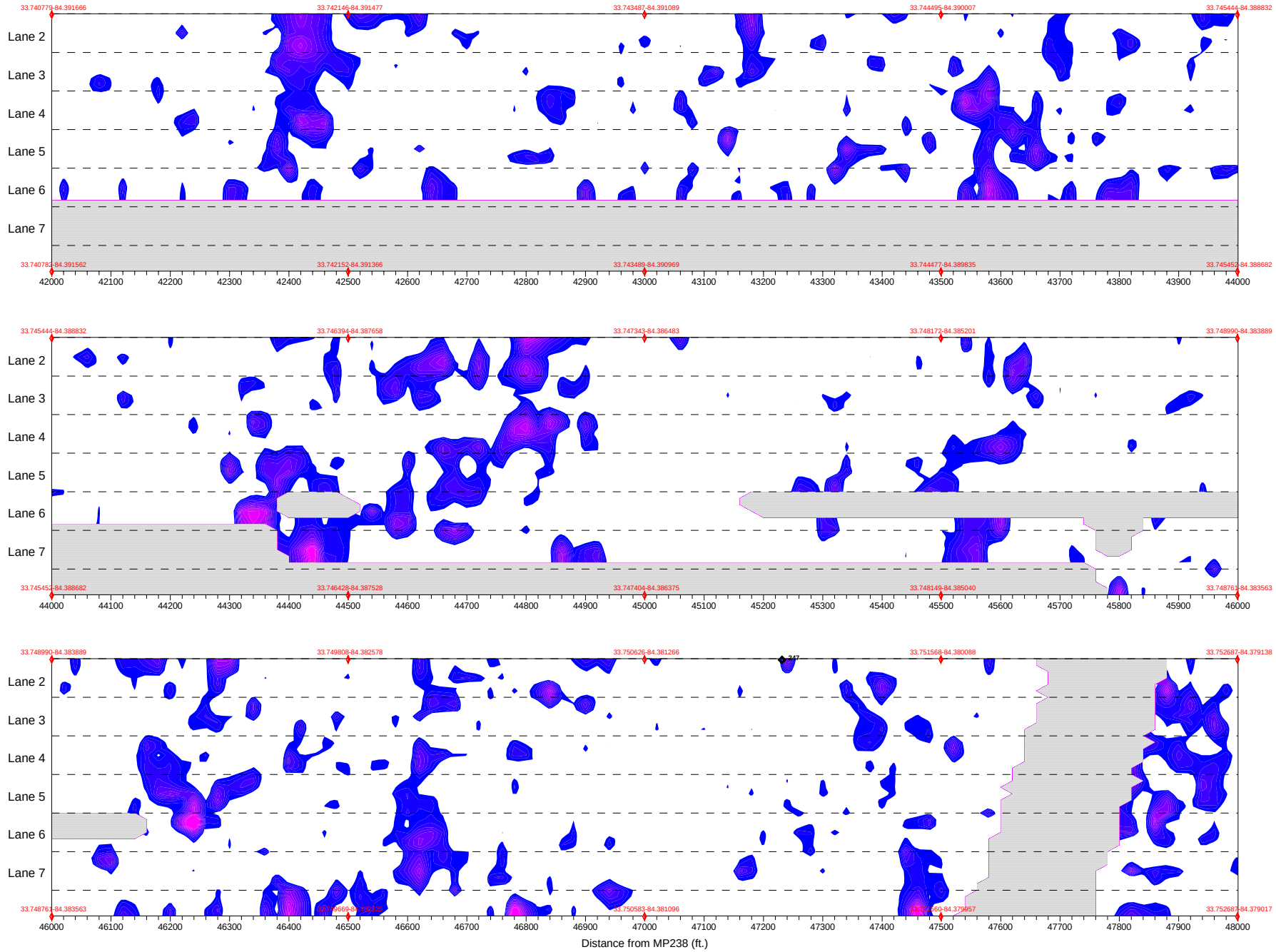
33.740779-84.391666
33.742146-84.391477
33.743487-84.391089
33.744495-84.390007
33.745444-84.388832
Lane 2
Lane 3
Lane 4
Lane 5
Lane 6
Lane 7
33.740782-84.391562
33.742152-84.391366
33.743489-84.390969
33.744477-84.389835
33.745452-84.388682
42000 42100 42200 42300 42400 42500 42600 42700 42800 42900 43000 43100 43200 43300 43400 43500 43600 43700 43800 43900 44000
33.745444-84.388832
33.746394-84.387658
33.747343-84.386483
33.748172-84.385201
33.748990-84.383889
Lane 2
Lane 3
Lane 4
Lane 5
Lane 6
Lane 7
33.745452-84.388682
33.746428-84.387528
33.747404-84.386375
33.748149-84.385040
33.748761-84.383563
44000 44100 44200 44300 44400 44500 44600 44700 44800 44900 45000 45100 45200 45300 45400 45500 45600 45700 45800 45900 46000
33.748990-84.383889
33.749808-84.382578
33.750626-84.381266
247
33.751568-84.380088
33.752687-84.379138
Lane 2
Lane 3
Lane 4
Lane 5
Lane 6
Lane 7
33.748761-84.383563
33.750583-84.381096
33.752687-84.379017
46000 46100 46200 46300 46400 46500 46600 46700 46800 46900 47000 47100 47200 47300 47400 47500 47600 47700 47800 47900 48000
Distance from MP238 (ft.)

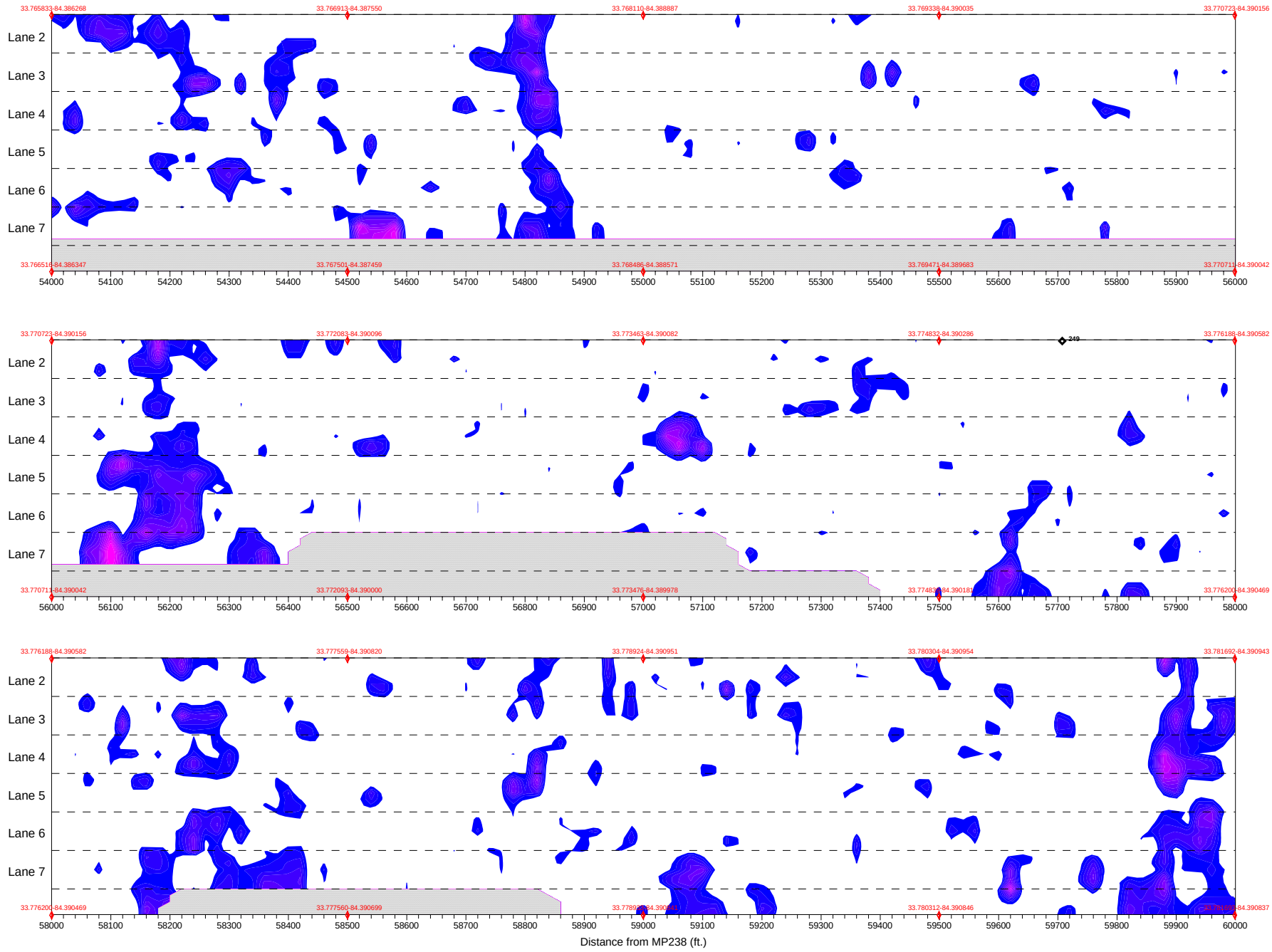
33.765833-84.386268
33.766913-84.387550
33.768110-84.388887
33.769338-84.390035
33.770723-84.390156
Lane 2
Lane 3
Lane 4
Lane 5
Lane 6
Lane 7
33.766516-84.386347
33.767501-84.387459
33.768486-84.388571
33.769471-84.389683
33.770711-84.390042
54000 54100 54200 54300 54400 54500 54600 54700 54800 54900 55000 55100 55200 55300 55400 55500 55600 55700 55800 55900 56000
33.770723-84.390156
33.772093-84.390096
33.773463-84.390082
33.774832-84.390286
249
33.776188-84.390582
33.770711-84.390042
33.772093-84.390000
33.773476-84.389978
33.774839-84.390181
33.776200-84.390469
56000 56100 56200 56300 56400 56500 56600 56700 56800 56900 57000 57100 57200 57300 57400 57500 57600 57700 57800 57900 58000
33.776188-84.390582
33.777559-84.390820
33.778924-84.390951
33.780304-84.390954
33.781692-84.390943
33.776200-84.390469
33.777560-84.390699
33.780312-84.390846
58000 58100 58200 58300 58400 58500 58600 58700 58800 58900 59000 59100 59200 59300 59400 59500 59600 59700 59800 59900 60000
Distance from MP238 (ft.)

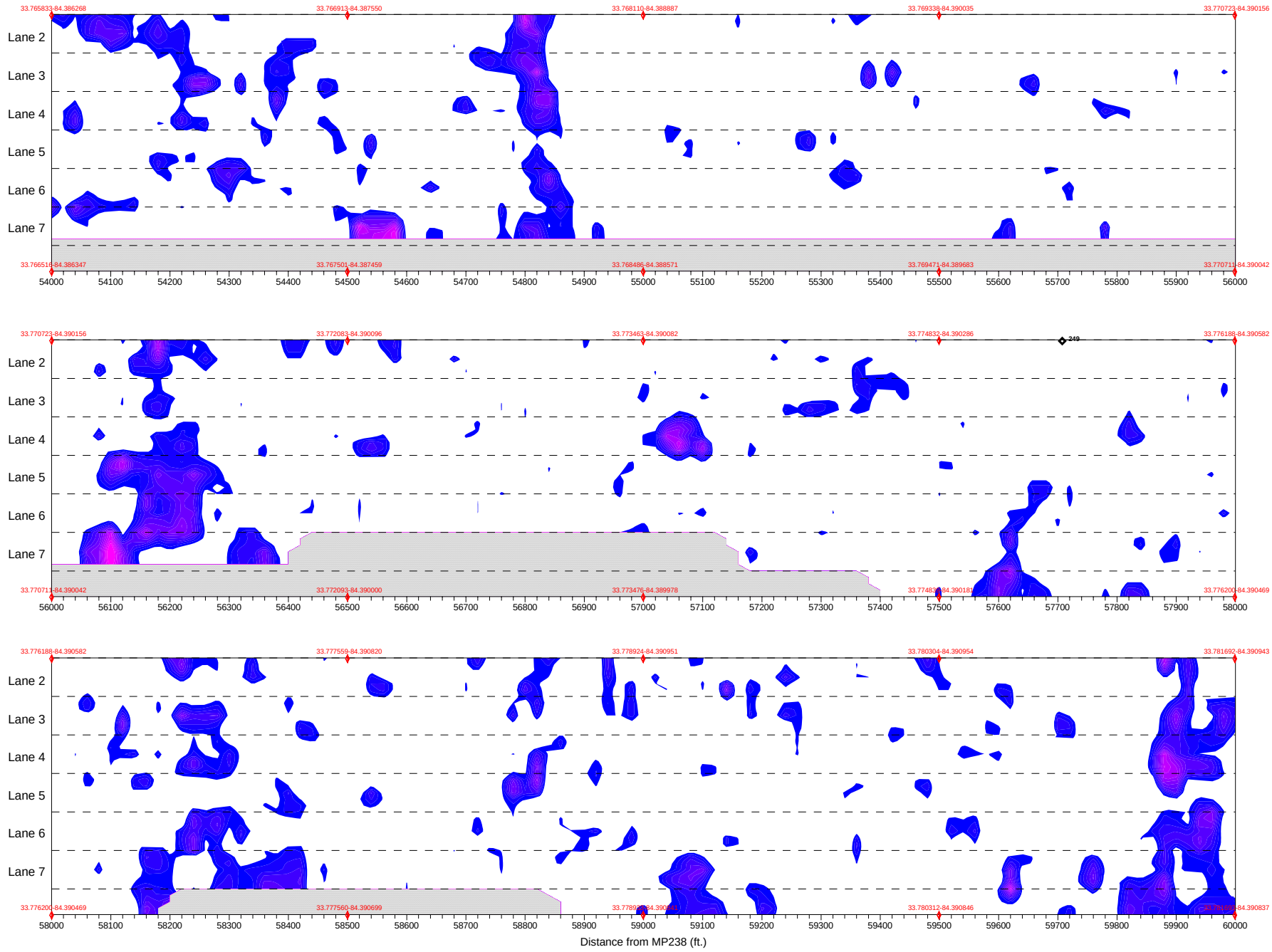
33.765833-84.386268
33.766913-84.387550
33.768110-84.388887
33.769338-84.390035
33.770723-84.390156
Lane 2
Lane 3
Lane 4
Lane 5
Lane 6
Lane 7
33.766516-84.386347
33.767501-84.387459
33.768486-84.388571
33.769471-84.389683
33.770711-84.390042
54000 54100 54200 54300 54400 54500 54600 54700 54800 54900 55000 55100 55200 55300 55400 55500 55600 55700 55800 55900 56000
33.770723-84.390156
33.772093-84.390096
33.773463-84.390082
33.774832-84.390286
249
33.776188-84.390582
33.770711-84.390042
33.772093-84.390000
33.773476-84.389978
33.776200-84.390469
56000 56100 56200 56300 56400 56500 56600 56700 56800 56900 57000 57100 57200 57300 57400 57500 57600 57700 57800 57900 58000
33.776188-84.390582
33.777559-84.390820
33.778924-84.390951
33.780304-84.390954
33.781692-84.390943
33.776200-84.390469
33.777560-84.390699
33.780312-84.390846
58000 58100 58200 58300 58400 58500 58600 58700 58800 58900 59000 59100 59200 59300 59400 59500 59600 59700 59800 59900 60000
Distance from MP238 (ft.)

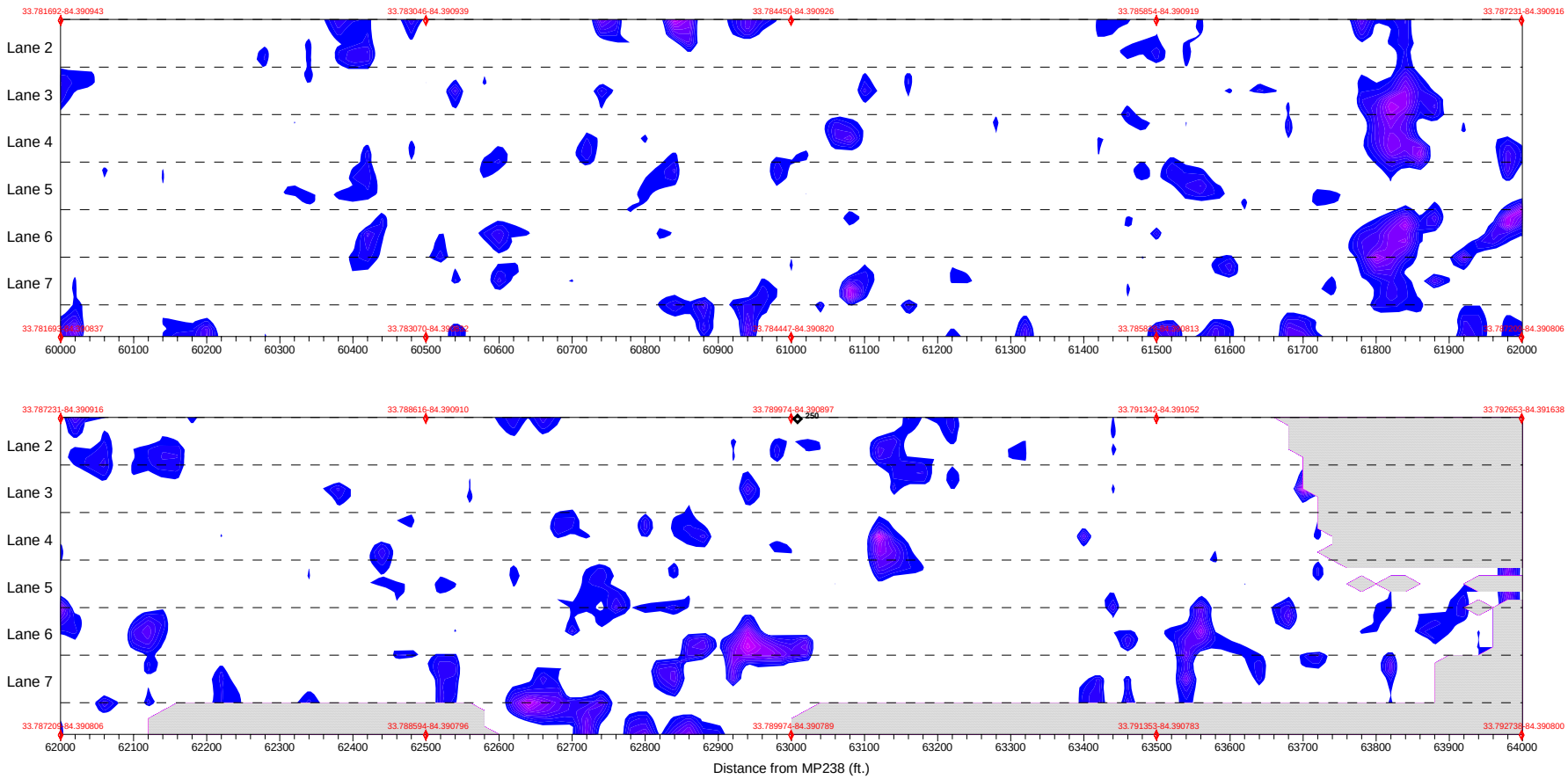
33.781692-84.390943
33.783046-84.390939
33.784450-84.390926
33.785854-84.390919
33.787231-84.390916
Lane 2
Lane 3
Lane 4
Lane 5
Lane 6
Lane 7
60000
60100
60200
60300
60400
60500
60600
60700
60800
60900
61000
61100
61200
61300
61400
61500
61600
61700
61800
61900
62000
33.787231-84.390916
33.788616-84.390910
33.789974-84.390897
250
33.791342-84.391052
33.792653-84.391638
33.789974-84.390789
33.791353-84.390783
62000
62100
62200
62300
62400
62500
62600
62700
62800
62900
63000
63100
63200
63300
63400
63500
63600
63700
63800
63900
64000
Distance from MP238 (ft.)

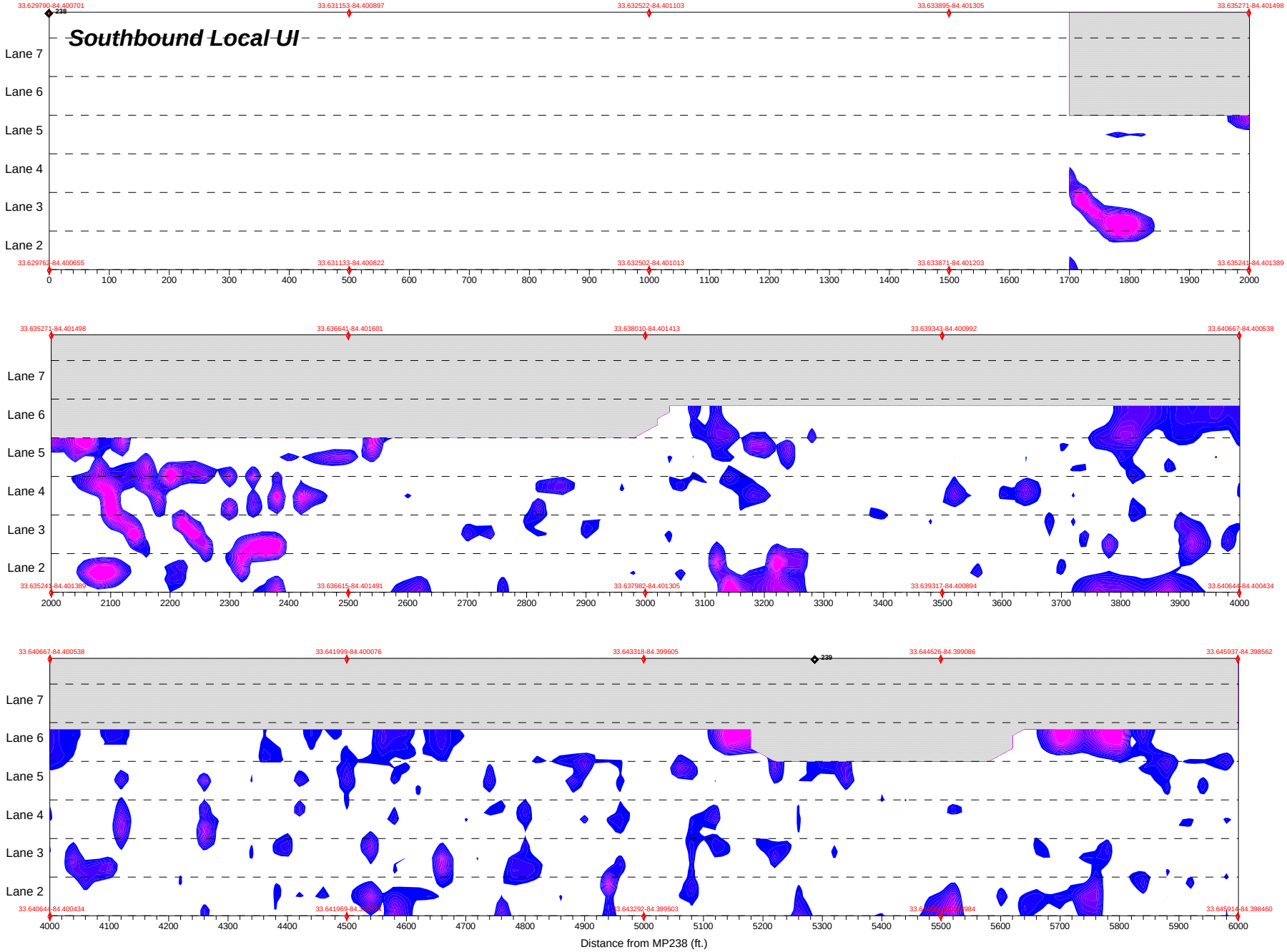
Southbound Local UI
Lane 7
Lane 6
Lane 5
Lane 4
Lane 3
Lane 2
33.629790-84.400701
238
33.631153-84.400897
33.632522-84.401103
33.633895-84.401305
33.635271-84.401498
33.629762-84.400655
33.631133-84.400822
33.632502-84.401013
33.633871-84.401203
33.635243-84.401389
0 100 200 300 400 500 600 700 800 900 1000 1100 1200 1300 1400 1500 1600 1700 1800 1900 2000
33.635271-84.401498
33.636641-84.401601
33.638010-84.401413
33.639343-84.400992
33.640667-84.400538
33.635243-84.401389
33.636615-84.401491
33.637982-84.401305
33.639317-84.400894
33.640644-84.400434
2000 2100 2200 2300 2400 2500 2600 2700 2800 2900 3000 3100 3200 3300 3400 3500 3600 3700 3800 3900 4000
33.640667-84.400538
33.641999-84.400076
33.643318-84.399605
239
33.644626-84.399086
33.645937-84.398562
33.640644-84.400434
33.641969-84.399
33.643292-84.399503
33.645914-84.398460
4000 4100 4200 4300 4400 4500 4600 4700 4800 4900 5000 5100 5200 5300 5400 5500 5600 5700 5800 5900 6000
Distance from MP238 (ft.)

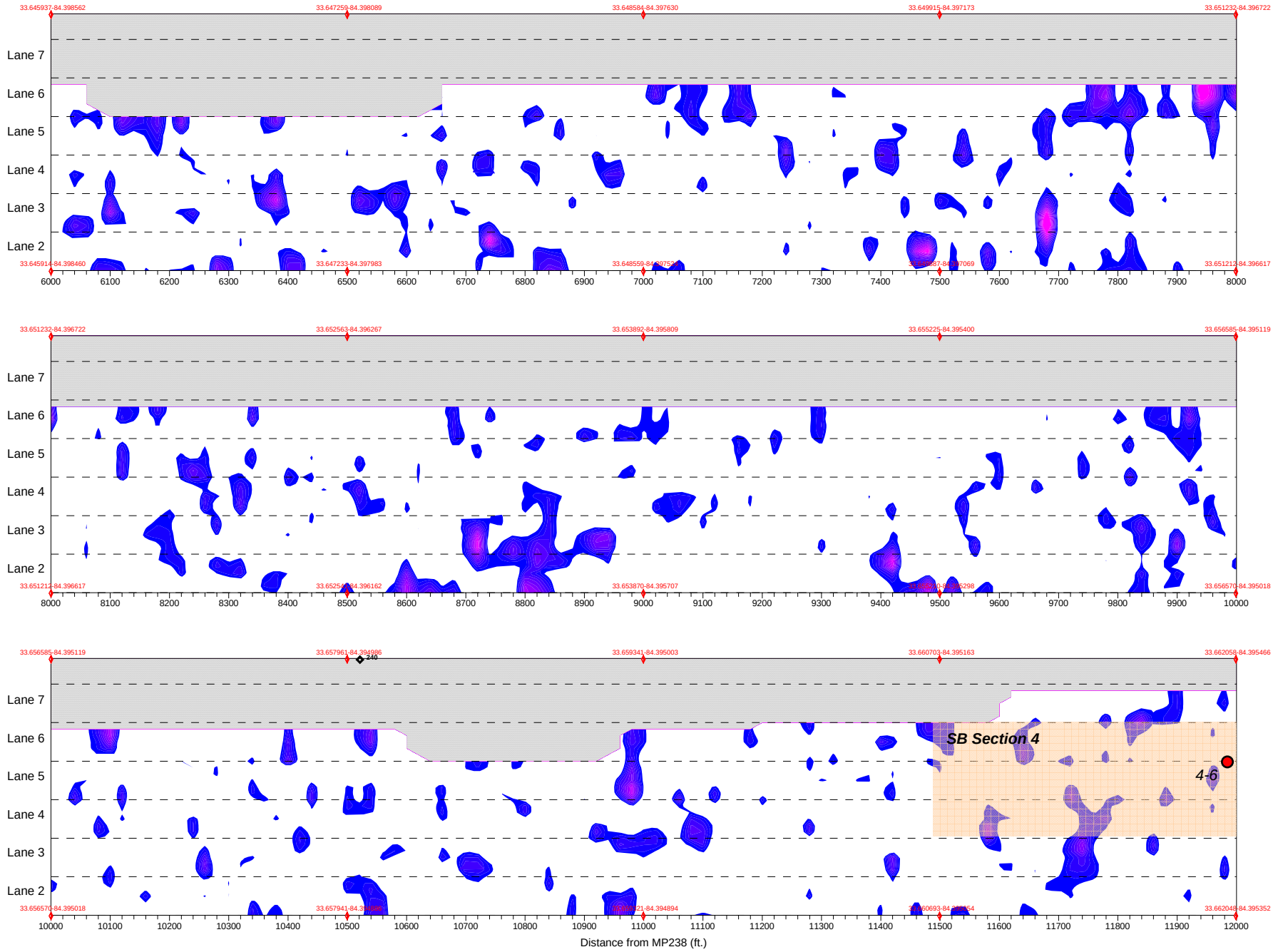
33.645937-84.398562
33.647259-84.398089
33.648584-84.397630
33.649915-84.397173
33.651232-84.396722
Lane 7
Lane 6
Lane 5
Lane 4
Lane 3
Lane 2
33.645914-84.398460
33.647233-84.397983
33.651212-84.396617
6000 6100 6200 6300 6400 6500 6600 6700 6800 6900 7000 7100 7200 7300 7400 7500 7600 7700 7800 7900 8000
33.651232-84.396722
33.652563-84.396267
33.653892-84.395809
33.655225-84.395400
33.656585-84.395119
33.651212-84.396617
33.653870-84.395707
33.656570-84.395018
8000 8100 8200 8300 8400 8500 8600 8700 8800 8900 9000 9100 9200 9300 9400 9500 9600 9700 9800 9900 10000
33.656585-84.395119
33.657961-84.394986
240
33.659341-84.395003
33.660703-84.395163
33.662058-84.395466
SB Section 4
4-6
33.656570-84.395018
33.659321-84.394894
33.662048-84.395352
10000 10100 10200 10300 10400 10500 10600 10700 10800 10900 11000 11100 11200 11300 11400 11500 11600 11700 11800 11900 12000
Distance from MP238 (ft.)

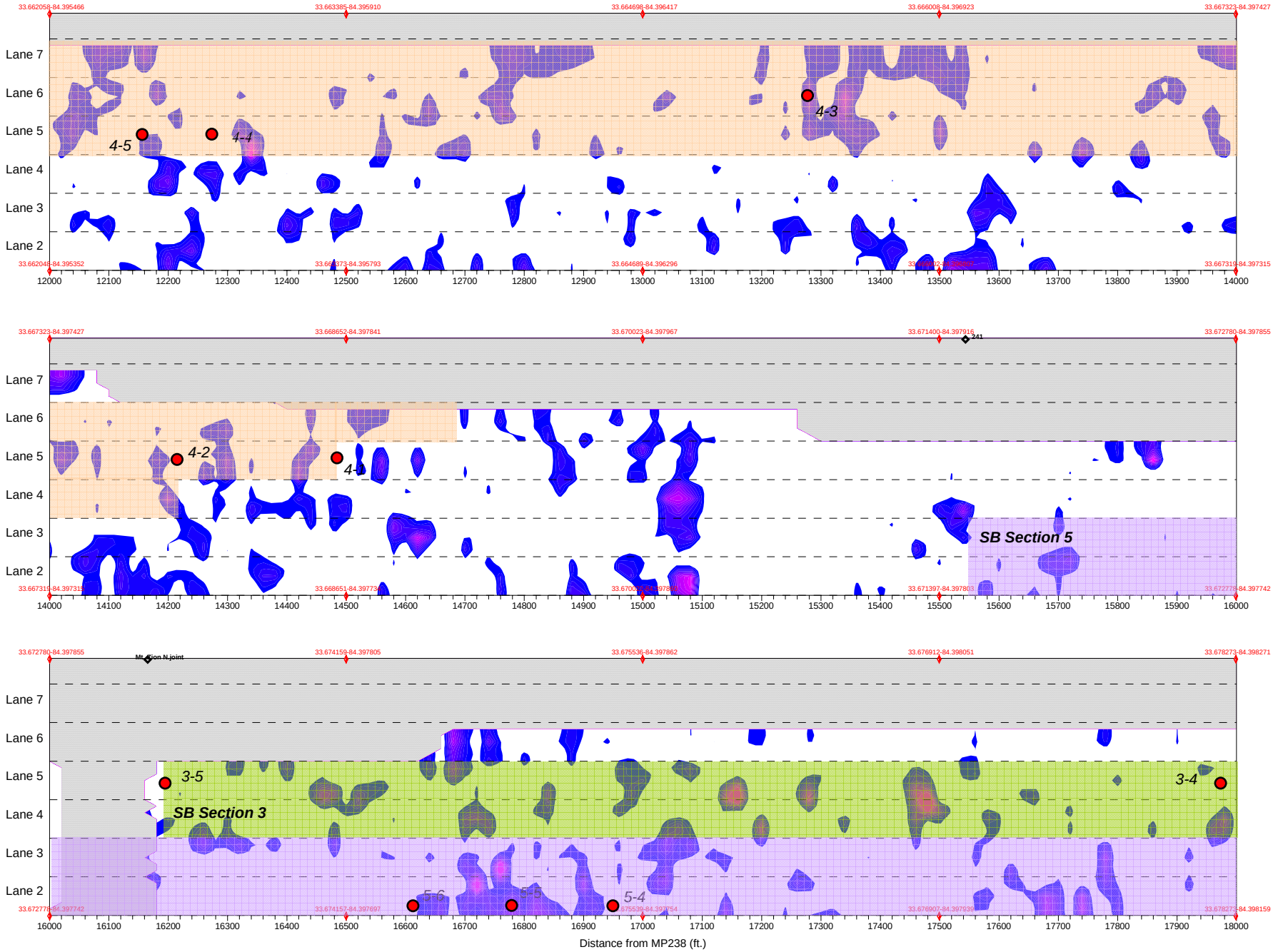
Lane 7
Lane 6
Lane 5
Lane 4
Lane 3
Lane 2
4-5
4-4
4-3
4-2
4-1
SB Section 5
3-5
SB Section 3
3-4
5-6
5-5
5-4
Distance from MP238 (ft.)

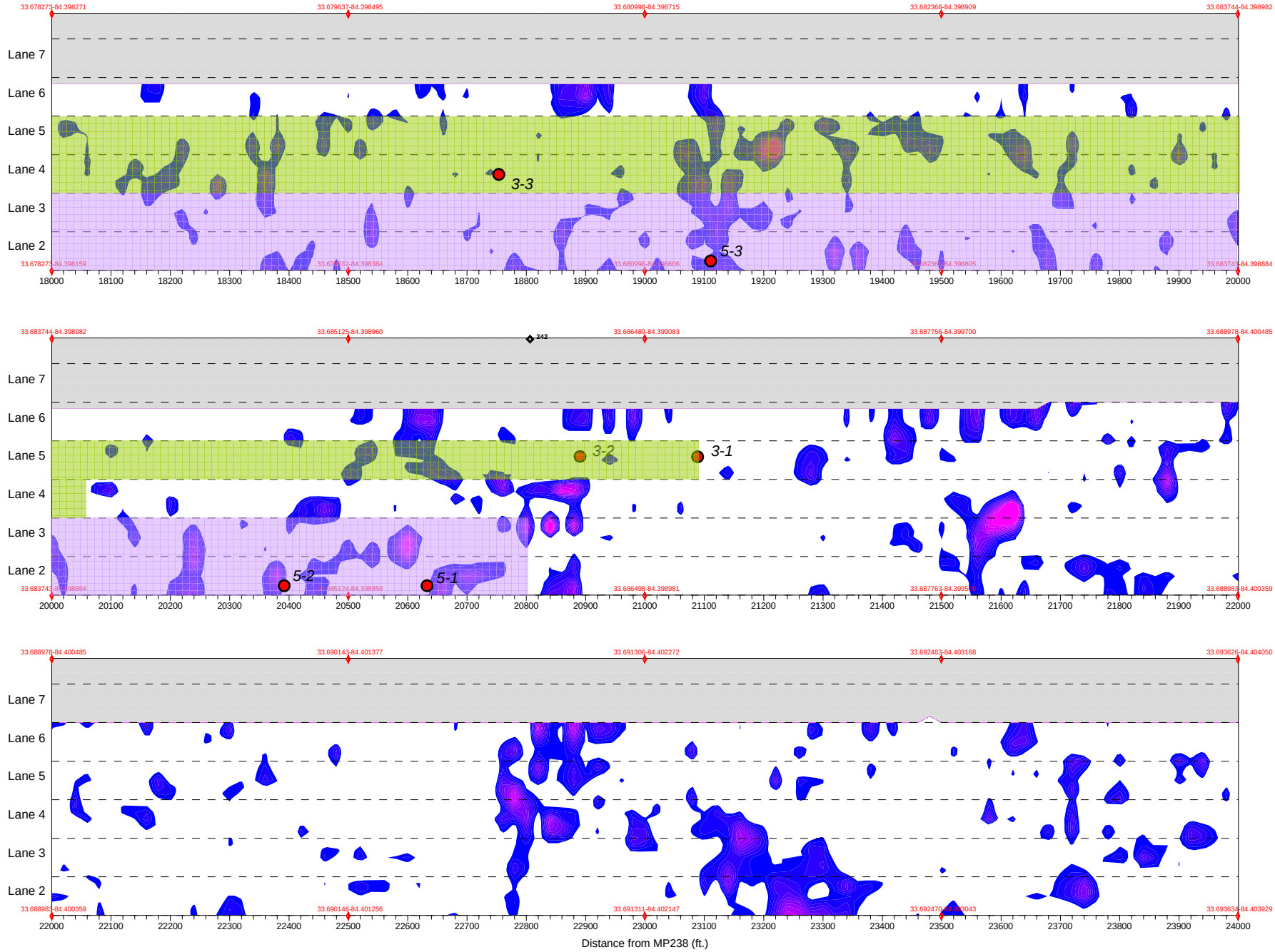
33.678273-84.398271
33.679637-84.398495
33.680998-84.398715
33.682368-84.398909
33.683744-84.398982
Lane 7
Lane 6
Lane 5
Lane 4
Lane 3
Lane 2
3-3
5-3
33.678273-84.398159
33.683743-84.398884
18000
18100
18200
18300
18400
18500
18600
18700
18800
18900
19000
19100
19200
19300
19400
19500
19600
19700
19800
19900
20000
33.683744-84.398982
33.685125-84.398960
242
33.686489-84.399083
33.687756-84.399700
33.688978-84.400485
3-2
3-1
5-2
5-1
33.685124-84.398858
33.686498-84.398981
33.688983-84.400359
20000
20100
20200
20300
20400
20500
20600
20700
20800
20900
21000
21100
21200
21300
21400
21500
21600
21700
21800
21900
22000
33.688978-84.400485
33.690143-84.401377
33.691306-84.402272
33.692463-84.403168
33.693626-84.404050
33.688983-84.400359
33.690146-84.401256
33.691311-84.402147
33.693634-84.403929
22000
22100
22200
22300
22400
22500
22600
22700
22800
22900
23000
23100
23200
23300
23400
23500
23600
23700
23800
23900
24000
Distance from MP238 (ft.)

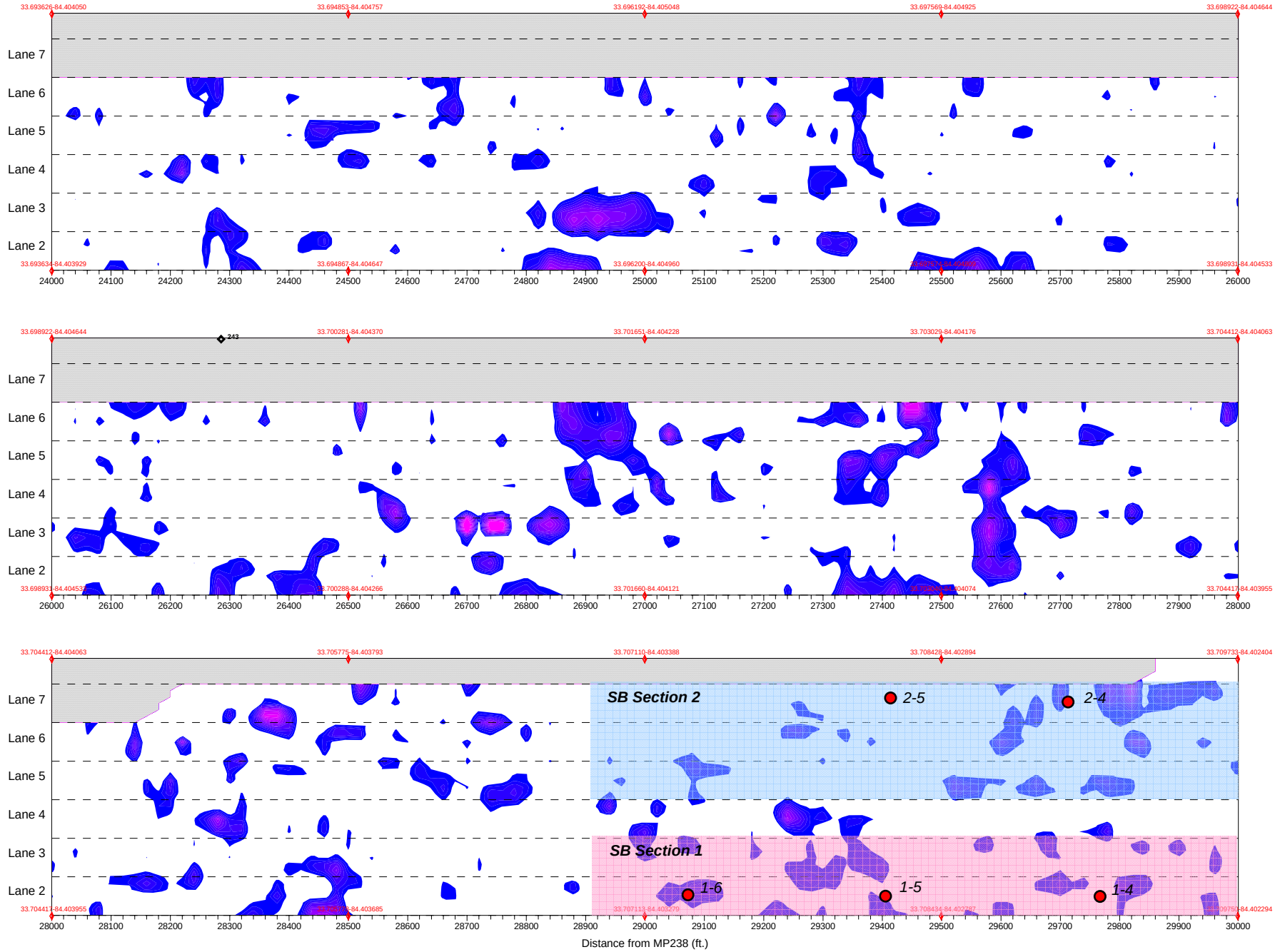
Lane 7
Lane 6
Lane 5
Lane 4
Lane 3
Lane 2
SB Section 2
2-5
2-4
SB Section 1
1-6
1-5
1-4
Distance from MP238 (ft.)

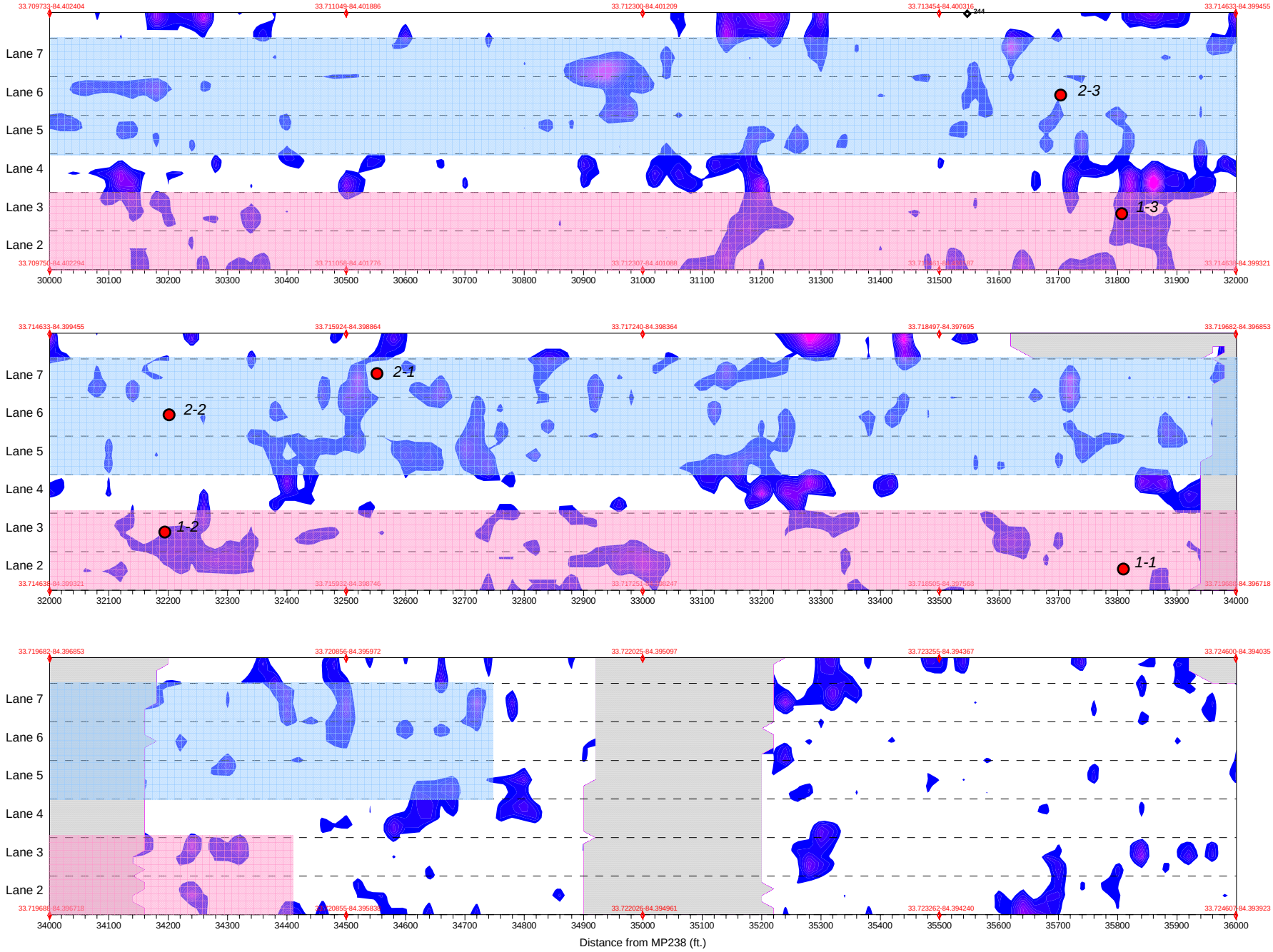
33.709733-84.402404
33.711049-84.401886
33.712300-84.401209
33.713454-84.400316
244
33.714633-84.399455
Lane 7
Lane 6
Lane 5
Lane 4
Lane 3
Lane 2
2-3
1-3
33.709750-84.402294
33.711058-84.401776
33.712307-84.401088
33.714638-84.399321
30000
30100
30200
30300
30400
30500
30600
30700
30800
30900
31000
31100
31200
31300
31400
31500
31600
31700
31800
31900
32000
33.714633-84.399455
33.715924-84.398864
33.717240-84.398364
33.718497-84.397695
33.719682-84.396853
2-1
2-2
1-2
1-1
33.714638-84.399321
33.715932-84.398746
33.718505-84.397568
33.719688-84.396718
32000
32100
32200
32300
32400
32500
32600
32700
32800
32900
33000
33100
33200
33300
33400
33500
33600
33700
33800
33900
34000
33.719682-84.396853
33.720856-84.395972
33.722025-84.395097
33.723255-84.394367
33.724600-84.394035
33.719688-84.396718
33.720855-84.395838
33.722026-84.394961
33.723262-84.394240
33.724607-84.393923
34000
34100
34200
34300
34400
34500
34600
34700
34800
34900
35000
35100
35200
35300
35400
35500
35600
35700
35800
35900
36000
Distance from MP238 (ft.)

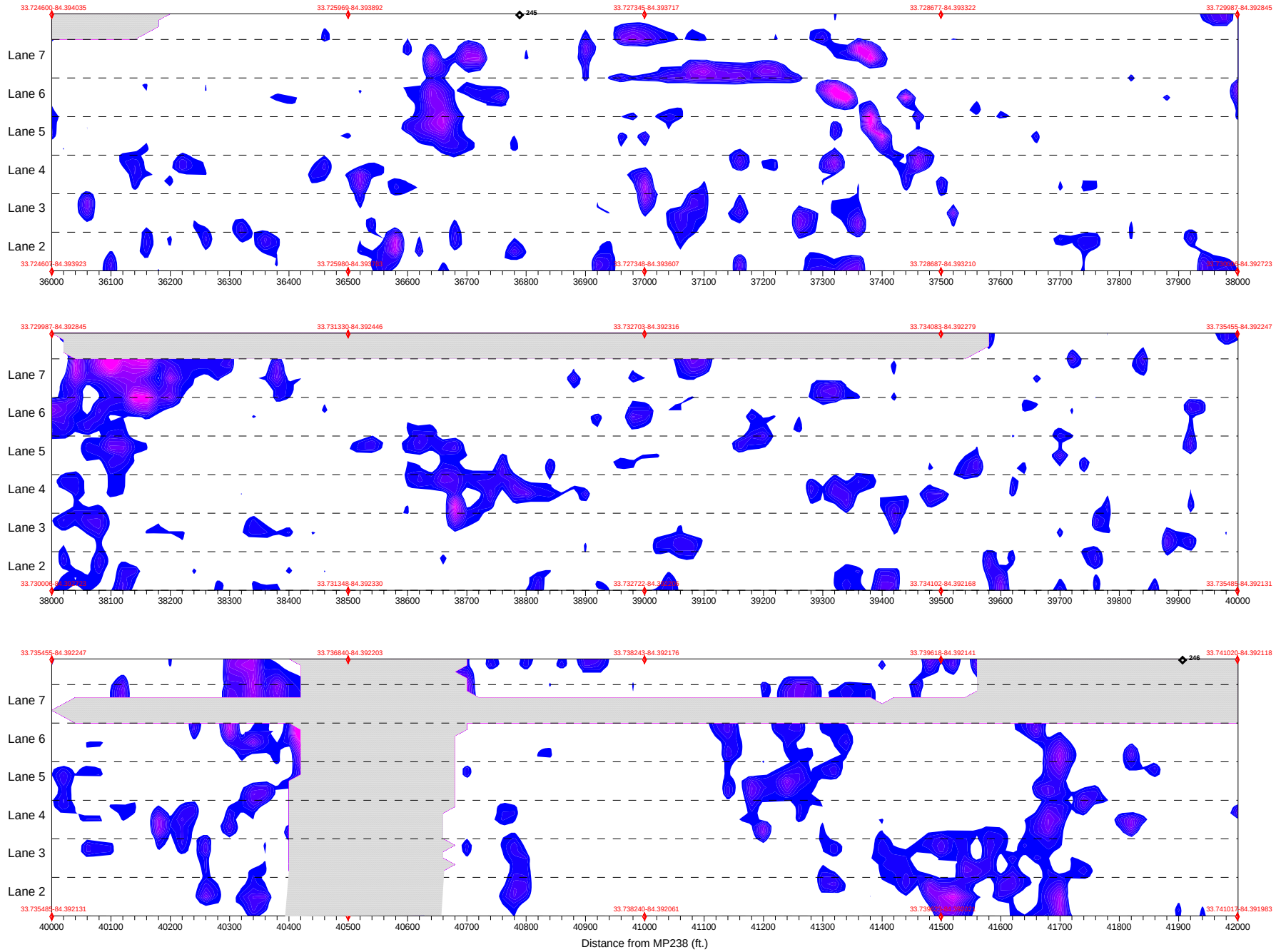
33.724600-84.394035
33.725969-84.393892
245
33.727345-84.393717
33.728677-84.393322
33.729987-84.392845
Lane 7
Lane 6
Lane 5
Lane 4
Lane 3
Lane 2
33.724601-84.393923
33.725980-84.393
33.727348-84.393607
33.728687-84.393210
33.729987-84.392723
36000 36100 36200 36300 36400 36500 36600 36700 36800 36900 37000 37100 37200 37300 37400 37500 37600 37700 37800 37900 38000
33.729987-84.392845
33.731330-84.392446
33.732703-84.392316
33.734083-84.392279
33.735455-84.392247
33.731348-84.392330
33.734102-84.392168
33.735485-84.392131
38000 38100 38200 38300 38400 38500 38600 38700 38800 38900 39000 39100 39200 39300 39400 39500 39600 39700 39800 39900 40000
33.735455-84.392247
33.736840-84.392203
33.738243-84.392176
33.739618-84.392141
246
33.741020-84.392118
33.735485-84.392131
33.738240-84.392061
33.741017-84.391983
40000 40100 40200 40300 40400 40500 40600 40700 40800 40900 41000 41100 41200 41300 41400 41500 41600 41700 41800 41900 42000
Distance from MP238 (ft.)

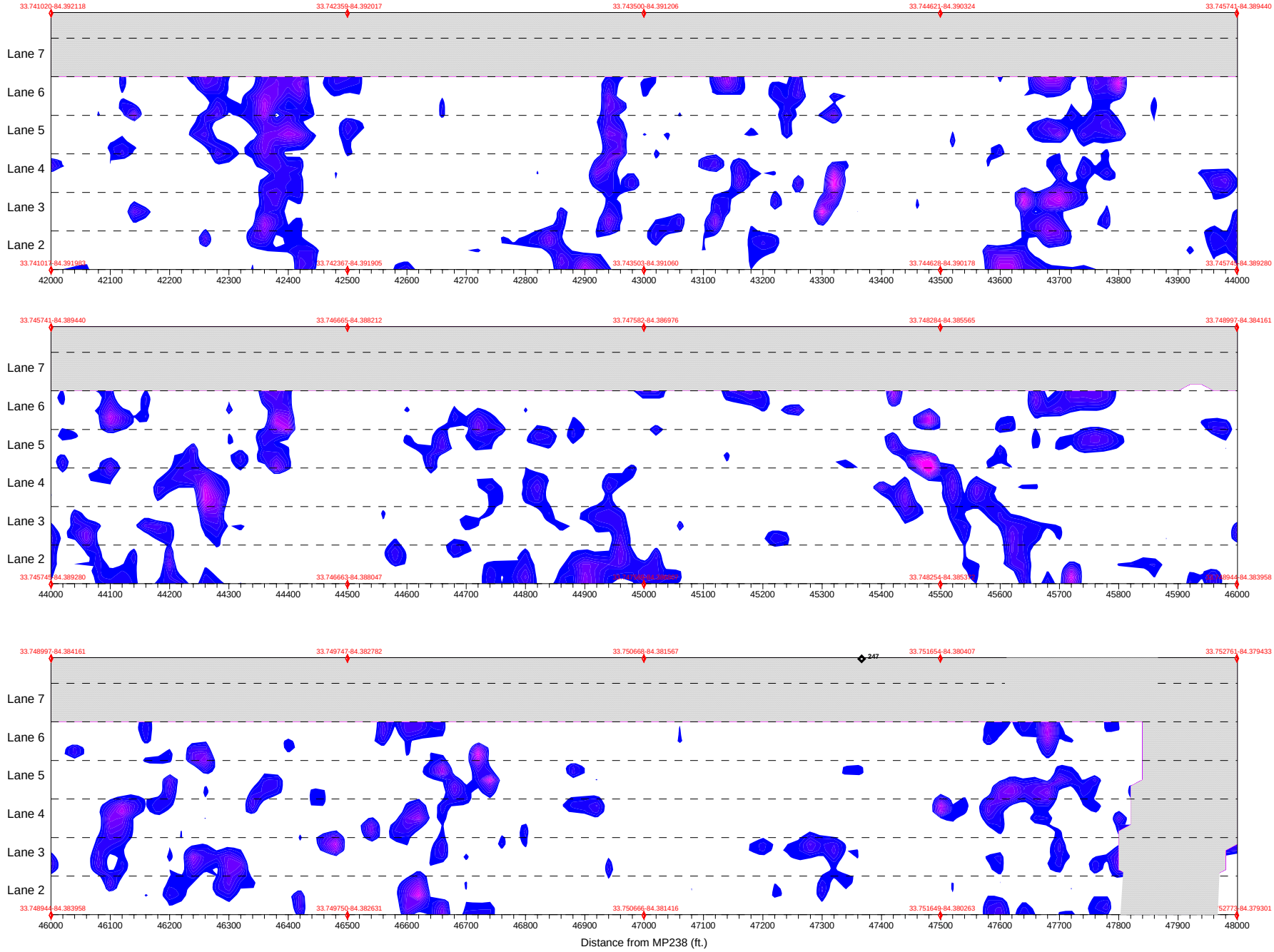
33.741020-84.392118
33.742359-84.392017
33.743500-84.391206
33.744621-84.390324
33.745741-84.389440
Lane 7
Lane 6
Lane 5
Lane 4
Lane 3
Lane 2
33.741013-84.391983
33.742367-84.391905
33.743503-84.391060
33.744628-84.390178
33.745743-84.389280
42000 42100 42200 42300 42400 42500 42600 42700 42800 42900 43000 43100 43200 43300 43400 43500 43600 43700 43800 43900 44000
33.745741-84.389440
33.746665-84.388212
33.747582-84.386976
33.748284-84.385565
33.748997-84.384161
33.745749-84.389280
33.746663-84.388047
33.748254-84.3853
33.748944-84.383958
44000 44100 44200 44300 44400 44500 44600 44700 44800 44900 45000 45100 45200 45300 45400 45500 45600 45700 45800 45900 46000
33.748997-84.384161
33.749747-84.382782
33.750668-84.381567
247
33.751654-84.380407
33.752761-84.379433
33.748944-84.383958
33.749750-84.382631
33.750666-84.381416
33.751649-84.380263
52773-84.379301
46000 46100 46200 46300 46400 46500 46600 46700 46800 46900 47000 47100 47200 47300 47400 47500 47600 47700 47800 47900 48000
Distance from MP238 (ft.)

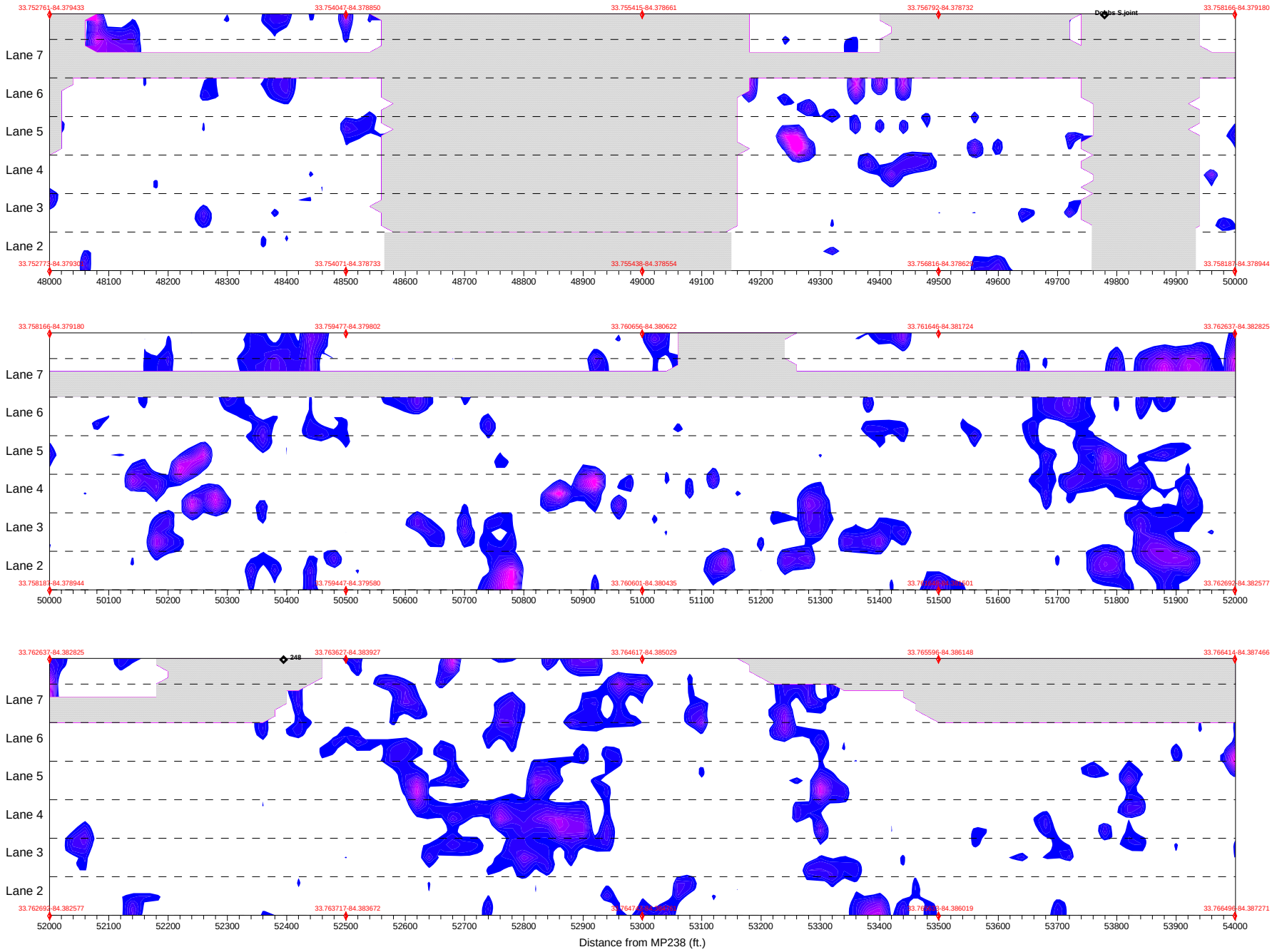
33.752761-84.379433
33.754047-84.378850
33.755415-84.378661
33.756792-84.378732
Dobbs S joint
33.758166-84.379180
Lane 7
Lane 6
Lane 5
Lane 4
Lane 3
Lane 2
33.752773-84.379300
33.754071-84.378733
33.755438-84.378554
33.756816-84.378629
33.758187-84.378944
48000 48100 48200 48300 48400 48500 48600 48700 48800 48900 49000 49100 49200 49300 49400 49500 49600 49700 49800 49900 50000
33.758166-84.379180
33.759477-84.379802
33.760656-84.380622
33.761646-84.381724
33.762637-84.382825
33.758187-84.378944
33.759447-84.379580
33.760601-84.380435
33.762692-84.382577
50000 50100 50200 50300 50400 50500 50600 50700 50800 50900 51000 51100 51200 51300 51400 51500 51600 51700 51800 51900 52000
33.762637-84.382825
248
33.763627-84.383927
33.764617-84.385029
33.765596-84.386148
33.766414-84.387466
33.762692-84.382577
33.763717-84.383672
33.765596-84.386019
33.766496-84.387271
52000 52100 52200 52300 52400 52500 52600 52700 52800 52900 53000 53100 53200 53300 53400 53500 53600 53700 53800 53900 54000
Distance from MP238 (ft.)

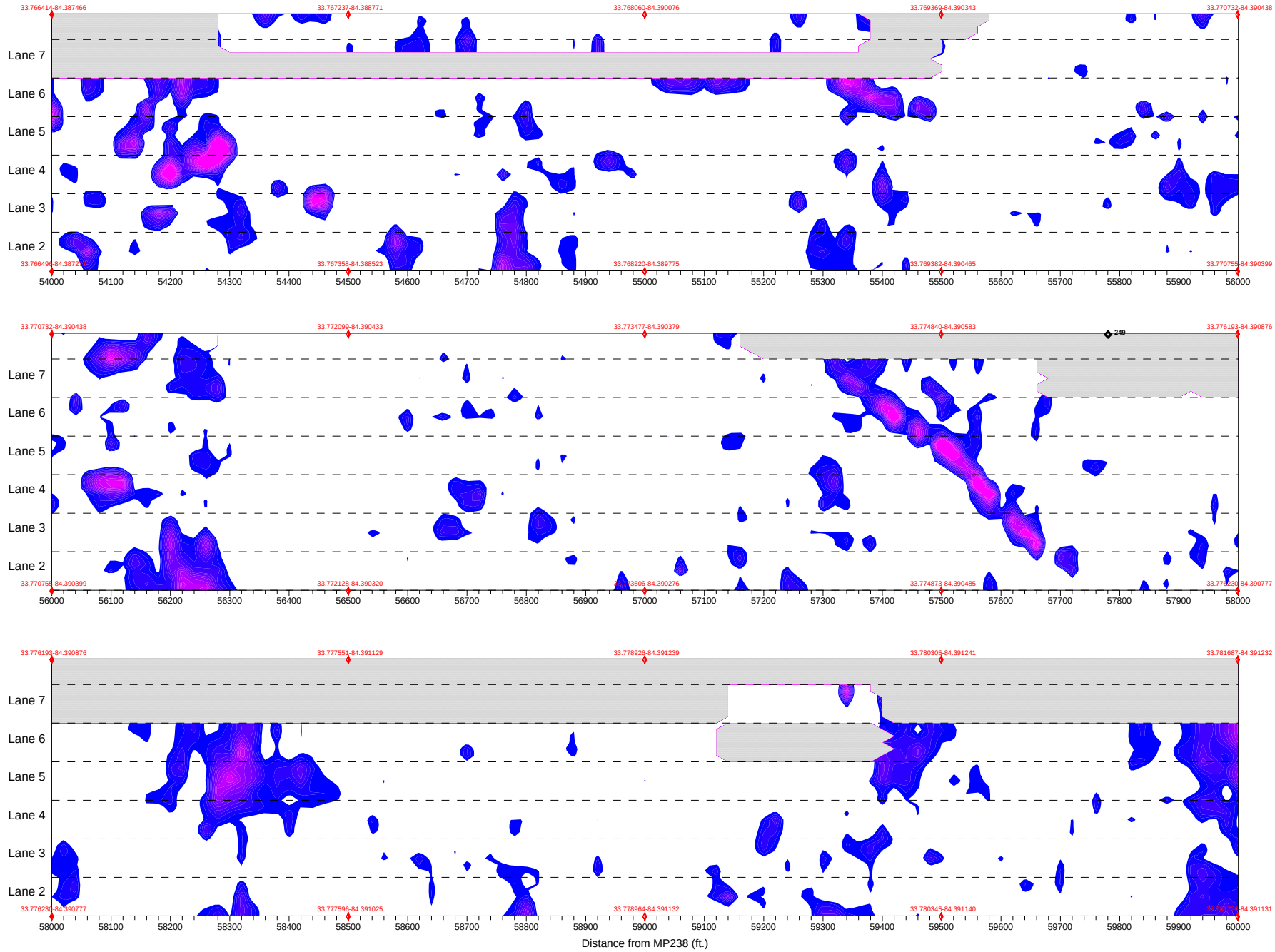
33.766414-84.387466
33.767237-84.388771
33.768060-84.390076
33.769369-84.390343
33.770732-84.390438
Lane 7
Lane 6
Lane 5
Lane 4
Lane 3
Lane 2
33.767358-84.388523
33.768220-84.389775
33.769382-84.390465
33.770755-84.390399
54000 54100 54200 54300 54400 54500 54600 54700 54800 54900 55000 55100 55200 55300 55400 55500 55600 55700 55800 55900 56000
33.770732-84.390438
33.772099-84.390433
33.773477-84.390379
33.774840-84.390583
249
33.776193-84.390876
33.770755-84.390399
33.772128-84.390320
33.773506-84.390276
33.774873-84.390485
33.776230-84.390777
56000 56100 56200 56300 56400 56500 56600 56700 56800 56900 57000 57100 57200 57300 57400 57500 57600 57700 57800 57900 58000
33.776193-84.390876
33.777551-84.391129
33.778926-84.391239
33.780305-84.391241
33.781687-84.391232
33.776230-84.390777
33.777596-84.391025
33.778964-84.391132
33.780345-84.391140
33.781728-84.391131
58000 58100 58200 58300 58400 58500 58600 58700 58800 58900 59000 59100 59200 59300 59400 59500 59600 59700 59800 59900 60000
Distance from MP238 (ft.)

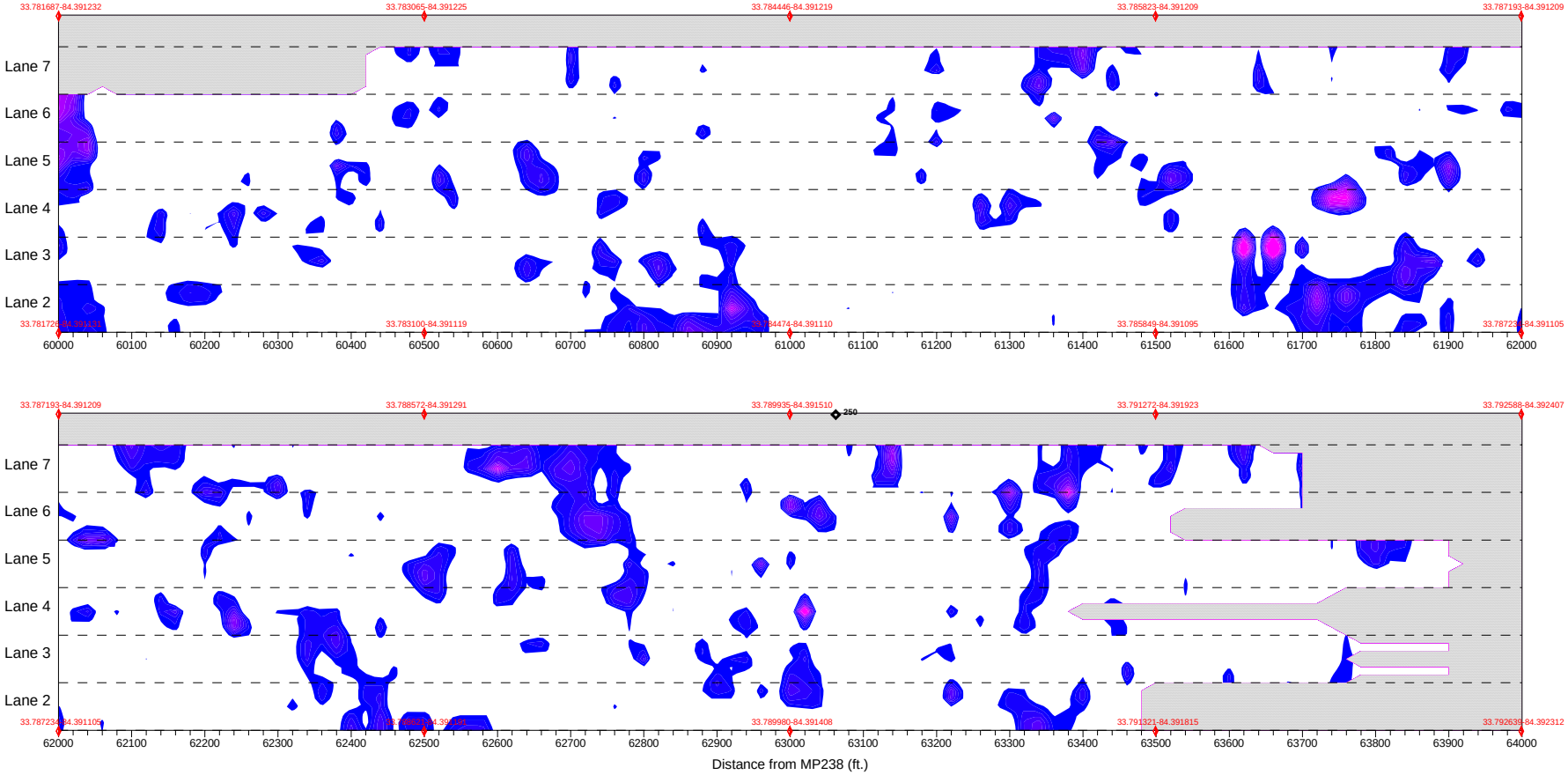
33.781687-84.391232
33.783065-84.391225
33.784446-84.391219
33.785823-84.391209
33.787193-84.391209
Lane 7
Lane 6
Lane 5
Lane 4
Lane 3
Lane 2
33.783100-84.391119
33.784474-84.391110
33.785849-84.391095
60000
60100
60200
60300
60400
60500
60600
60700
60800
60900
61000
61100
61200
61300
61400
61500
61600
61700
61800
61900
62000
33.787193-84.391209
33.788572-84.391291
33.789935-84.391510
250
33.791272-84.391923
33.792588-84.392407
33.789980-84.391408
33.791321-84.391815
62000
62100
62200
62300
62400
62500
62600
62700
62800
62900
63000
63100
63200
63300
63400
63500
63600
63700
63800
63900
64000
Distance from MP238 (ft.)

APPENDIX B. GLOBAL UNIFORMITY INDEX PROFILES

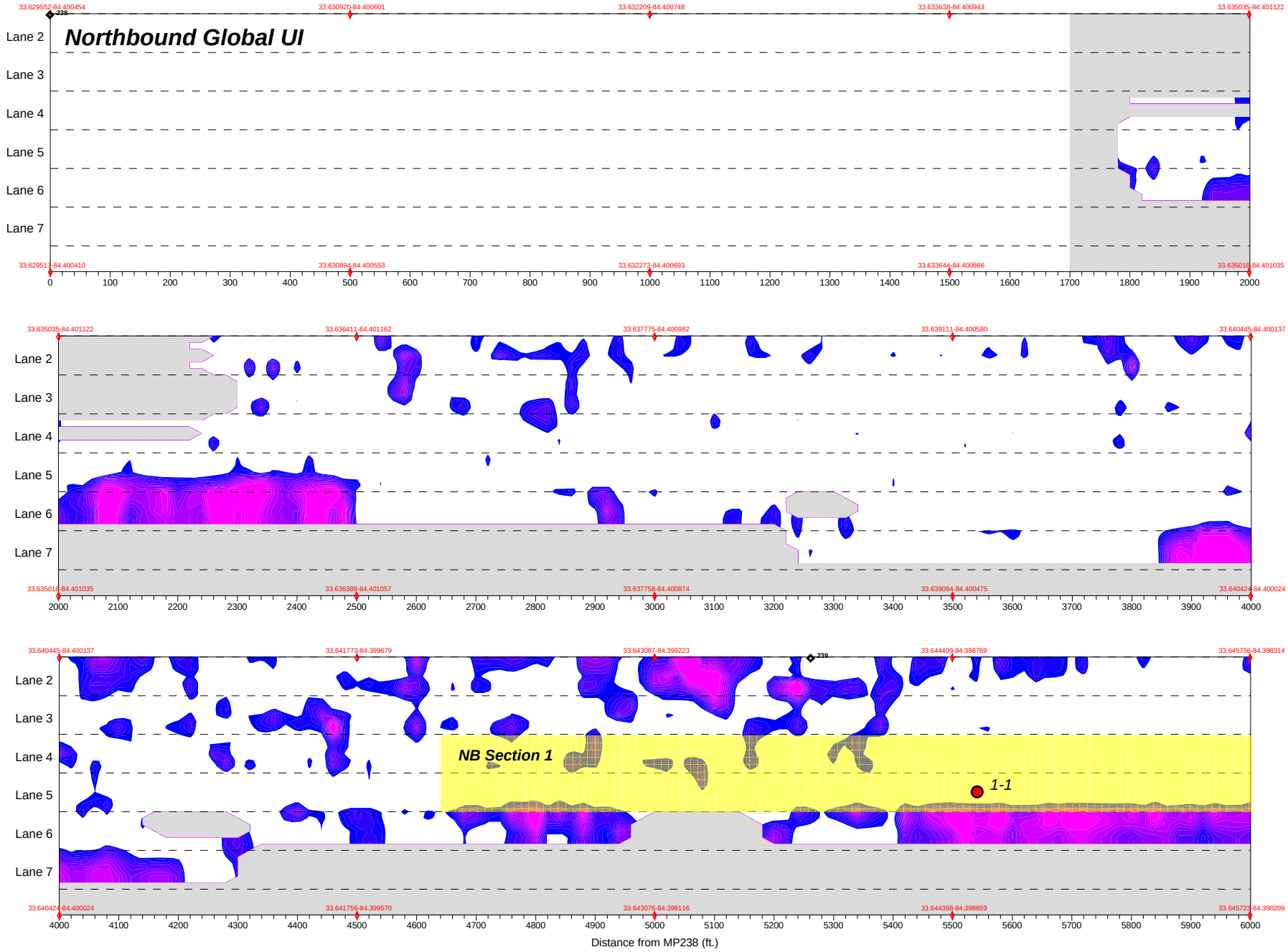
Northbound Global UI
Lane 2
Lane 3
Lane 4
Lane 5
Lane 6
Lane 7
NB Section 1
1-1
Distance from MP238 (ft.)

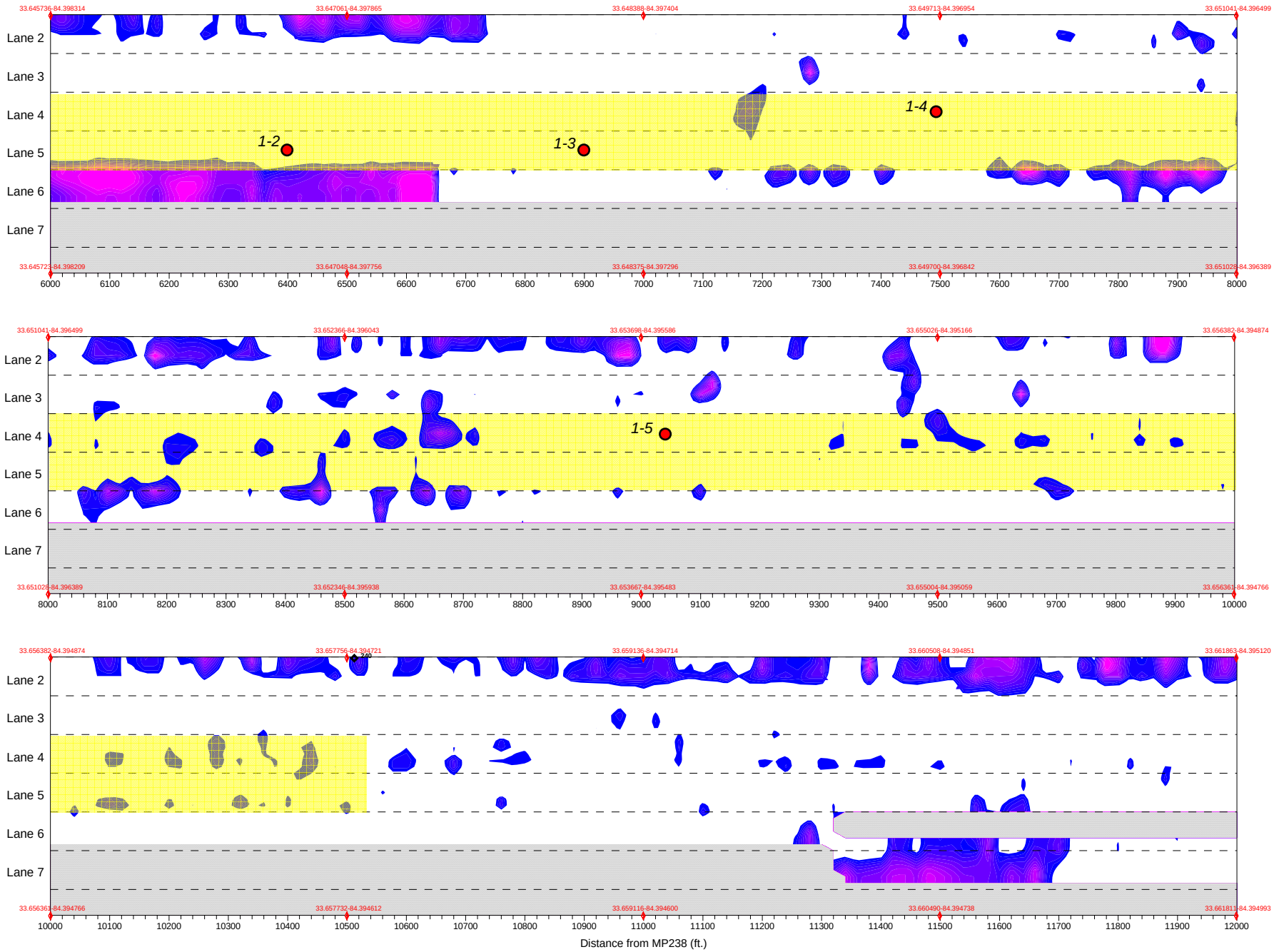
33.645736-84.398314
33.647061-84.397865
33.648388-84.397404
33.649713-84.396954
33.651041-84.396499
Lane 2
Lane 3
Lane 4
Lane 5
Lane 6
Lane 7
1-2
1-3
1-4
33.645723-84.398209
33.647048-84.397756
33.648375-84.397296
33.649700-84.396842
33.651028-84.396389
6000 6100 6200 6300 6400 6500 6600 6700 6800 6900 7000 7100 7200 7300 7400 7500 7600 7700 7800 7900 8000
33.651041-84.396499
33.652366-84.396043
33.653698-84.395586
33.655026-84.395166
33.656382-84.394874
1-5
33.651028-84.396389
33.652346-84.395938
33.653667-84.395483
33.655004-84.395059
33.656363-84.394766
8000 8100 8200 8300 8400 8500 8600 8700 8800 8900 9000 9100 9200 9300 9400 9500 9600 9700 9800 9900 10000
33.656382-84.394874
33.657756-84.394721
240
33.659136-84.394714
33.660508-84.394851
33.661863-84.395120
33.656363-84.394766
33.657732-84.394612
33.659116-84.394600
33.660490-84.394738
33.661813-84.394993
10000 10100 10200 10300 10400 10500 10600 10700 10800 10900 11000 11100 11200 11300 11400 11500 11600 11700 11800 11900 12000
Distance from MP238 (ft.)

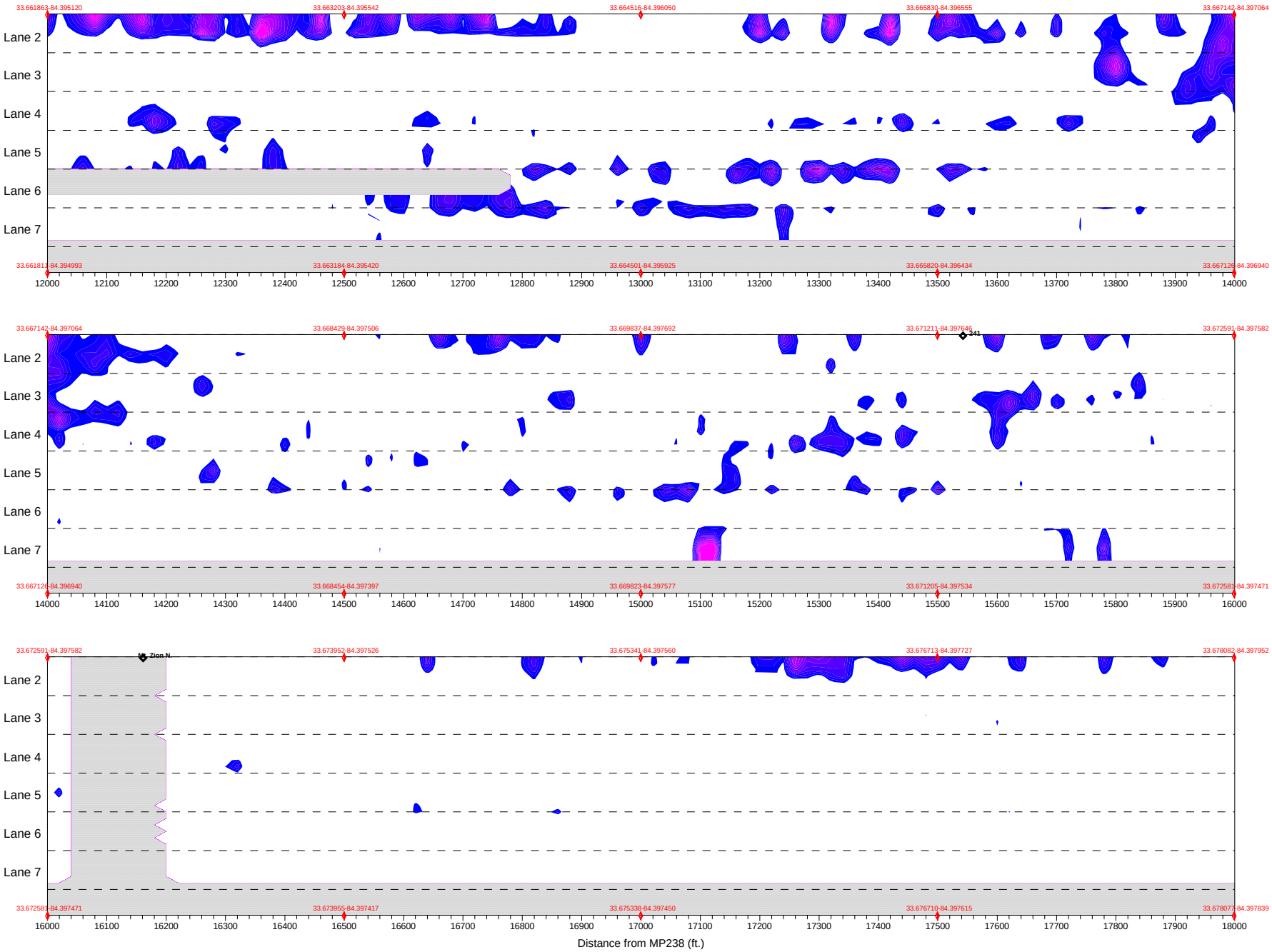
33.661863-84.395120
33.663203-84.395542
33.664516-84.396050
33.665830-84.396555
33.667142-84.397064
Lane 2
Lane 3
Lane 4
Lane 5
Lane 6
Lane 7
33.661811-84.394993
33.663184-84.395420
33.664501-84.395925
33.665820-84.396434
33.667126-84.396940
12000 12100 12200 12300 12400 12500 12600 12700 12800 12900 13000 13100 13200 13300 13400 13500 13600 13700 13800 13900 14000
33.667142-84.397064
33.668429-84.397506
33.669837-84.397692
33.671211-84.397646
241
33.672591-84.397582
33.667126-84.396940
33.668454-84.397397
33.669823-84.397577
33.671205-84.397534
33.672581-84.397471
14000 14100 14200 14300 14400 14500 14600 14700 14800 14900 15000 15100 15200 15300 15400 15500 15600 15700 15800 15900 16000
33.672591-84.397582
Mt. Zion N.
33.673952-84.397526
33.675341-84.397560
33.676713-84.397727
33.678082-84.397952
33.672581-84.397471
33.673955-84.397417
33.675338-84.397450
33.676710-84.397615
33.678077-84.397839
16000 16100 16200 16300 16400 16500 16600 16700 16800 16900 17000 17100 17200 17300 17400 17500 17600 17700 17800 17900 18000
Distance from MP238 (ft.)

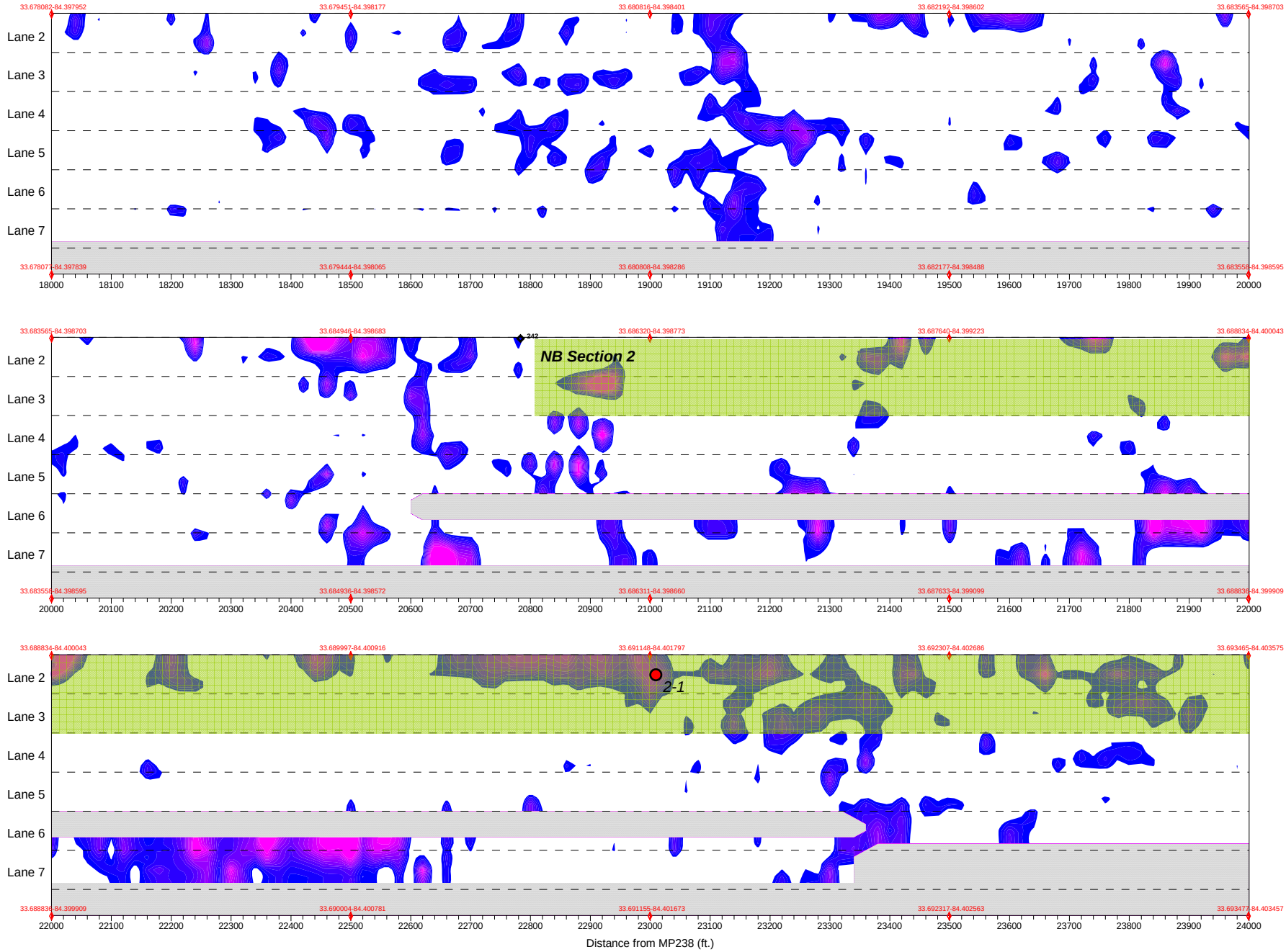
33.678082-84.397952
33.679451-84.398177
33.680816-84.398401
33.682192-84.398602
33.683565-84.398703
Lane 2
Lane 3
Lane 4
Lane 5
Lane 6
Lane 7
33.678077-84.397839
33.679444-84.398065
33.680808-84.398286
33.682177-84.398488
33.683558-84.398595
18000 18100 18200 18300 18400 18500 18600 18700 18800 18900 19000 19100 19200 19300 19400 19500 19600 19700 19800 19900 20000
33.683565-84.398703
33.684946-84.398683
242
33.686320-84.398773
33.687640-84.399223
33.688834-84.400043
NB Section 2
33.683555-84.398595
33.684936-84.398572
33.686311-84.398660
33.687633-84.399099
33.688836-84.399909
20000 20100 20200 20300 20400 20500 20600 20700 20800 20900 21000 21100 21200 21300 21400 21500 21600 21700 21800 21900 22000
33.688834-84.400043
33.689997-84.400916
33.691148-84.401797
33.692307-84.402686
33.693465-84.403575
2-1
33.688836-84.399909
33.690004-84.400781
33.691155-84.401673
33.692317-84.402563
33.693477-84.403457
22000 22100 22200 22300 22400 22500 22600 22700 22800 22900 23000 23100 23200 23300 23400 23500 23600 23700 23800 23900 24000
Distance from MP238 (ft.)

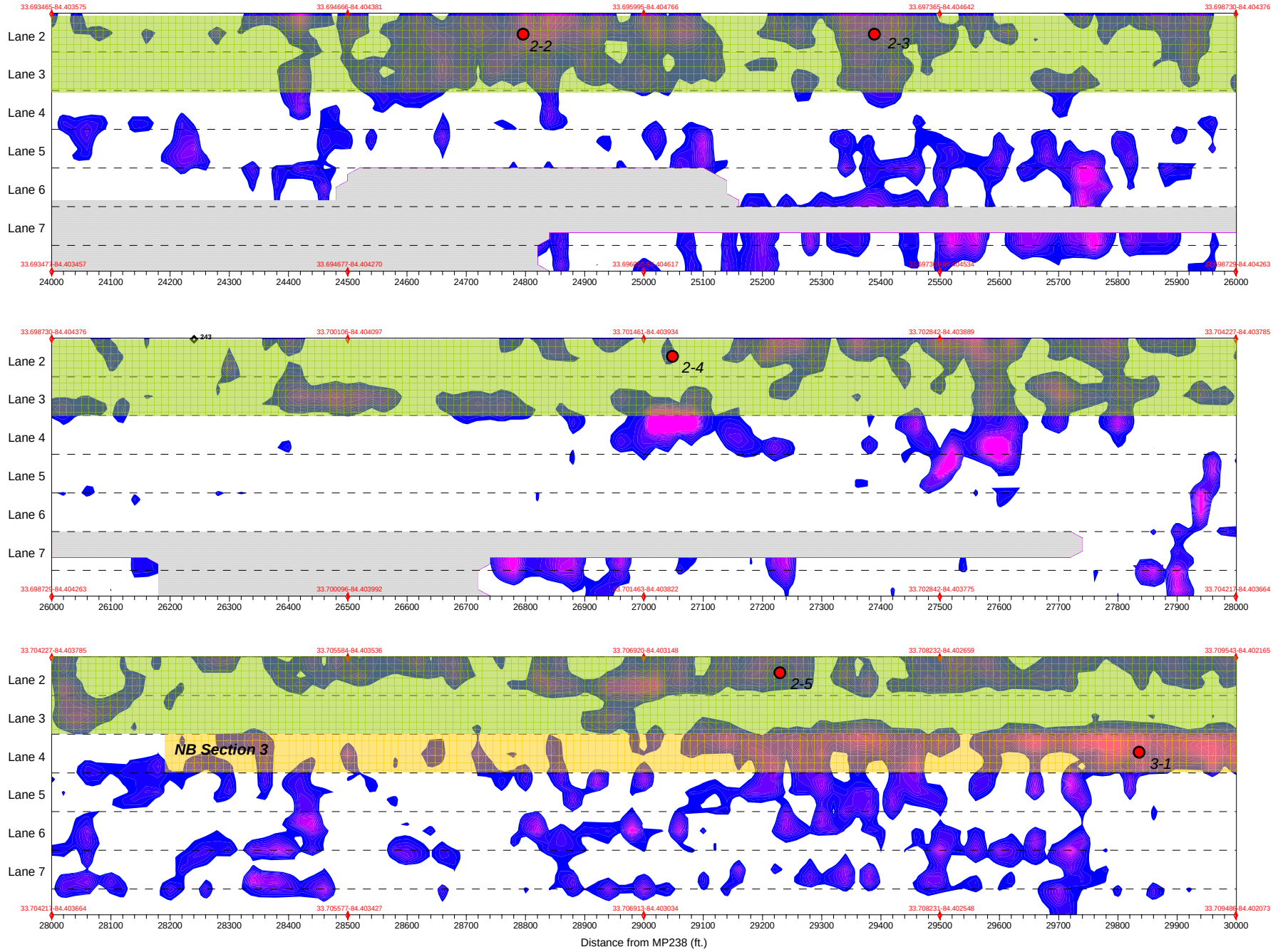
Lane 2
Lane 3
Lane 4
Lane 5
Lane 6
Lane 7
2-2
2-3
2-4
2-5
3-1
NB Section 3
Distance from MP238 (ft.)

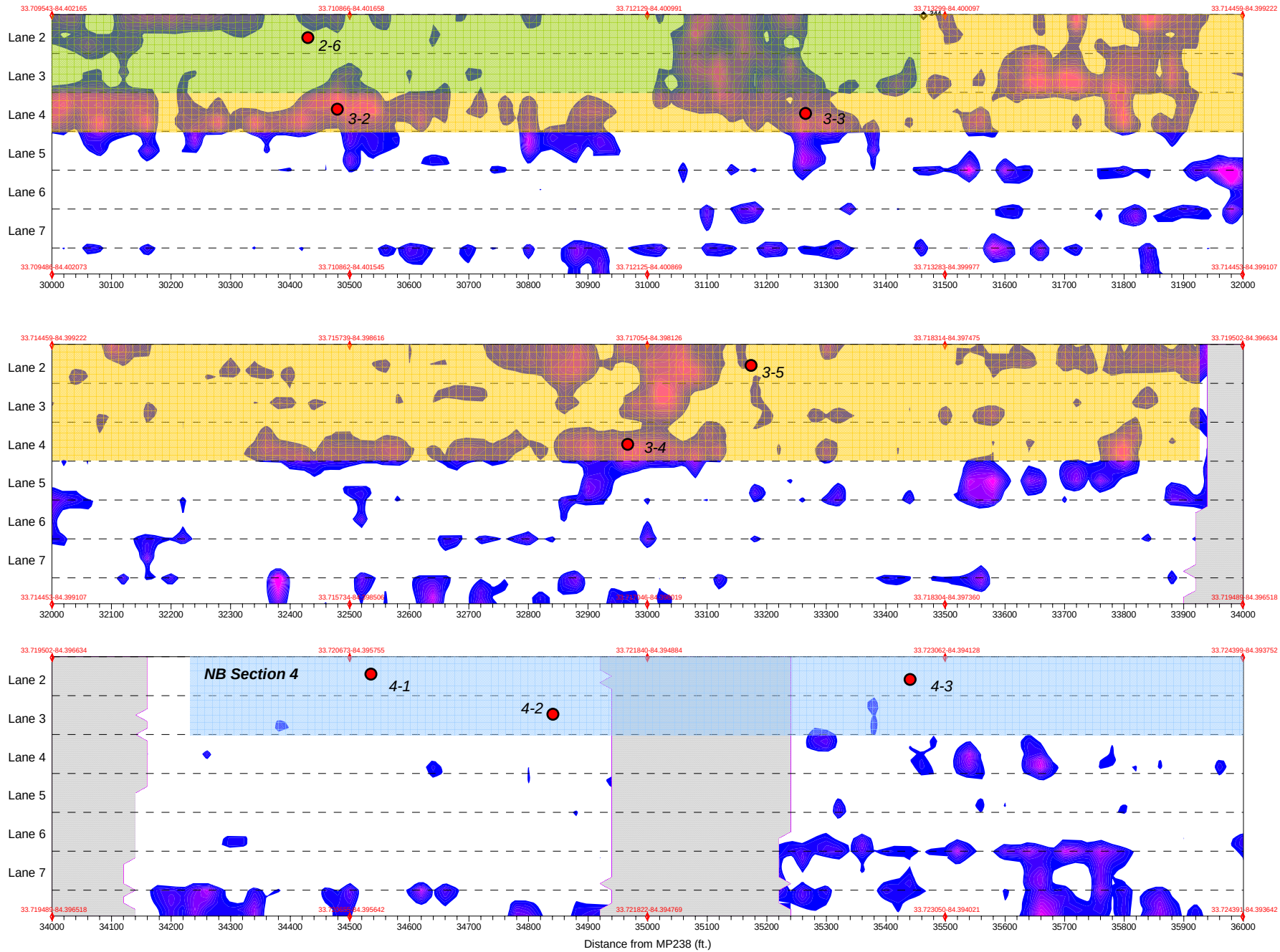
Lane 2
Lane 3
Lane 4
Lane 5
Lane 6
Lane 7
2-6
3-2
3-3
3-5
3-4
NB Section 4
4-1
4-2
4-3
Distance from MP238 (ft.)

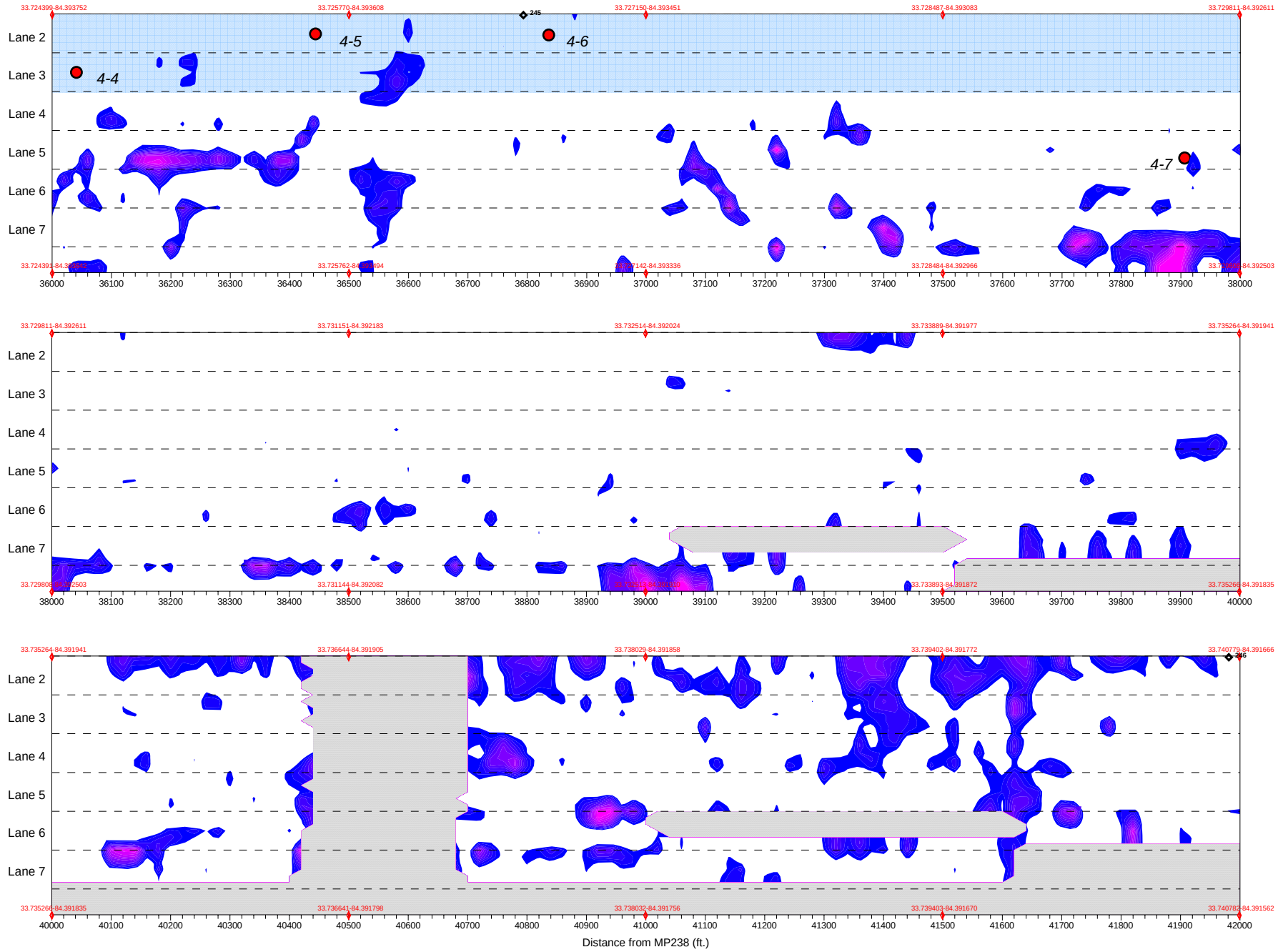
Lane 2
Lane 3
Lane 4
Lane 5
Lane 6
Lane 7
4-4
4-5
4-6
4-7
Distance from MP238 (ft.)

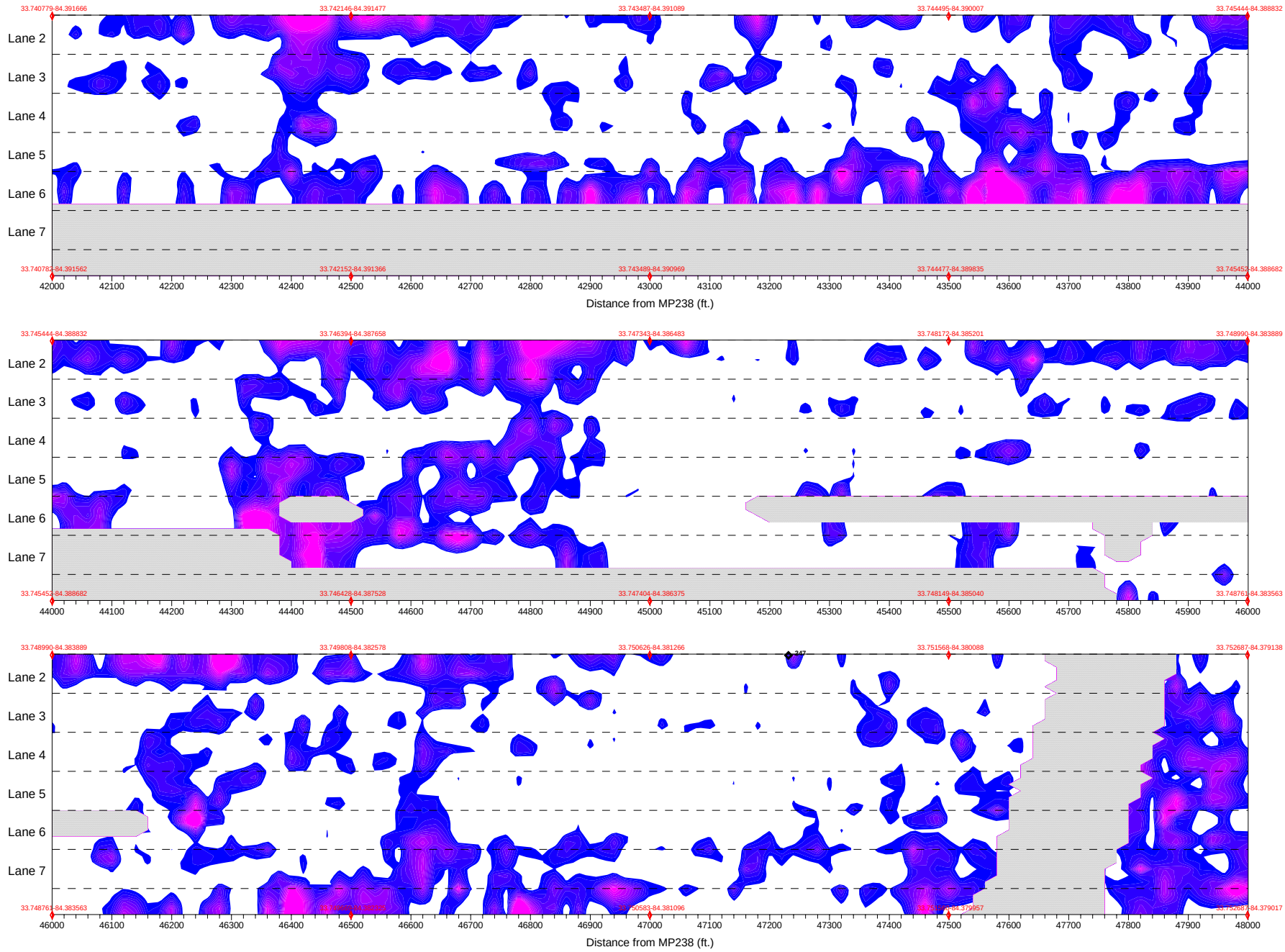
33.740779-84.391666
33.742146-84.391477
33.743487-84.391089
33.744495-84.390007
33.745444-84.388832
Lane 2
Lane 3
Lane 4
Lane 5
Lane 6
Lane 7
33.740782-84.391562
33.742152-84.391366
33.743489-84.390969
33.744477-84.389835
33.745452-84.388682
42000 42100 42200 42300 42400 42500 42600 42700 42800 42900 43000 43100 43200 43300 43400 43500 43600 43700 43800 43900 44000
Distance from MP238 (ft.)
33.745444-84.388832
33.746394-84.387658
33.747343-84.386483
33.748172-84.385201
33.748990-84.383889
Lane 2
Lane 3
Lane 4
Lane 5
Lane 6
Lane 7
33.745452-84.388682
33.746428-84.387528
33.747404-84.386375
33.748149-84.385040
33.748761-84.383563
44000 44100 44200 44300 44400 44500 44600 44700 44800 44900 45000 45100 45200 45300 45400 45500 45600 45700 45800 45900 46000
33.748990-84.383889
33.749808-84.382578
33.750626-84.381266
247
33.751568-84.380088
33.752687-84.379138
Lane 2
Lane 3
Lane 4
Lane 5
Lane 6
Lane 7
33.748761-84.383563
33.750583-84.381096
33.752687-84.379017
46000 46100 46200 46300 46400 46500 46600 46700 46800 46900 47000 47100 47200 47300 47400 47500 47600 47700 47800 47900 48000
Distance from MP238 (ft.)

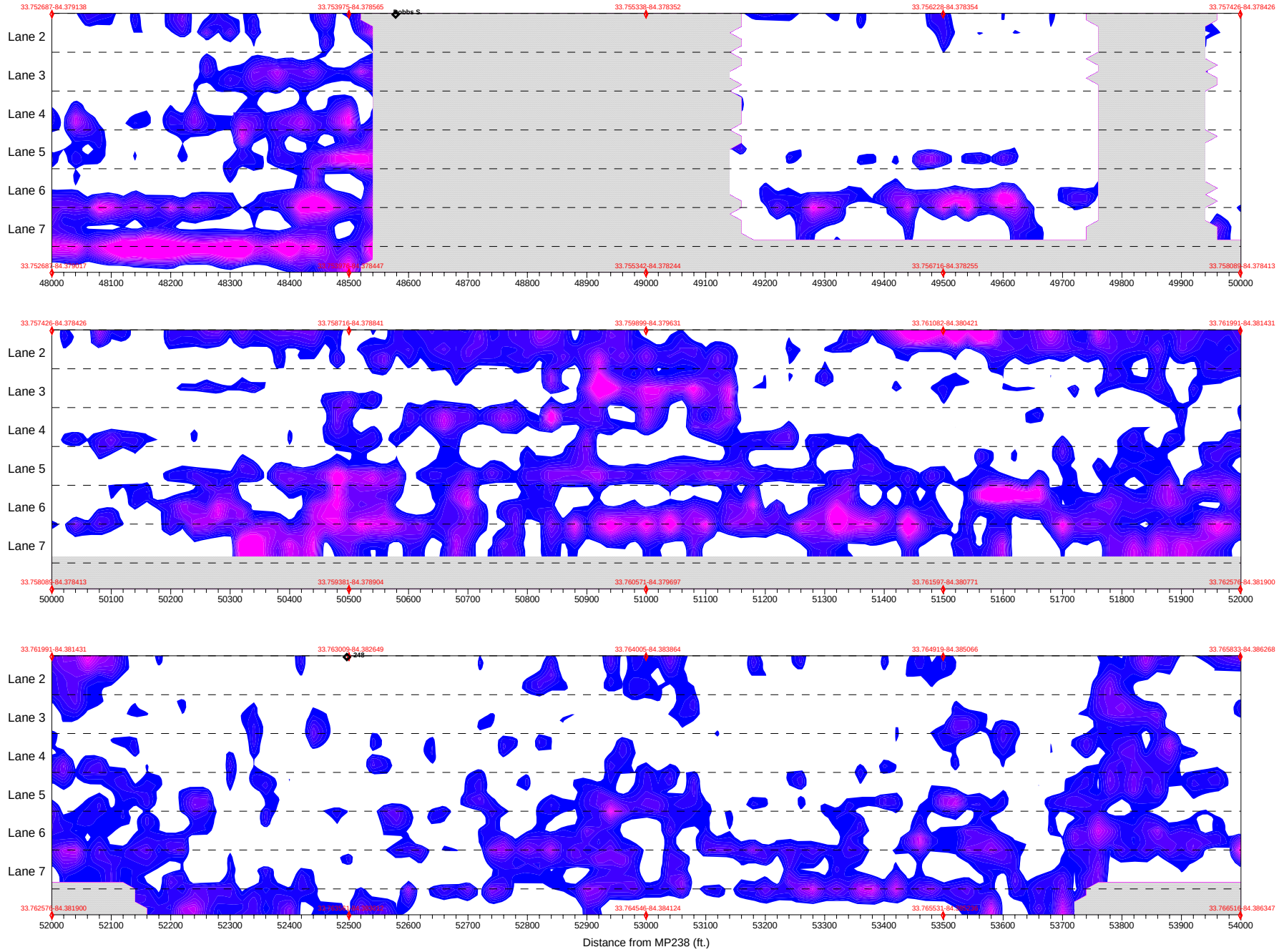
33.752687-84.379138
33.753975-84.378565
Robbs S.
33.755338-84.378352
33.756228-84.378354
33.757426-84.378426
Lane 2
Lane 3
Lane 4
Lane 5
Lane 6
Lane 7
33.752687-84.379017
33.755342-84.378244
33.756716-84.378255
33.758089-84.378413
48000 48100 48200 48300 48400 48500 48600 48700 48800 48900 49000 49100 49200 49300 49400 49500 49600 49700 49800 49900 50000
33.757426-84.378426
33.758716-84.378841
33.759899-84.379631
33.761082-84.380421
33.761991-84.381431
33.758089-84.378413
33.759381-84.378904
33.760571-84.379697
33.761597-84.380771
33.762576-84.381900
50000 50100 50200 50300 50400 50500 50600 50700 50800 50900 51000 51100 51200 51300 51400 51500 51600 51700 51800 51900 52000
33.761991-84.381431
33.763009-84.382649
248
33.764005-84.383864
33.764919-84.385066
33.765833-84.386268
33.762576-84.381900
33.764546-84.384124
33.765531-84.385
33.766516-84.386347
52000 52100 52200 52300 52400 52500 52600 52700 52800 52900 53000 53100 53200 53300 53400 53500 53600 53700 53800 53900 54000
Distance from MP238 (ft.)

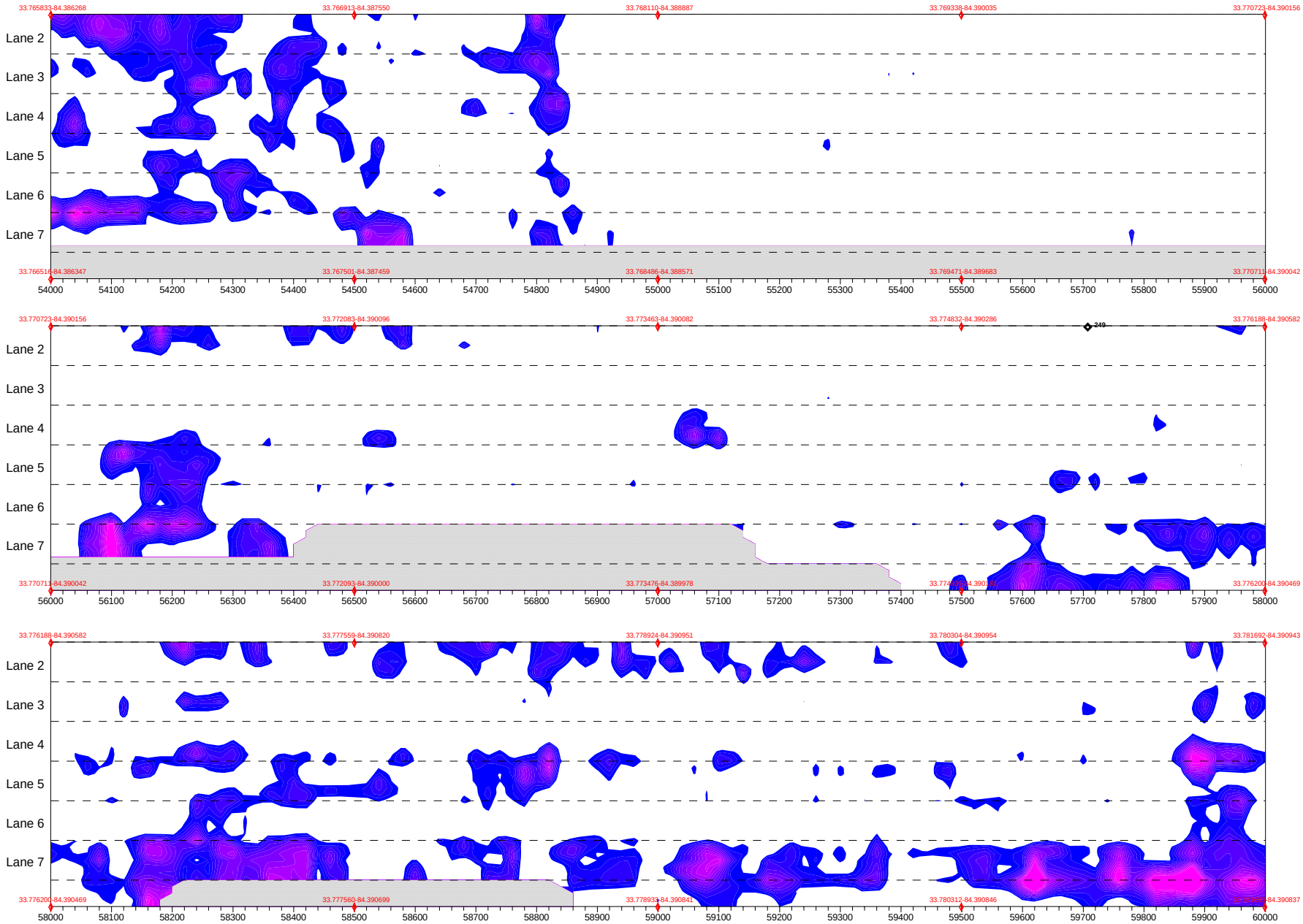
33.765833-84.386268
33.766913-84.387550
33.768110-84.388887
33.769338-84.390035
33.770723-84.390156
Lane 2
Lane 3
Lane 4
Lane 5
Lane 6
Lane 7
33.766516-84.386347
33.767501-84.387459
33.768486-84.388571
33.769471-84.389683
33.770713-84.390042
54000 54100 54200 54300 54400 54500 54600 54700 54800 54900 55000 55100 55200 55300 55400 55500 55600 55700 55800 55900 56000
33.770723-84.390156
33.772083-84.390096
33.773463-84.390082
33.774832-84.390286
249
33.776188-84.390582
33.770713-84.390042
33.772093-84.390000
33.773476-84.389978
33.776200-84.390469
56000 56100 56200 56300 56400 56500 56600 56700 56800 56900 57000 57100 57200 57300 57400 57500 57600 57700 57800 57900 58000
33.776188-84.390582
33.777559-84.390820
33.778924-84.390951
33.780304-84.390954
33.781692-84.390943
33.776200-84.390469
33.777560-84.390699
33.778933-84.390841
33.780312-84.390846
58000 58100 58200 58300 58400 58500 58600 58700 58800 58900 59000 59100 59200 59300 59400 59500 59600 59700 59800 59900 60000

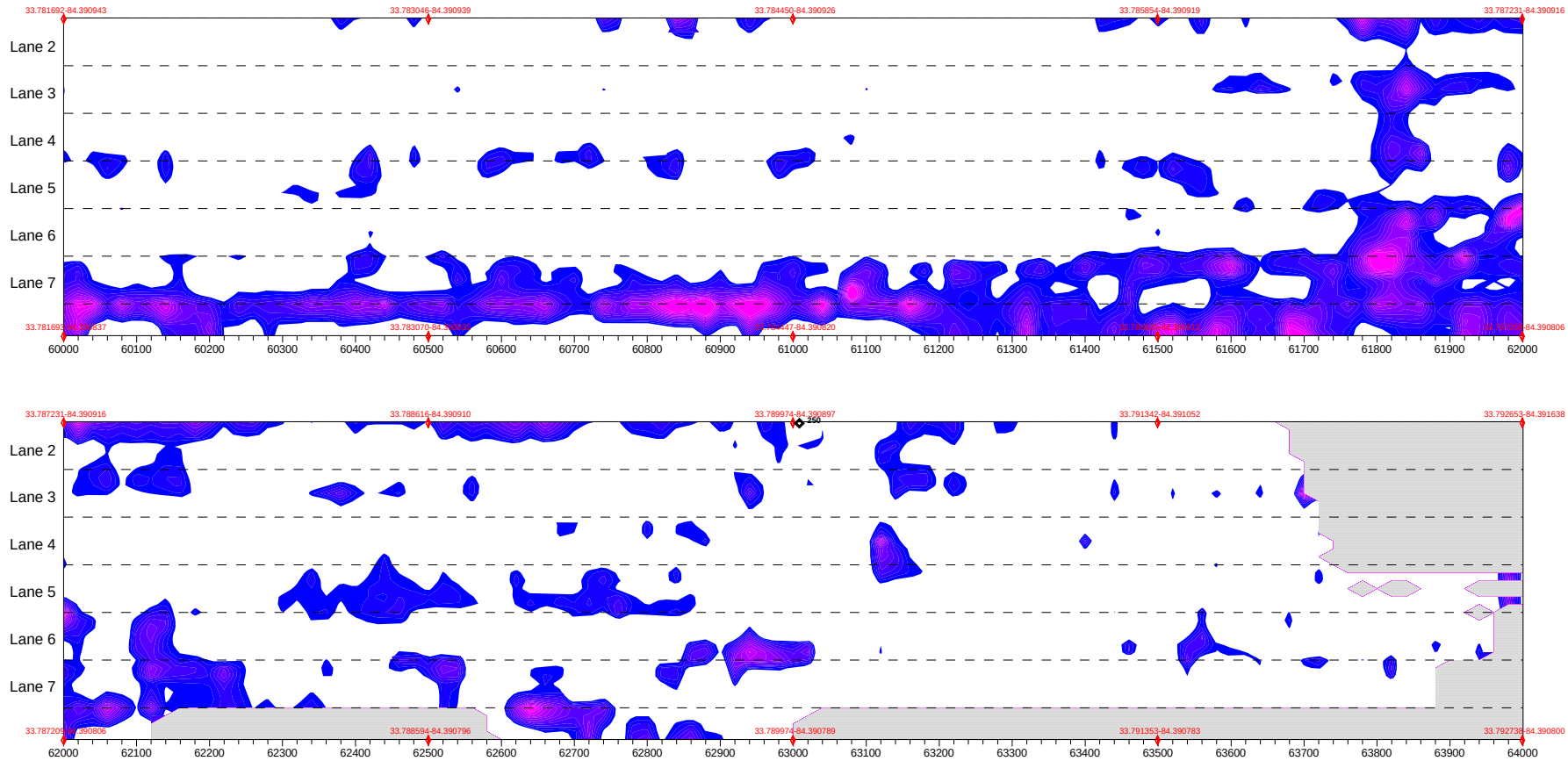
33.781692-84.390943
33.783046-84.390939
33.784450-84.390926
33.785854-84.390919
33.787231-84.390916
Lane 2
Lane 3
Lane 4
Lane 5
Lane 6
Lane 7
60000
60100
60200
60300
60400
60500
60600
60700
60800
60900
61000
61100
61200
61300
61400
61500
61600
61700
61800
61900
62000
33.787231-84.390916
33.788616-84.390910
33.789974-84.390897
250
33.791342-84.391052
33.792653-84.391638
Lane 2
Lane 3
Lane 4
Lane 5
Lane 6
Lane 7
33.788594-84.390796
33.789974-84.390789
33.791353-84.390783
33.792738-84.390800
62000
62100
62200
62300
62400
62500
62600
62700
62800
62900
63000
63100
63200
63300
63400
63500
63600
63700
63800
63900
64000

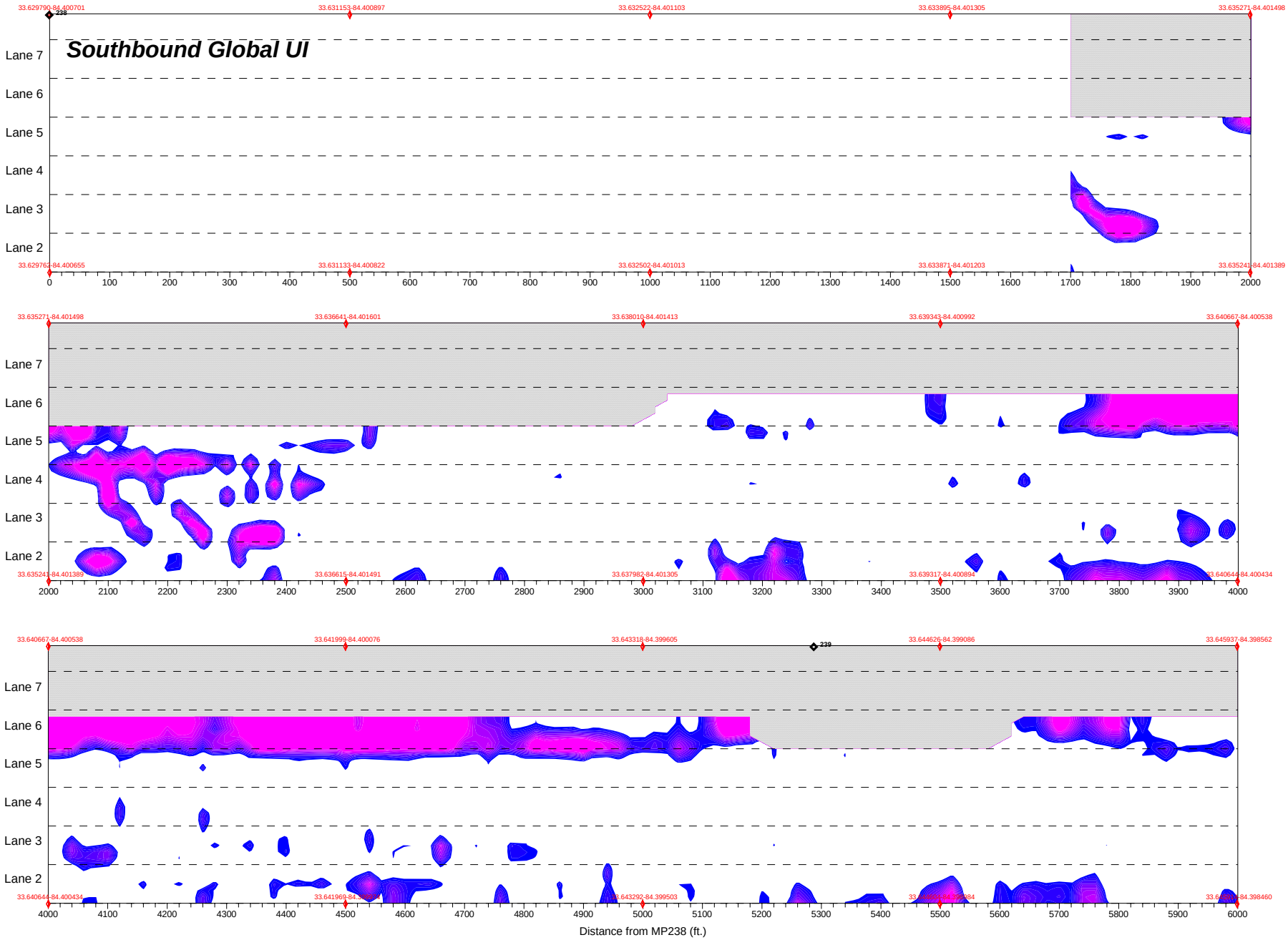
Southbound Global UI
Lane 7
Lane 6
Lane 5
Lane 4
Lane 3
Lane 2
238
239
33.629790-84.400701
33.631153-84.400897
33.632522-84.401103
33.633895-84.401305
33.635271-84.401498
33.629762-84.400655
33.631133-84.400822
33.632502-84.401013
33.633871-84.401203
33.635241-84.401389
33.636641-84.401601
33.638010-84.401413
33.639343-84.400992
33.640667-84.400538
33.636615-84.401491
33.637982-84.401305
33.639317-84.400894
33.640644-84.400434
33.641999-84.400076
33.643318-84.399605
33.644626-84.399086
33.645937-84.398562
33.641969-84.399914
33.643292-84.399503
33.645602-84.398984
33.646914-84.398460
0 100 200 300 400 500 600 700 800 900 1000 1100 1200 1300 1400 1500 1600 1700 1800 1900 2000
2000 2100 2200 2300 2400 2500 2600 2700 2800 2900 3000 3100 3200 3300 3400 3500 3600 3700 3800 3900 4000
4000 4100 4200 4300 4400 4500 4600 4700 4800 4900 5000 5100 5200 5300 5400 5500 5600 5700 5800 5900 6000
Distance from MP238 (ft.)

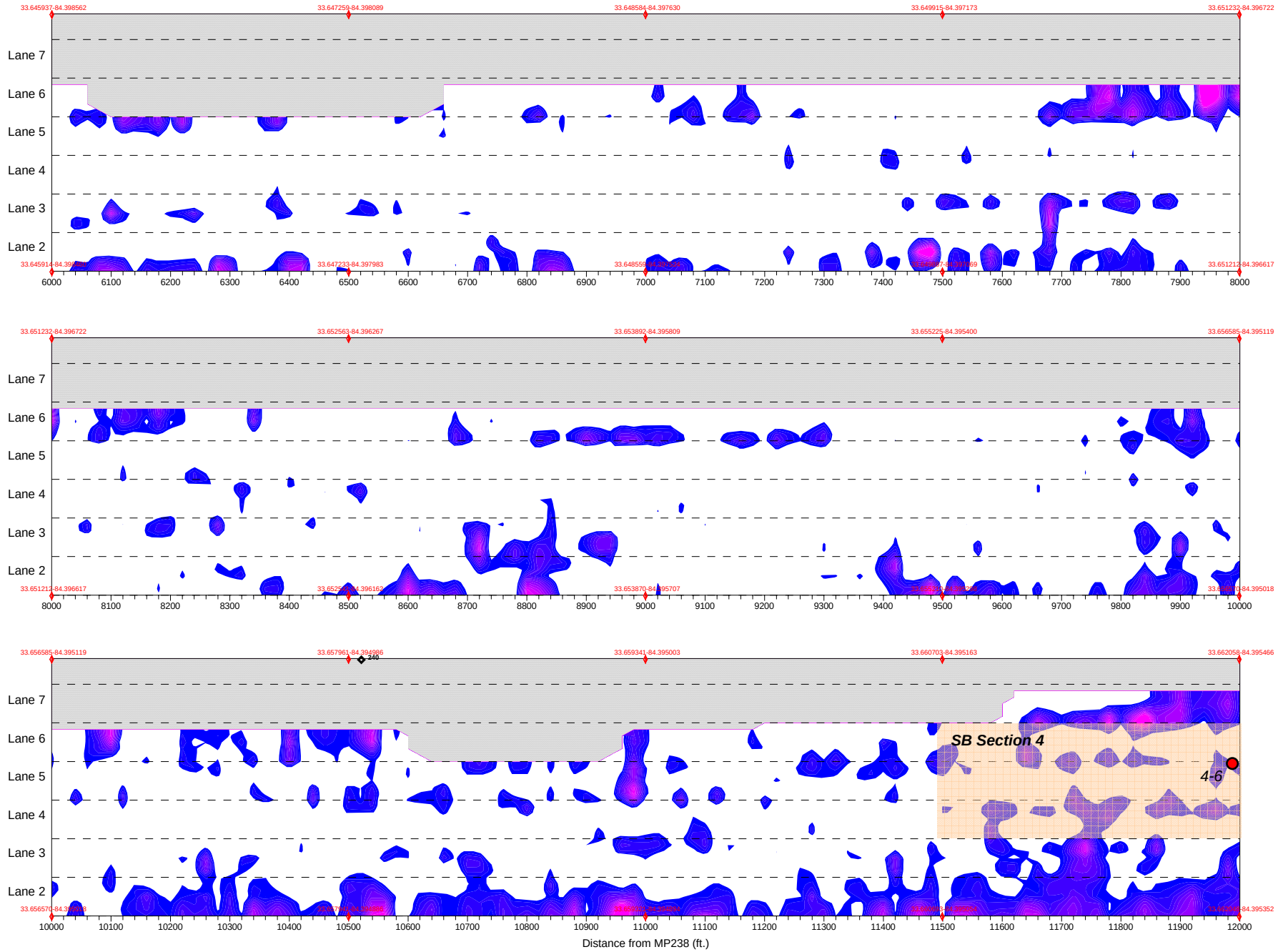
Lane 7
Lane 6
Lane 5
Lane 4
Lane 3
Lane 2
SB Section 4
4-6
Distance from MP238 (ft.)

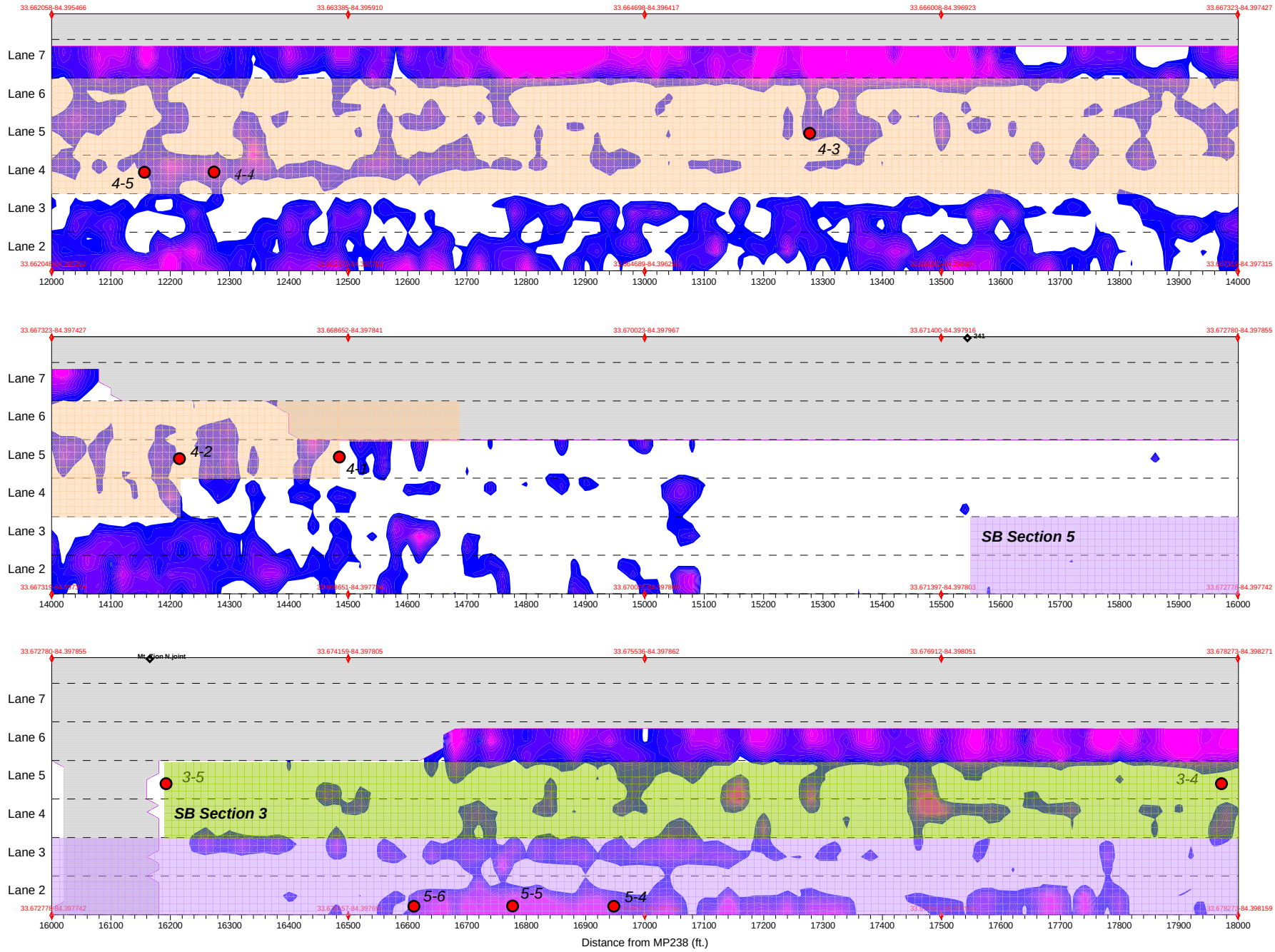
Lane 7
Lane 6
Lane 5
Lane 4
Lane 3
Lane 2
4-5
4-4
4-3
4-2
4-1
SB Section 5
3-5
SB Section 3
3-4
5-6
5-5
5-4
Distance from MP238 (ft.)

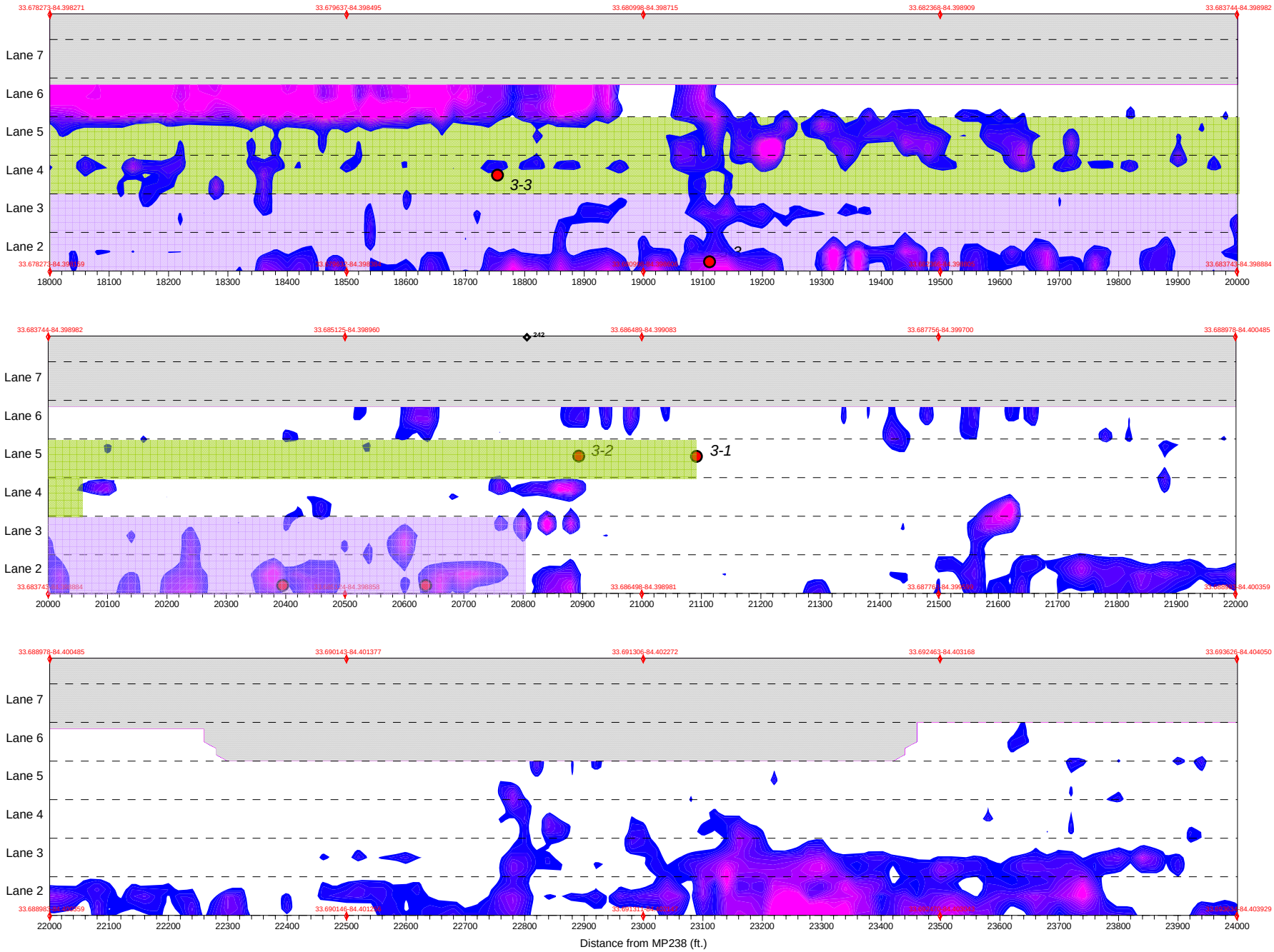
33.678273-84.398271
33.679637-84.398495
33.680998-84.398715
33.682368-84.398909
33.683744-84.398982
Lane 7
Lane 6
Lane 5
Lane 4
Lane 3
Lane 2
3-3
33.683743-84.398884
18000
18100
18200
18300
18400
18500
18600
18700
18800
18900
19000
19100
19200
19300
19400
19500
19600
19700
19800
19900
20000
33.683744-84.398982
33.685125-84.398960
242
33.686489-84.399083
33.687756-84.399700
33.688978-84.400485
3-2
3-1
33.686498-84.398981
33.688978-84.400485
33.690143-84.401377
33.691306-84.402272
33.692463-84.403168
33.693626-84.404050
33.690146-84.401377
33.693626-84.403929
20000
20100
20200
20300
20400
20500
20600
20700
20800
20900
21000
21100
21200
21300
21400
21500
21600
21700
21800
21900
22000
22100
22200
22300
22400
22500
22600
22700
22800
22900
23000
23100
23200
23300
23400
23500
23600
23700
23800
23900
24000
Distance from MP238 (ft.)

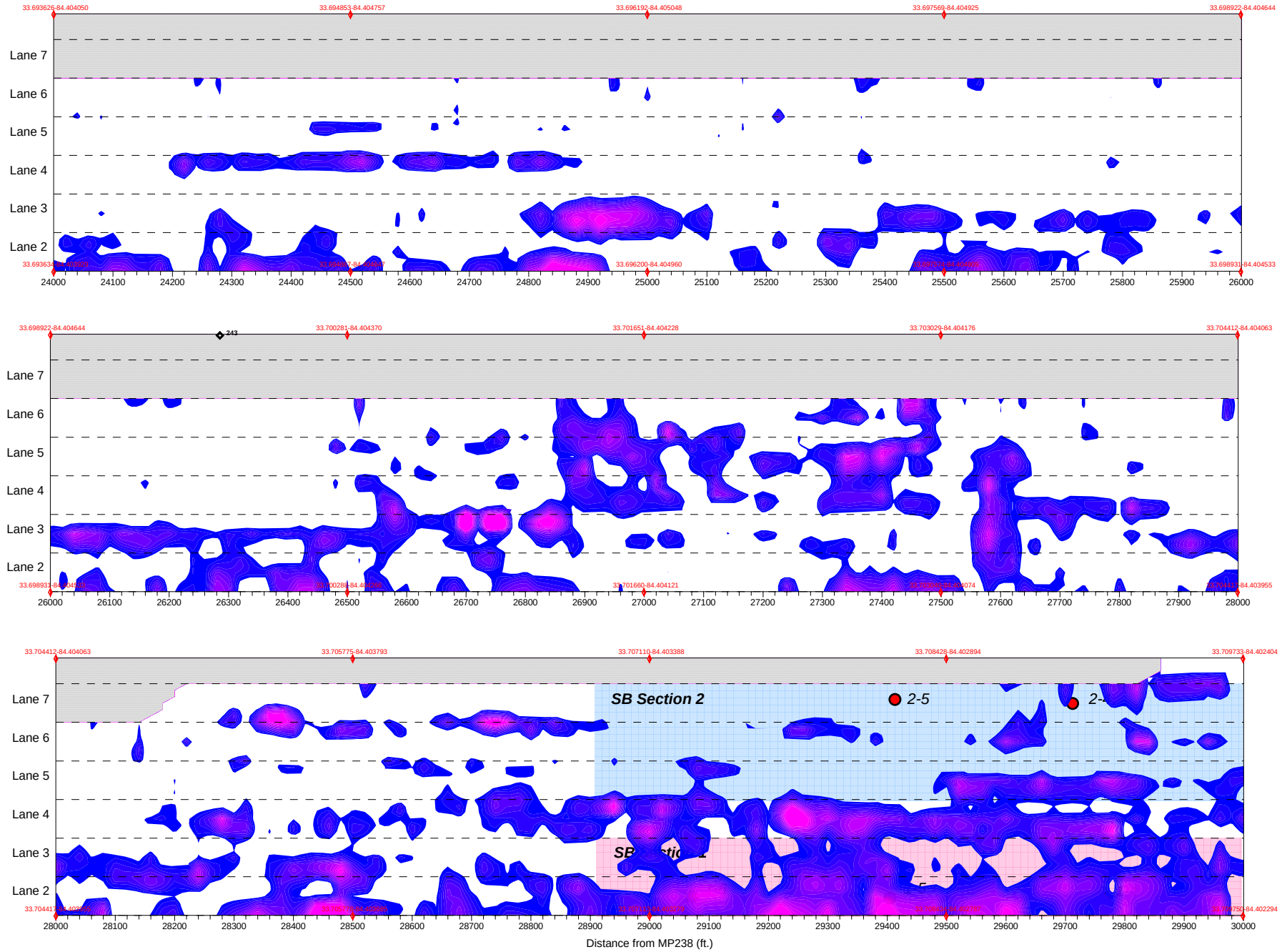
Lane 7
Lane 6
Lane 5
Lane 4
Lane 3
Lane 2
SB Section 2
2-5
Distance from MP238 (ft.)

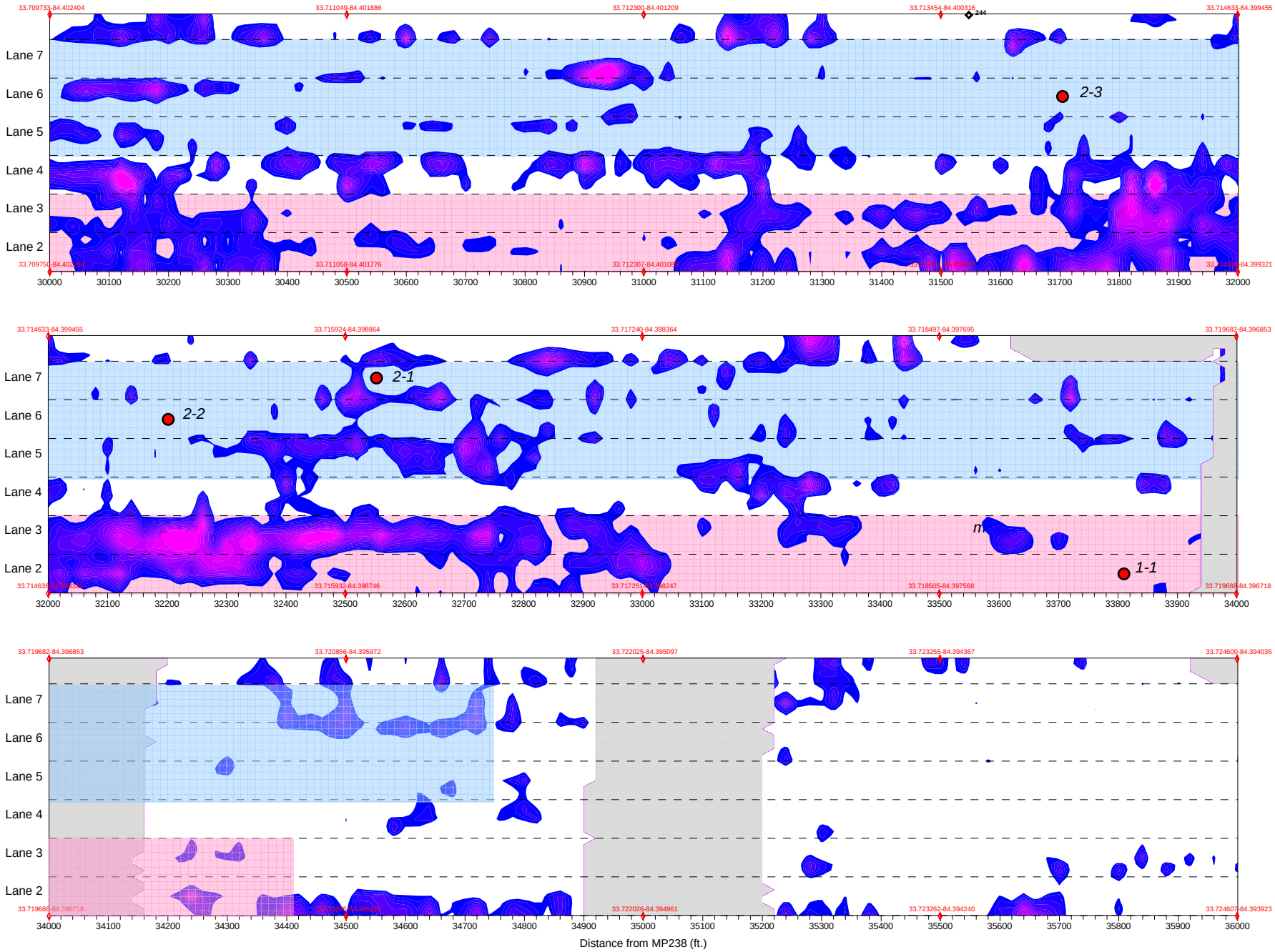
Lane 7
Lane 6
Lane 5
Lane 4
Lane 3
Lane 2
2-3
2-1
2-2
1-1
Distance from MP238 (ft.)

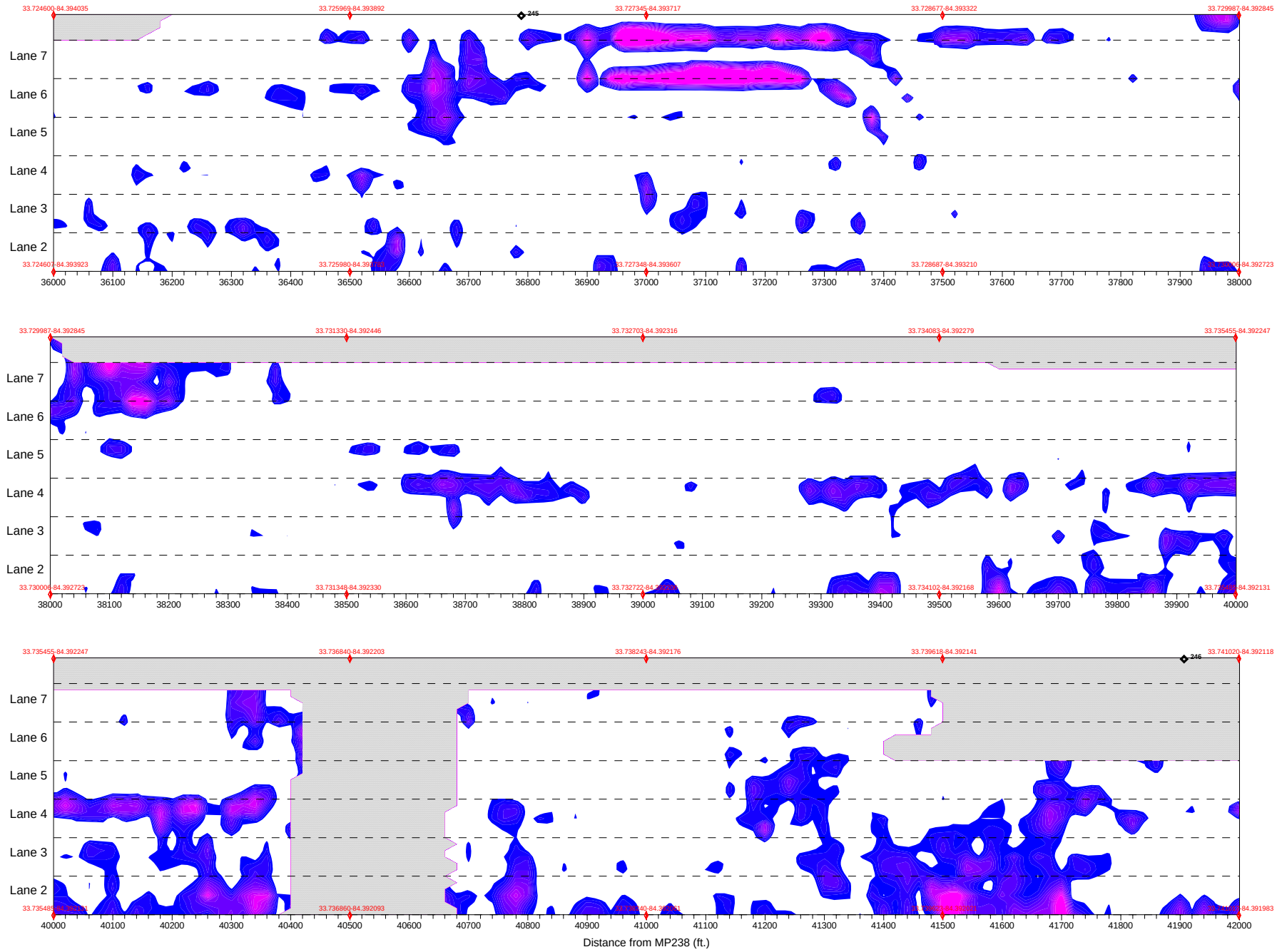
33.724600-84.394035
33.725969-84.393892
245
33.727345-84.393717
33.728677-84.393322
33.729987-84.392845
Lane 7
Lane 6
Lane 5
Lane 4
Lane 3
Lane 2
33.724607-84.393923
33.725980-84.393
33.727348-84.393607
33.728687-84.393210
33.729995-84.392723
36000 36100 36200 36300 36400 36500 36600 36700 36800 36900 37000 37100 37200 37300 37400 37500 37600 37700 37800 37900 38000
33.729987-84.392845
33.731330-84.392446
33.732703-84.392316
33.734083-84.392279
33.735455-84.392247
33.730006-84.392723
33.731348-84.392330
33.732722-84.392
33.734102-84.392168
33.735
-84.392131
38000 38100 38200 38300 38400 38500 38600 38700 38800 38900 39000 39100 39200 39300 39400 39500 39600 39700 39800 39900 40000
33.735455-84.392247
33.736840-84.392203
33.738243-84.392176
33.739618-84.392141
246
33.741020-84.392118
33.735485
33.736860-84.392093
33.738240-84.392061
33.739622-84.392011
33.741
-84.391983
40000 40100 40200 40300 40400 40500 40600 40700 40800 40900 41000 41100 41200 41300 41400 41500 41600 41700 41800 41900 42000
Distance from MP238 (ft.)

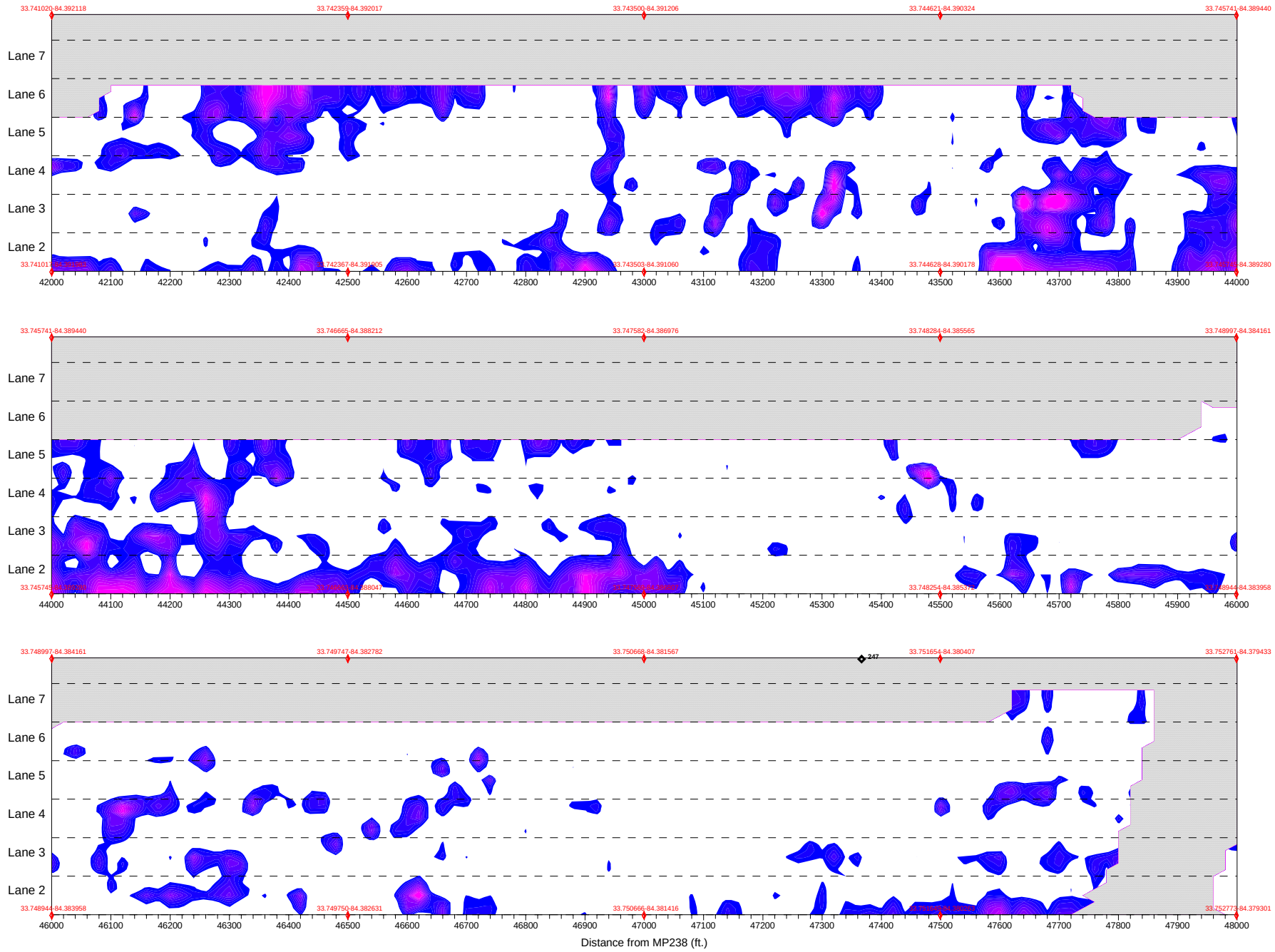
33.741020-84.392118
33.742359-84.392017
33.743500-84.391206
33.744621-84.390324
33.745741-84.389440
Lane 7
Lane 6
Lane 5
Lane 4
Lane 3
Lane 2
33.742367-84.391005
33.743503-84.391060
33.744628-84.390178
42000
42100
42200
42300
42400
42500
42600
42700
42800
42900
43000
43100
43200
43300
43400
43500
43600
43700
43800
43900
44000
33.745741-84.389440
33.746665-84.388212
33.747582-84.386976
33.748284-84.385565
33.748997-84.384161
44000
44100
44200
44300
44400
44500
44600
44700
44800
44900
45000
45100
45200
45300
45400
45500
45600
45700
45800
45900
46000
33.748997-84.384161
33.749747-84.382782
33.750668-84.381567
247
33.751654-84.380407
33.752761-84.379433
33.748944-84.383958
33.749750-84.382631
33.750666-84.381416
33.752773-84.379301
46000
46100
46200
46300
46400
46500
46600
46700
46800
46900
47000
47100
47200
47300
47400
47500
47600
47700
47800
47900
48000
Distance from MP238 (ft.)

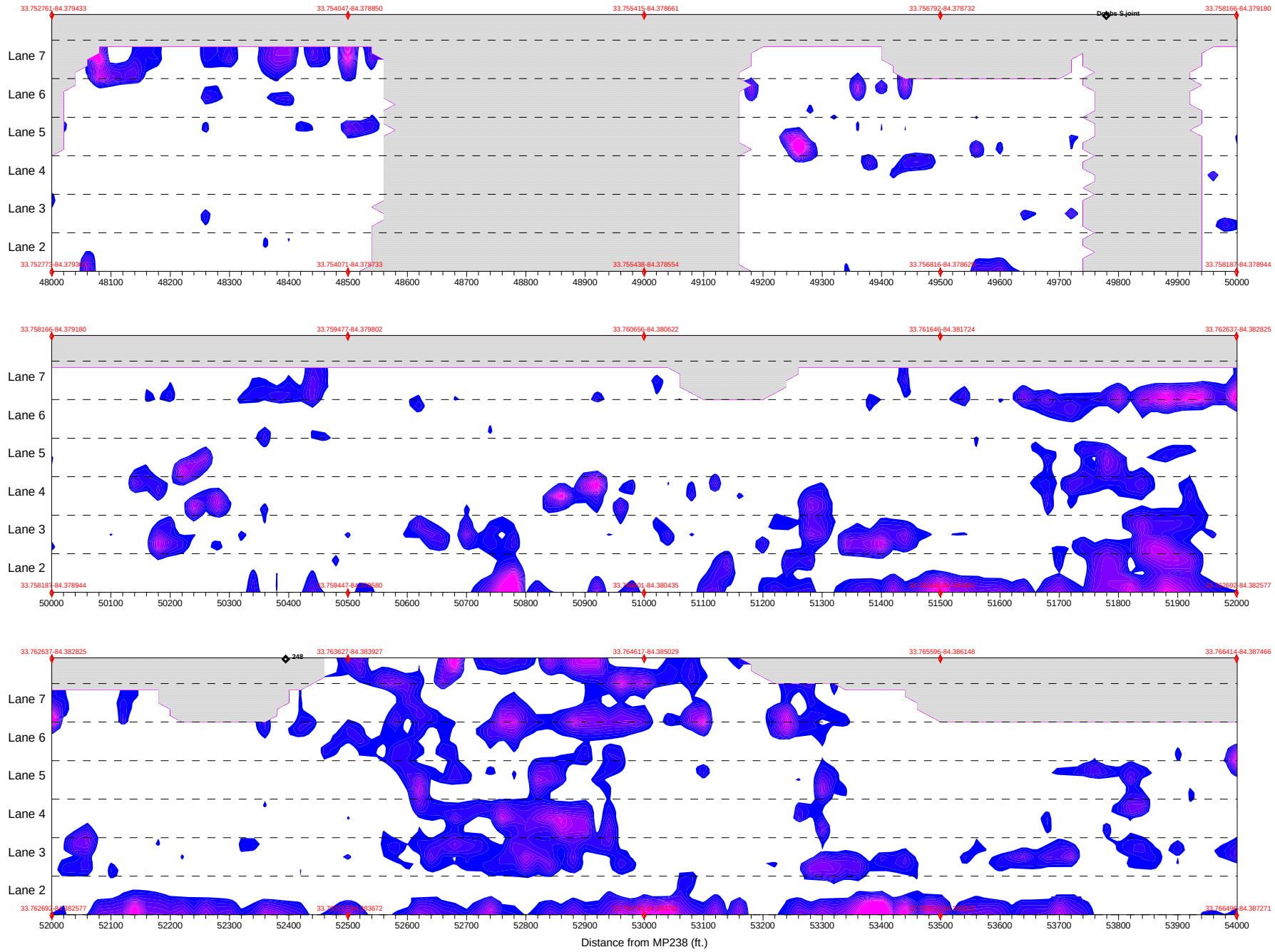
33.752761-84.379433
33.754047-84.378850
33.755415-84.378661
33.756792-84.378732
Dobbs S joint
33.758166-84.379180
Lane 7
Lane 6
Lane 5
Lane 4
Lane 3
Lane 2
33.752771-84.379
33.754071-84.379733
33.755439-84.378554
33.756816-84.378662
33.758187-84.378944
48000 48100 48200 48300 48400 48500 48600 48700 48800 48900 49000 49100 49200 49300 49400 49500 49600 49700 49800 49900 50000
33.758166-84.379180
33.759477-84.379802
33.760656-84.380622
33.761646-84.381724
33.762637-84.382825
33.758181-84.378944
33.759447-84.379580
33.760601-84.380435
33.762692-84.382577
50000 50100 50200 50300 50400 50500 50600 50700 50800 50900 51000 51100 51200 51300 51400 51500 51600 51700 51800 51900 52000
33.762637-84.382825
248
33.763627-84.383927
33.764617-84.385029
33.765596-84.386148
33.766414-84.387466
33.762692-84.382577
33.766496-84.387271
52000 52100 52200 52300 52400 52500 52600 52700 52800 52900 53000 53100 53200 53300 53400 53500 53600 53700 53800 53900 54000
Distance from MP238 (ft.)

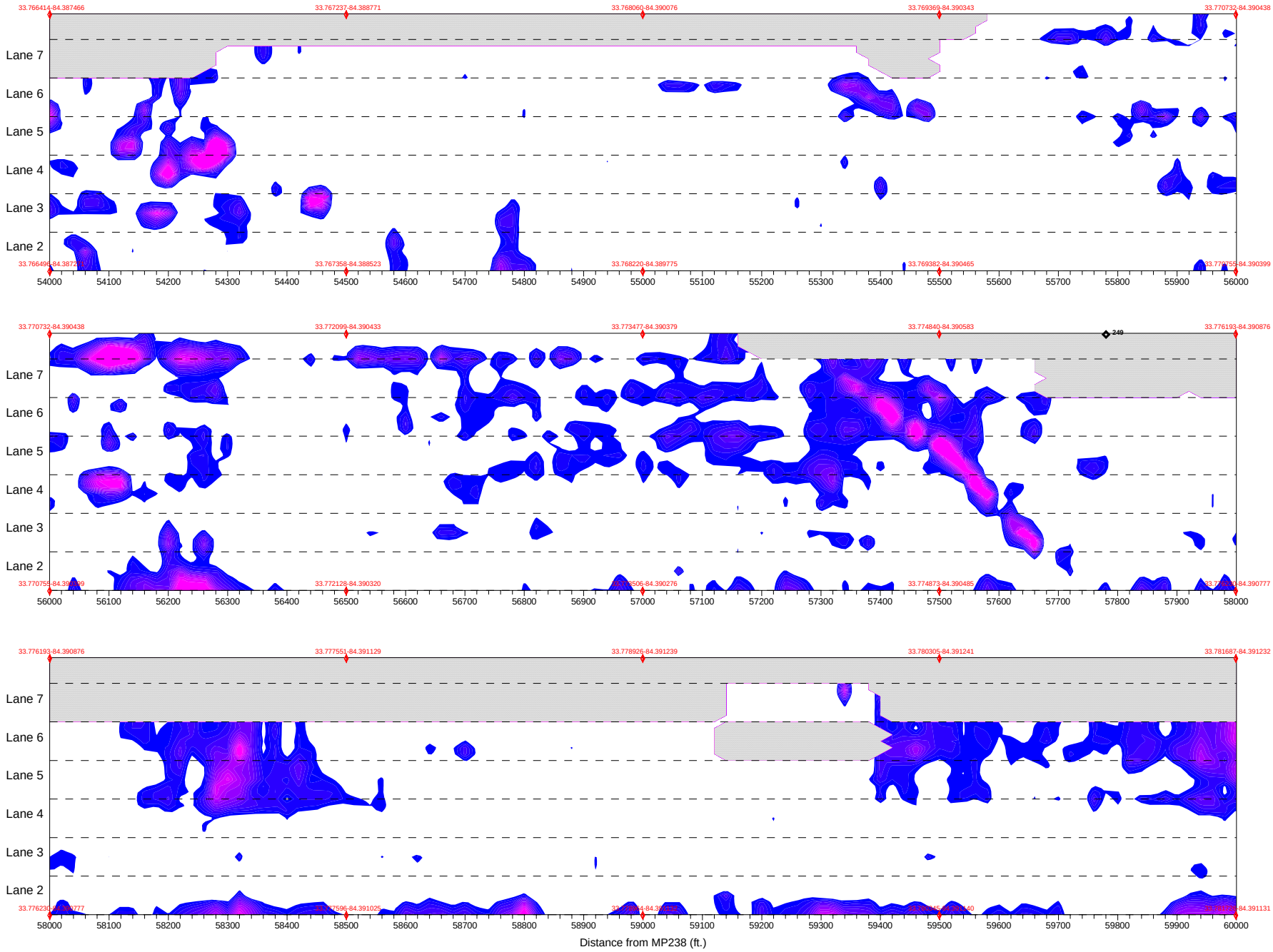
33.766414-84.387466
33.767237-84.388771
33.768060-84.390076
33.769369-84.390343
33.770732-84.390438
Lane 7
Lane 6
Lane 5
Lane 4
Lane 3
Lane 2
33.767359-84.388523
33.768220-84.389775
33.769382-84.390465
54000
54100
54200
54300
54400
54500
54600
54700
54800
54900
55000
55100
55200
55300
55400
55500
55600
55700
55800
55900
56000
33.770732-84.390438
33.772099-84.390433
33.773477-84.390379
33.774840-84.390583
33.776193-84.390876
249
33.772128-84.390320
33.774873-84.390485
56000
56100
56200
56300
56400
56500
56600
56700
56800
56900
57000
57100
57200
57300
57400
57500
57600
57700
57800
57900
58000
33.776193-84.390876
33.777551-84.391129
33.778926-84.391239
33.780305-84.391241
33.781687-84.391232
33.777596-84.391025
33.781687-84.391131
58000
58100
58200
58300
58400
58500
58600
58700
58800
58900
59000
59100
59200
59300
59400
59500
59600
59700
59800
59900
60000
Distance from MP238 (ft.)

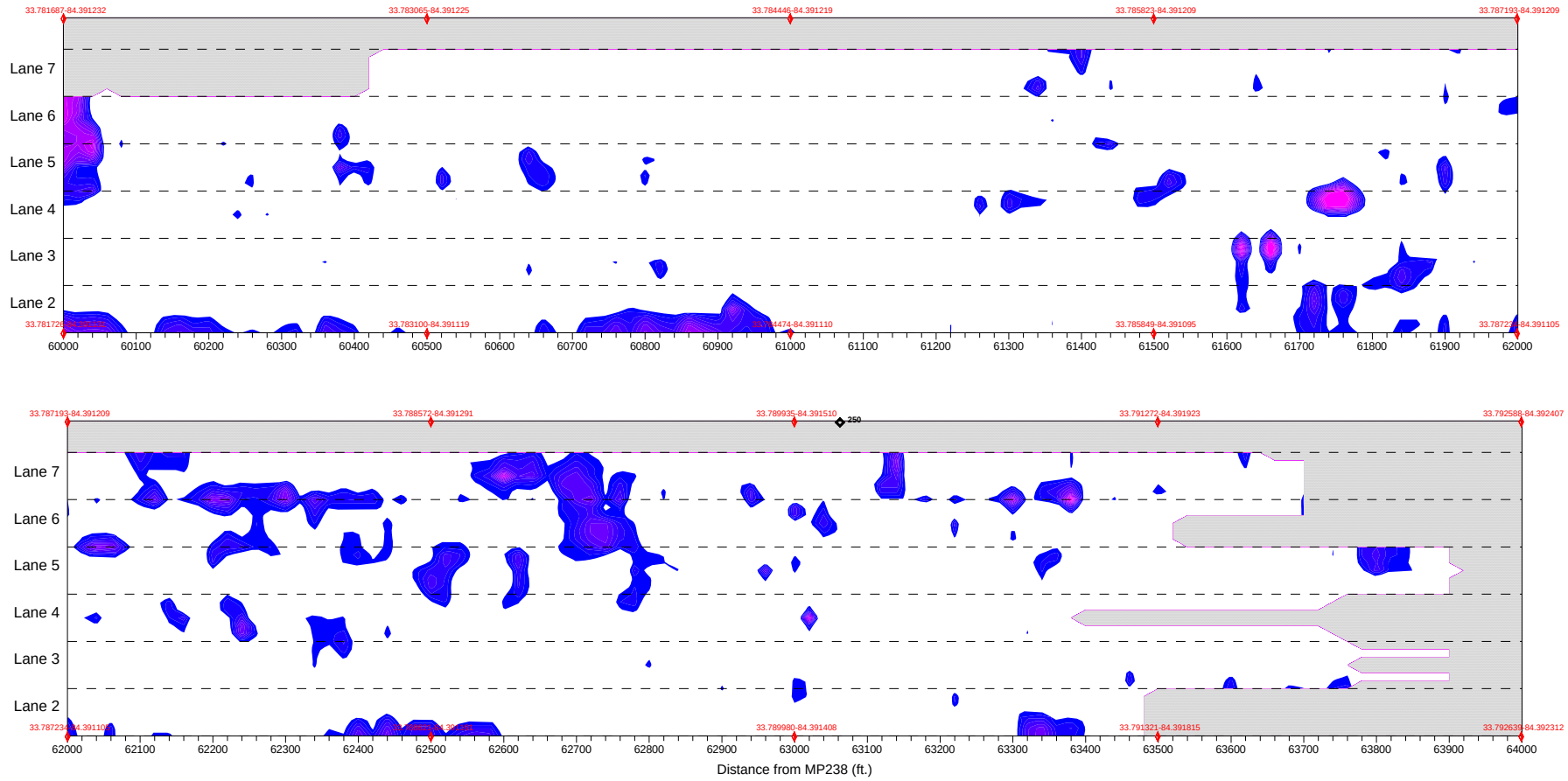
33.781687-84.391232
33.783065-84.391225
33.784446-84.391219
33.785823-84.391209
33.787193-84.391209
Lane 7
Lane 6
Lane 5
Lane 4
Lane 3
Lane 2
33.783100-84.391119
33.784474-84.391110
33.785849-84.391095
33.787223-84.391105
60000
60100
60200
60300
60400
60500
60600
60700
60800
60900
61000
61100
61200
61300
61400
61500
61600
61700
61800
61900
62000
33.787193-84.391209
33.788572-84.391291
33.789935-84.391510
250
33.791272-84.391923
33.792588-84.392407
Lane 7
Lane 6
Lane 5
Lane 4
Lane 3
Lane 2
33.789980-84.391408
33.791321-84.391815
33.792639-84.392312
62000
62100
62200
62300
62400
62500
62600
62700
62800
62900
63000
63100
63200
63300
63400
63500
63600
63700
63800
63900
64000
Distance from MP238 (ft.)

APPENDIX C. PHOTOGRAPHS OF CORES

NB 1-1 MP 239.05 (Lane 5)

NB 1-2 MP 239.21 (Lane 5)

NB 1-3 MP 239.31 (Lane 5)

NB 1-4 MP 239.42 (Lane 4)

NB 1-5 MP 239.71 (Lane 4)

NB 2-1 MP 242.36 (Lane 2)

NB 2-2 MP 242.70 (Lane 2)

NB 2-3 MP 242.81 (Lane 2)

NB 2-4 MP 243.24 (Lane 2)

NB 2-5 MP 243.54 (Lane 2)

NB 2-6 MP 243.91 (Lane 2)

NB 3-1 MP 243.65 (Lane 4)

NB 3-2 MP 243.77 (Lane 4)

NB 3-3 MP 243.92 (Lane 4)

NB 3-4 MP 244.24 (Lane 4)

NB 3-5 MP 244.28 (Lane 2)

NB 4-1B MP 244.54 (Lane 2)

NB 4-2 MP 244.60 (Lane 3)

NB 4-3 MP 244.71 (Lane 2)

NB 4-4 MP 244.83 (Lane 3)

NB 4-5 MP 244.90 (Lane 2)

NB 4-6 MP 244.98 (Lane 2)

NB 4-7 MP 245.17 (Lane 3)

SB 1-1 MP 244.40 (Lane 2)

SB 1-2 MP 244.10 (Lane 3)

SB 1-3 MP 244.02 (Lane 3)

SB 1-4 MP 243.64 (Lane 2)

SB 1-5 MP 243.57 (Lane 2)

SB 1-6 MP 243.51 (Lane 2)

SB 2-1 MP 244.17 (Lane 7)

SB 2-2 MP 244.10 (Lane 6)

SB 2-3 MP 244.00 (Lane 6)

SB 2-4 MP 243.63 (Lane 7)

SB 2-5 MP 243.57 (Lane 7)

SB 3-1 MP 242.20 (Lane 5)

SB 3-2 MP 241.96 (Lane 5)

SB 3-3 MP 241.55 (Lane 4)

SB 3-4 MP 241.40 (Lane 5)

SB 3-5 MP 241.07 (Lane 5)

SB 4-1 MP 240.74 (Lane 5)

SB 4-2 MP 240.69 (Lane 5)

SB 4-3 MP 240.52 (Lane 5)

SB 4-4 MP 240.30 (Lane 4)

SB 4-5 MP 240.27 (Lane 4)

SB 4-6 MP 240.24 (Lane 5/6)

SB 5-1 MP 241.91 (Lane 2)

SB 5-2 MP 241.86 (Lane 2)

SB 5-3 MP 241.62 (Lane 2)

SB 5-4 MP 241.21 (Lane 2)

SB 5-5 MP 241.18 (Lane 2)

SB 5-6 MP 241.15 (Lane 2)

APPENDIX D. STRESS-STRAIN CURVES

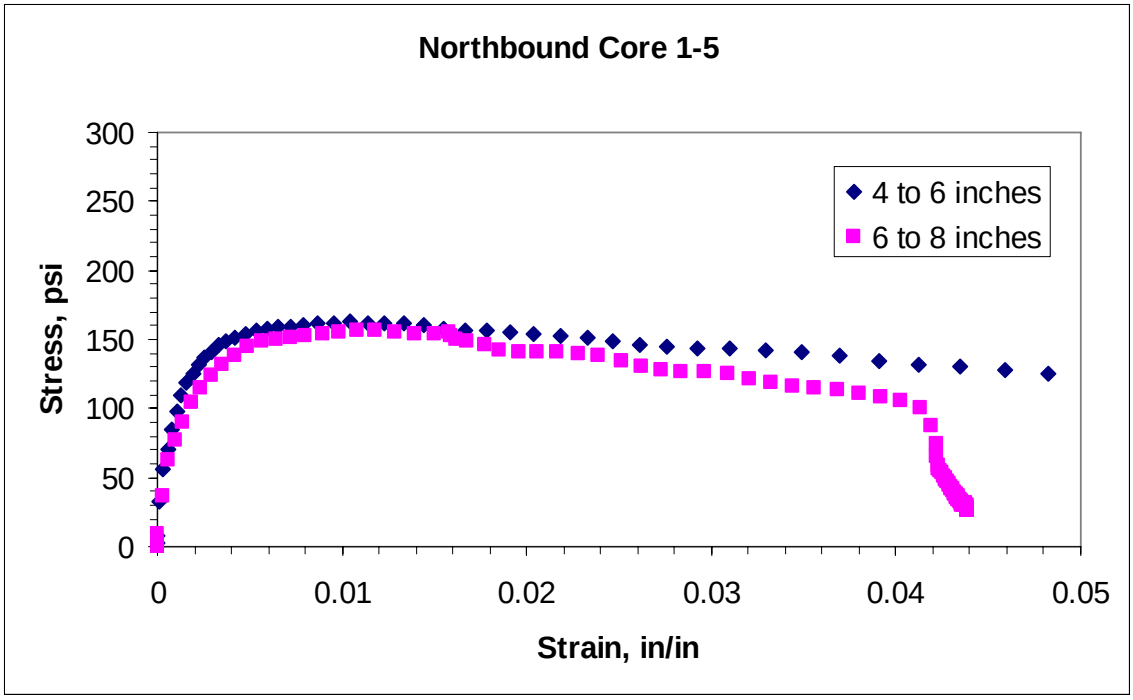
Northbound Core 1-5
Stress, psi
300
250
200
150
100
50
0
0
0.01
0.02
0.03
0.04
0.05
Strain, in/in
4 to 6 inches
6 to 8 inches

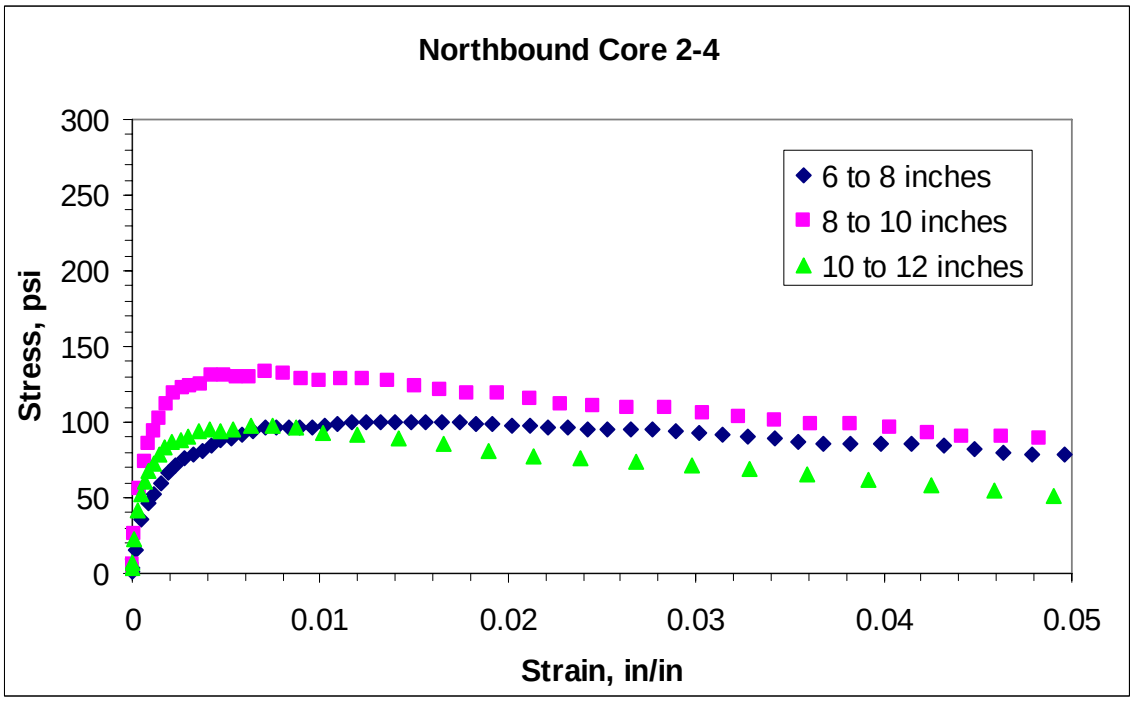
Northbound Core 2-4
Stress, psi
300
250
200
150
100
50
0
0
0.01
0.02
0.03
0.04
0.05
Strain, in/in
6 to 8 inches
8 to 10 inches
10 to 12 inches

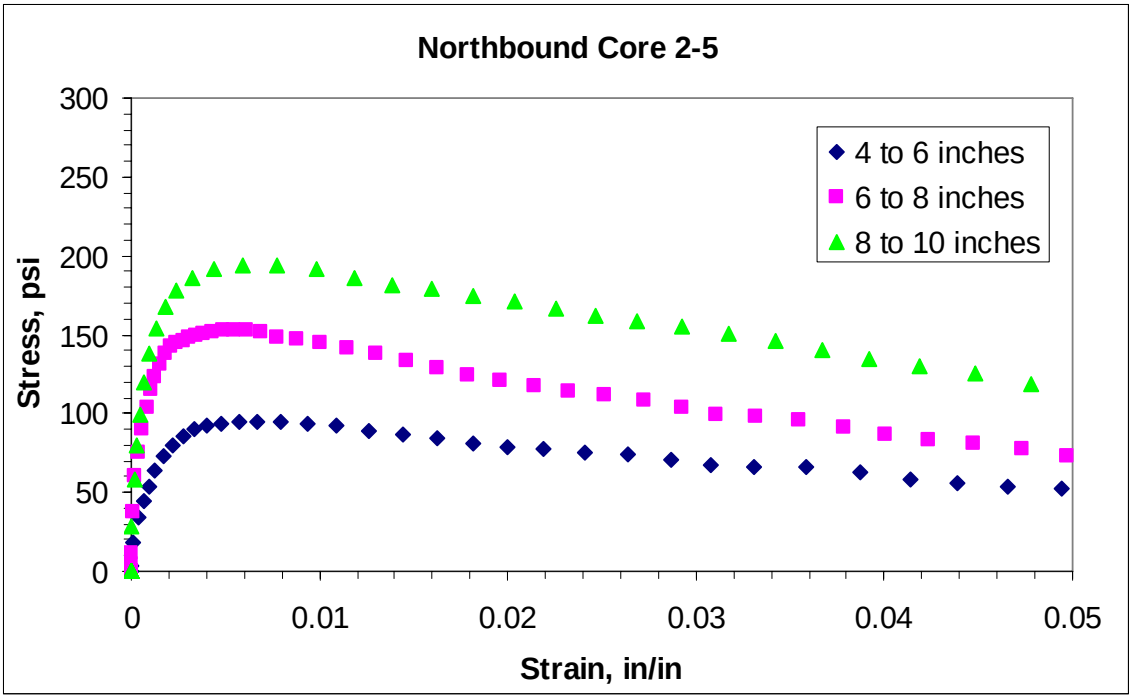
Northbound Core 2-5
Stress, psi
300
250
200
150
100
50
0
0
0.01
0.02
0.03
0.04
0.05
Strain, in/in
4 to 6 inches
6 to 8 inches
8 to 10 inches

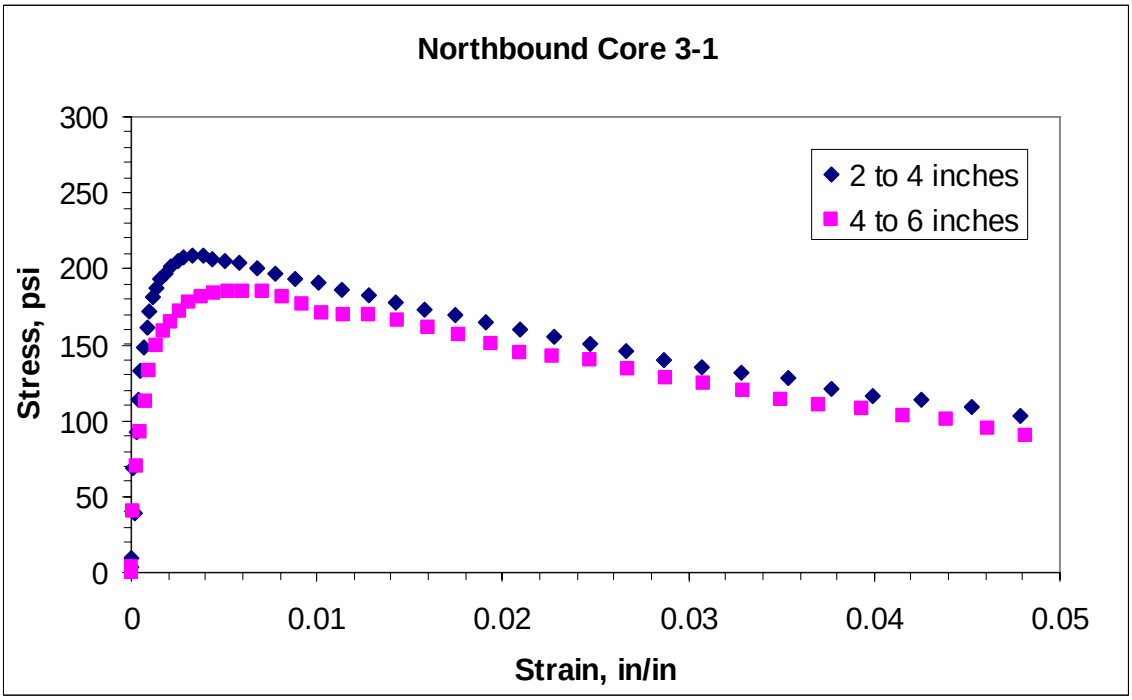
Northbound Core 3-1
Stress, psi
300
250
200
150
100
50
0
0
0.01
0.02
0.03
0.04
0.05
Strain, in/in
2 to 4 inches
4 to 6 inches

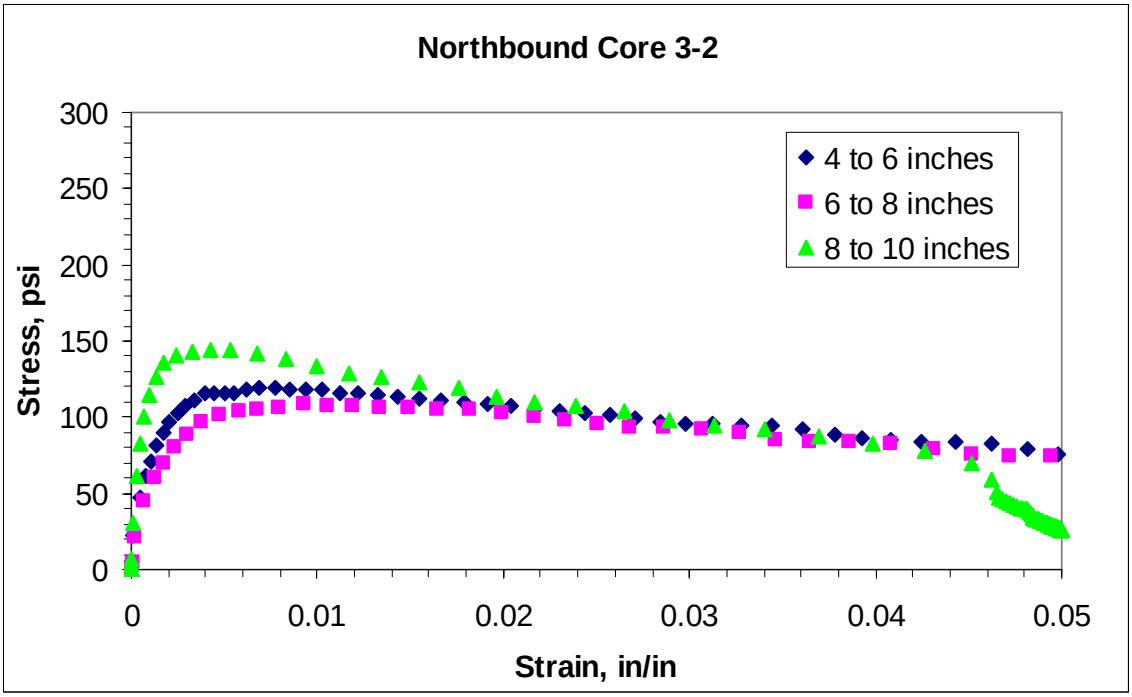
Northbound Core 3-2
Stress, psi
300
250
200
150
100
50
0
0
0.01
0.02
0.03
0.04
0.05
Strain, in/in
4 to 6 inches
6 to 8 inches
8 to 10 inches

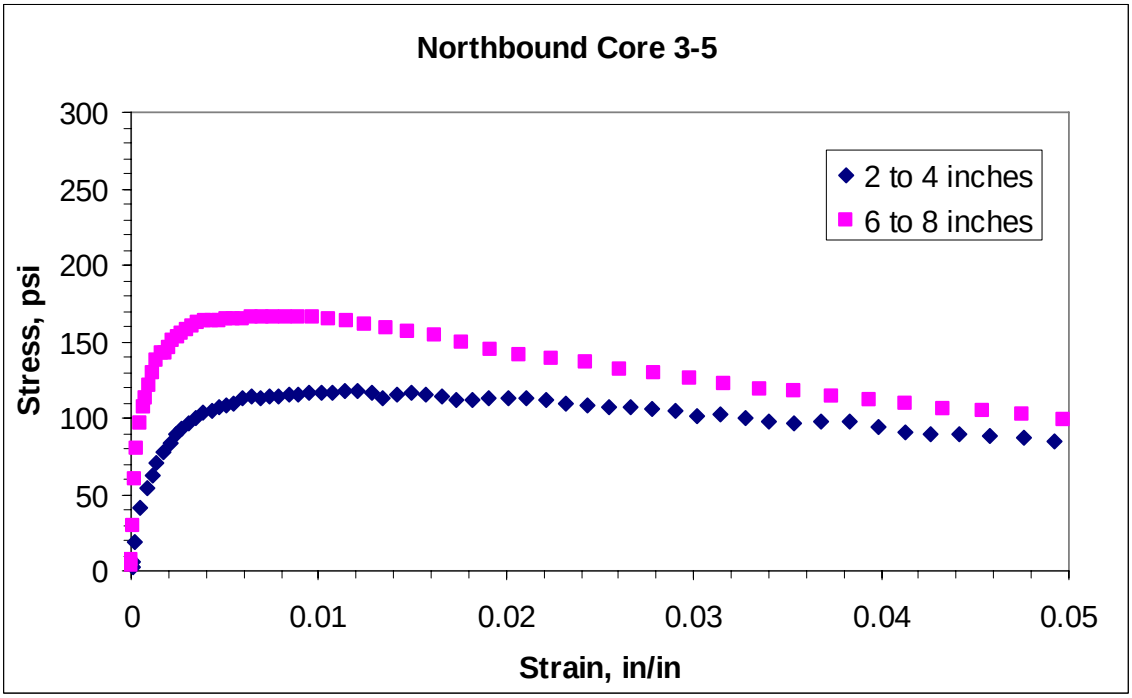
Northbound Core 3-5
Stress, psi
300
250
200
150
100
50
0
0
0.01
0.02
0.03
0.04
0.05
Strain, in/in
2 to 4 inches
6 to 8 inches

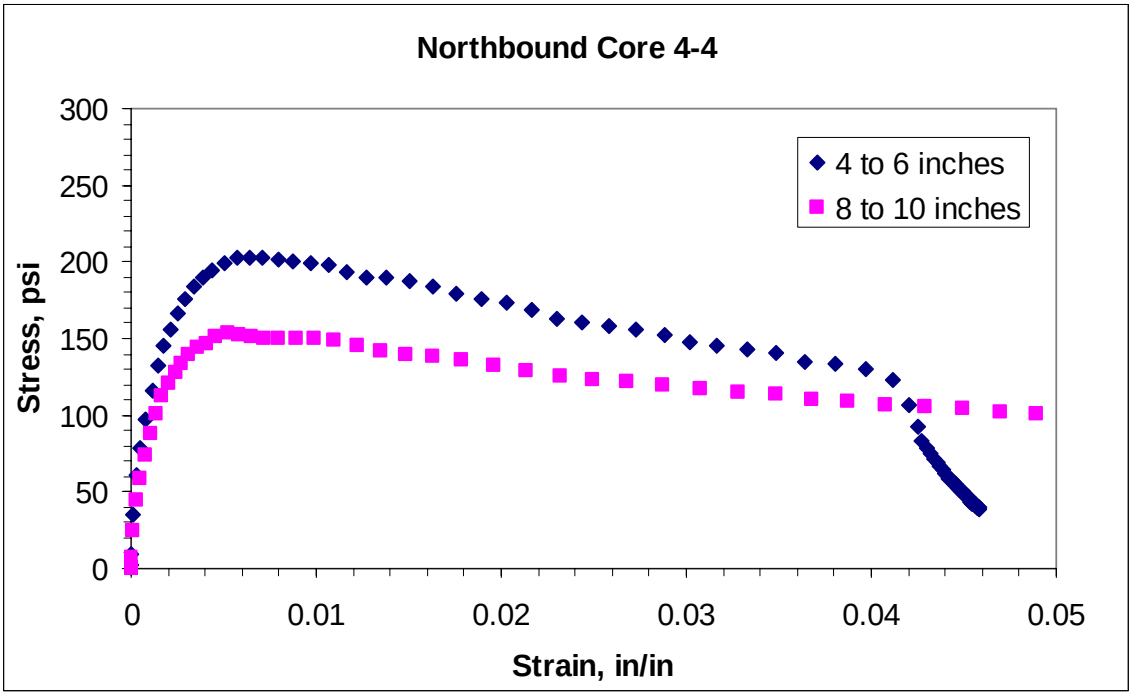
Northbound Core 4-4
Stress, psi
300
250
200
150
100
50
0
0
0.01
0.02
0.03
0.04
0.05
Strain, in/in
4 to 6 inches
8 to 10 inches

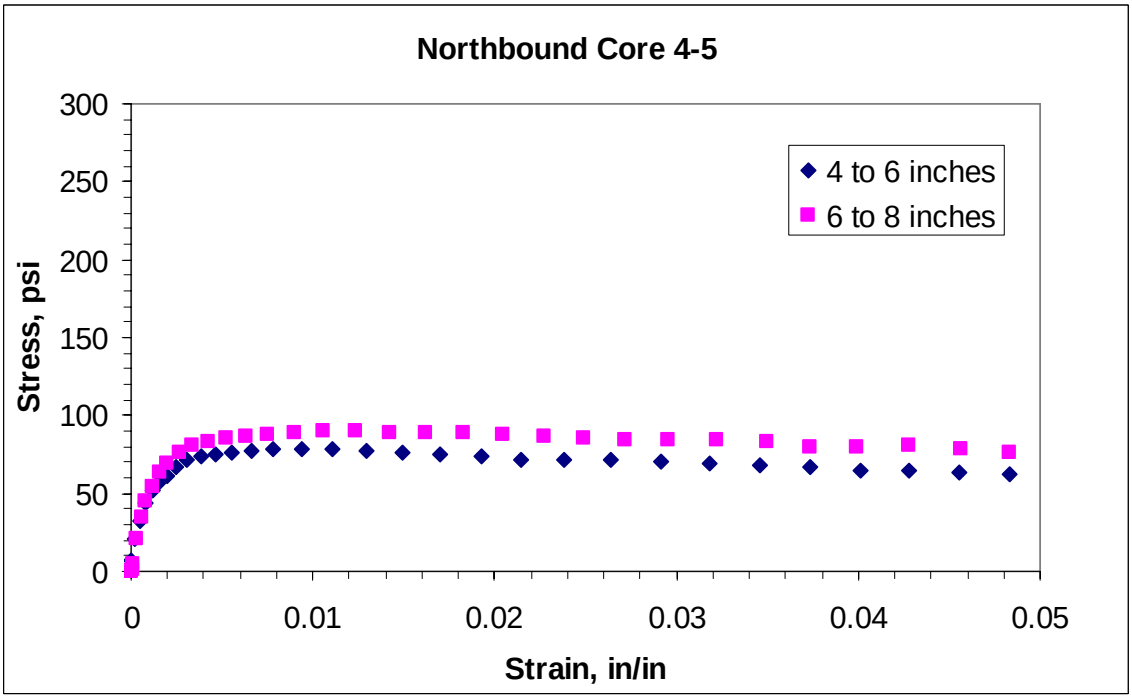
Northbound Core 4-5
Stress, psi
300
250
200
150
100
50
0
0
0.01
0.02
0.03
0.04
0.05
Strain, in/in
4 to 6 inches
6 to 8 inches

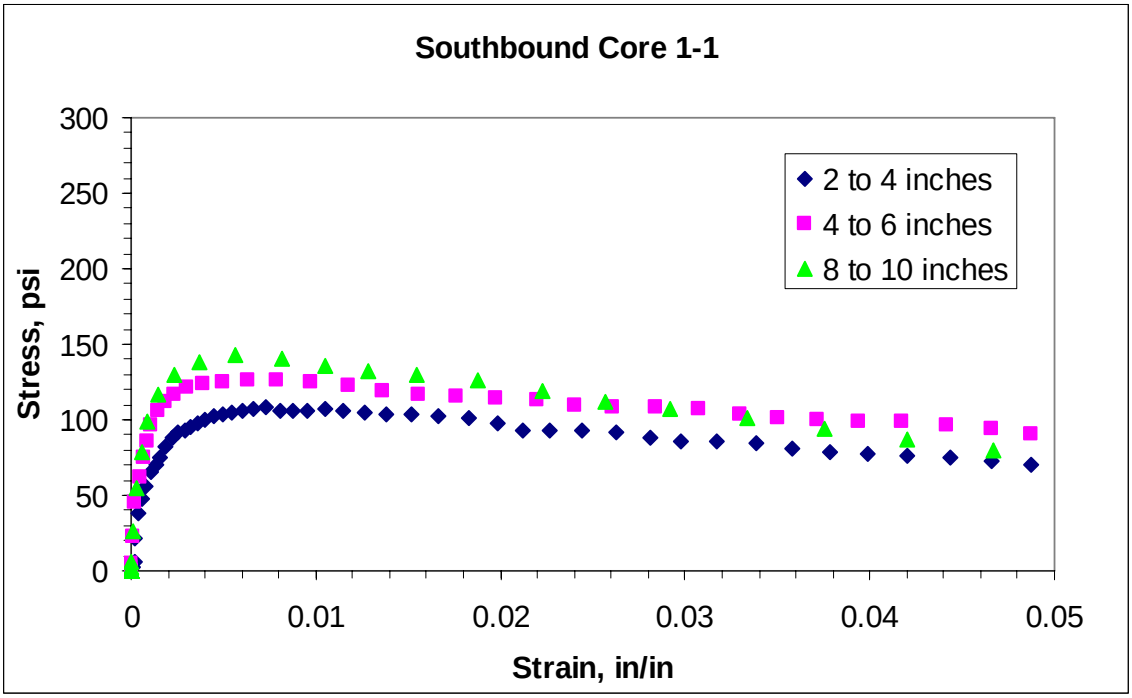
Southbound Core 1-1
Stress, psi
300
250
200
150
100
50
0
0
0.01
0.02
0.03
0.04
0.05
Strain, in/in
2 to 4 inches
4 to 6 inches
8 to 10 inches

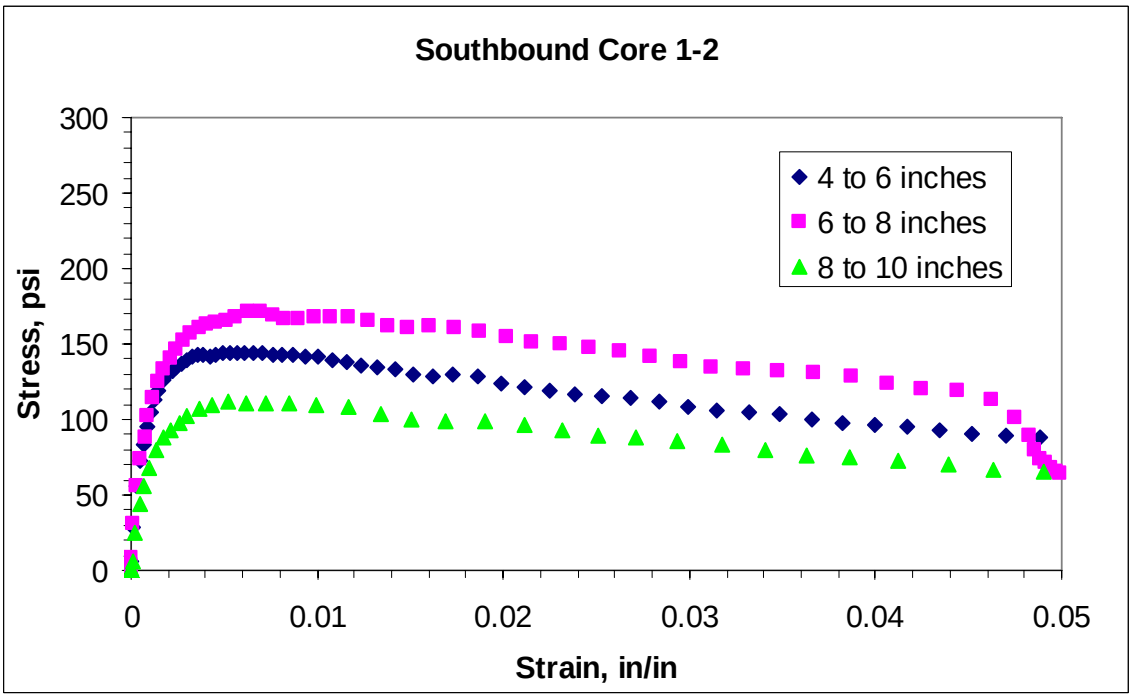
Southbound Core 1-2
Stress, psi
300
250
200
150
100
50
0
0
0.01
0.02
0.03
0.04
0.05
Strain, in/in
4 to 6 inches
6 to 8 inches
8 to 10 inches

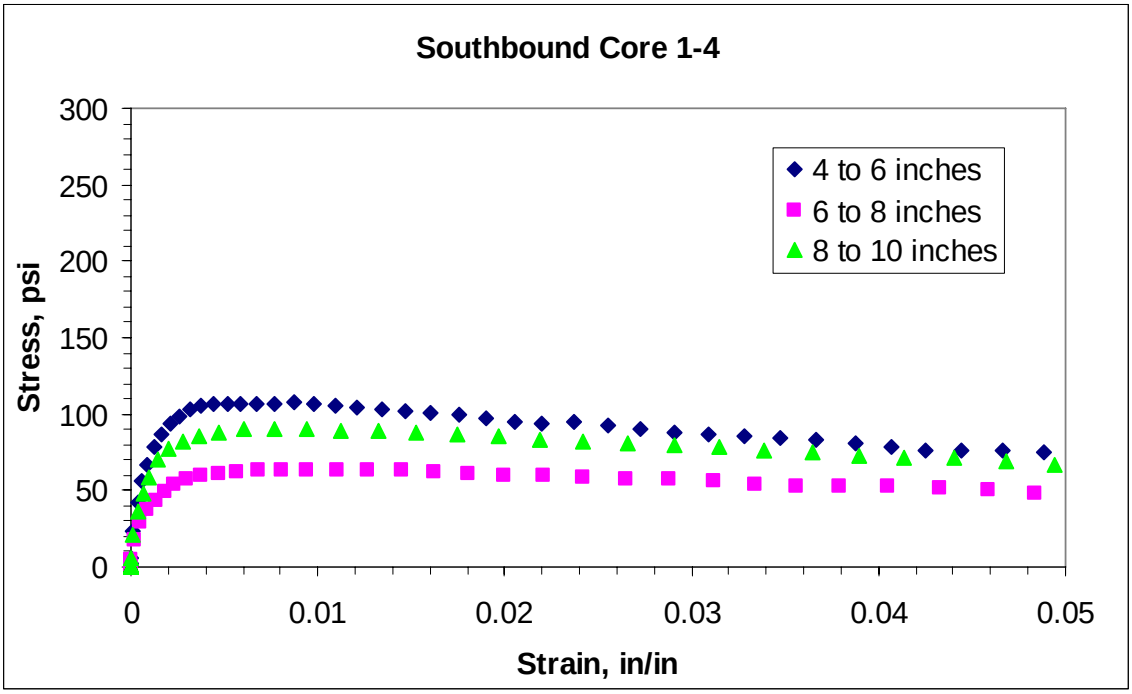
Southbound Core 1-4
Stress, psi
300
250
200
150
100
50
0
0
0.01
0.02
0.03
0.04
0.05
Strain, in/in
4 to 6 inches
6 to 8 inches
8 to 10 inches

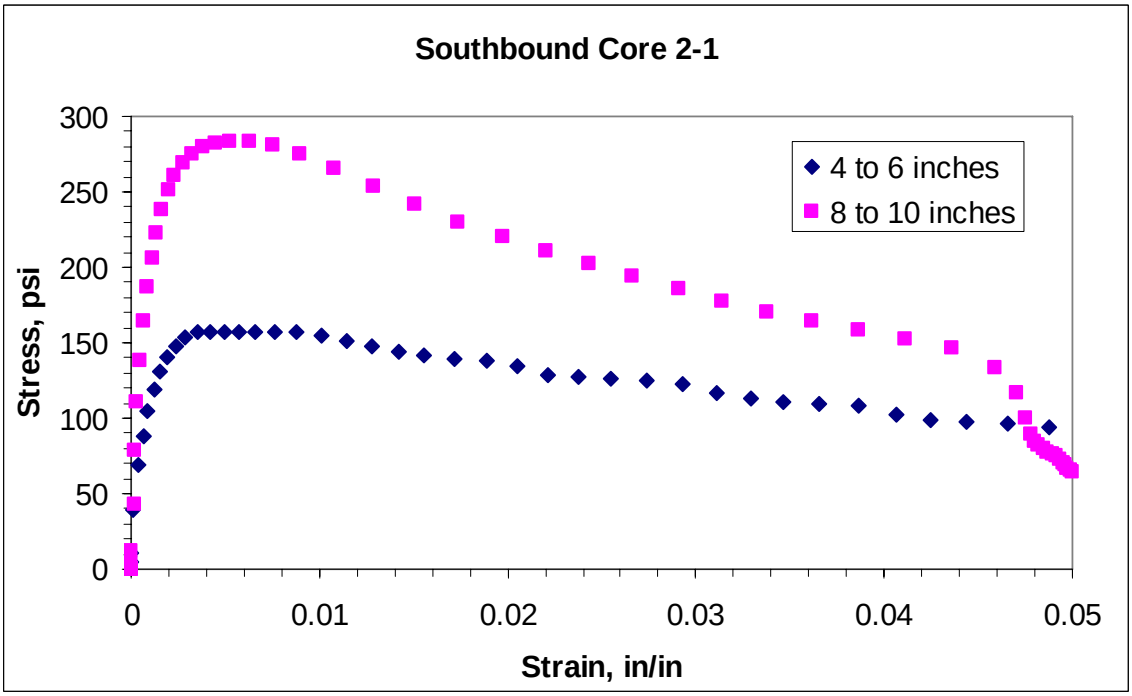
Southbound Core 2-1
Stress, psi
300
250
200
150
100
50
0
0
0.01
0.02
0.03
0.04
0.05
Strain, in/in
4 to 6 inches
8 to 10 inches

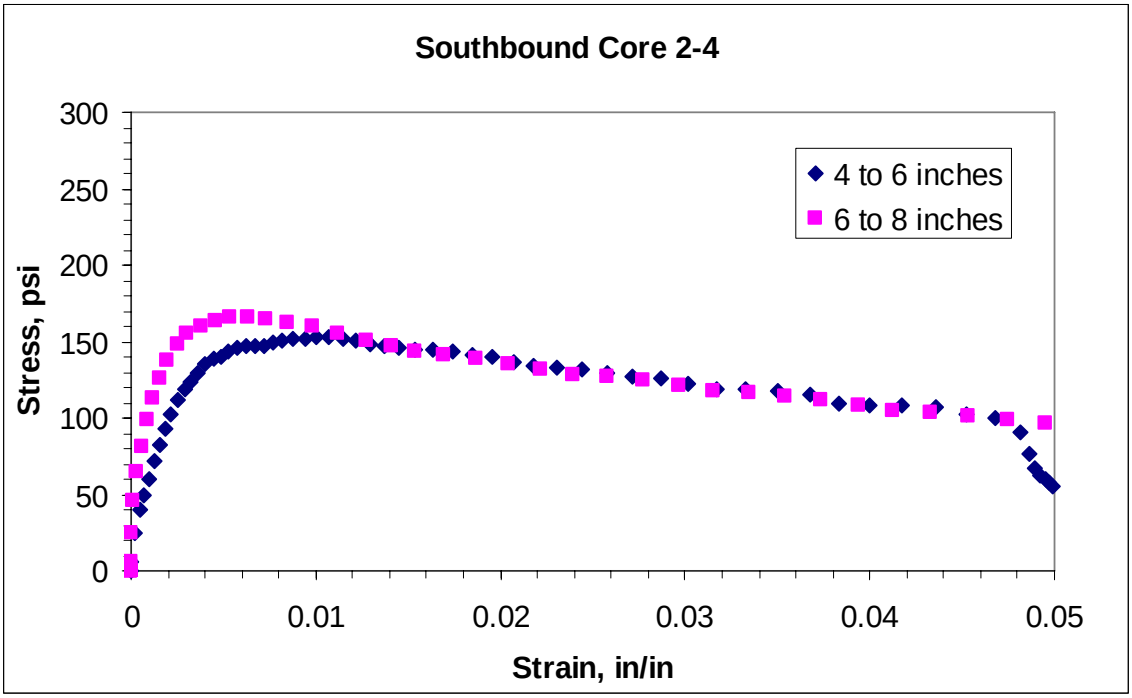
Southbound Core 2-4
Stress, psi
300
250
200
150
100
50
0
0
0.01
0.02
0.03
0.04
0.05
Strain, in/in
4 to 6 inches
6 to 8 inches

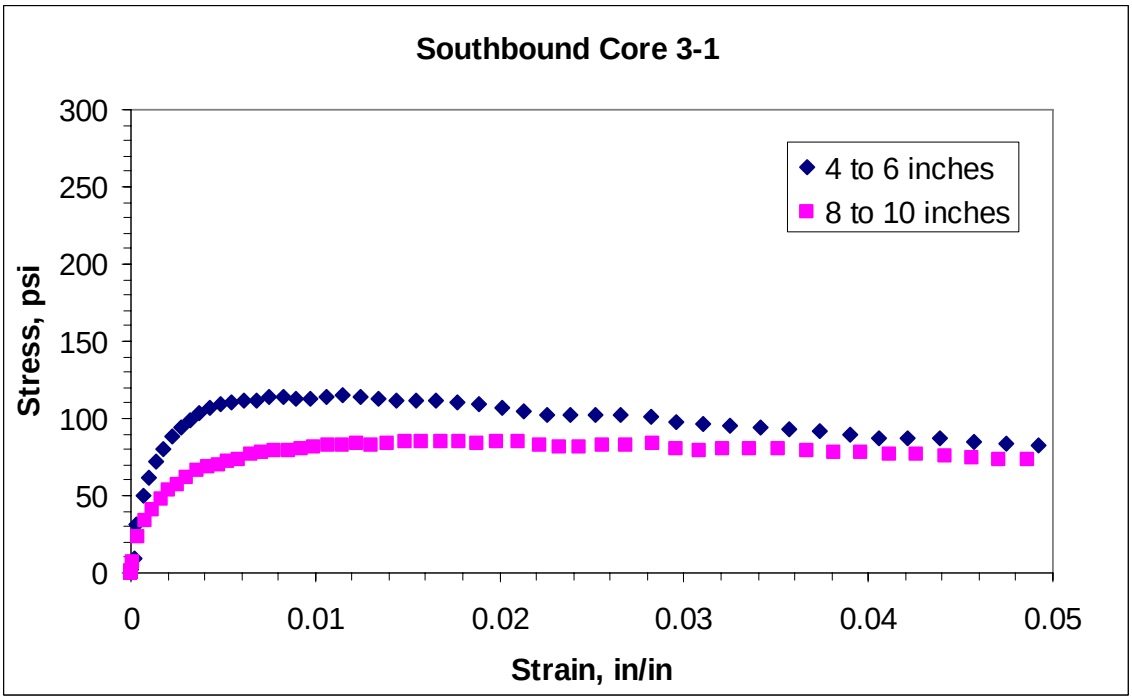
Southbound Core 3-1
Stress, psi
300
250
200
150
100
50
0
0
0.01
0.02
0.03
0.04
0.05
Strain, in/in
4 to 6 inches
8 to 10 inches

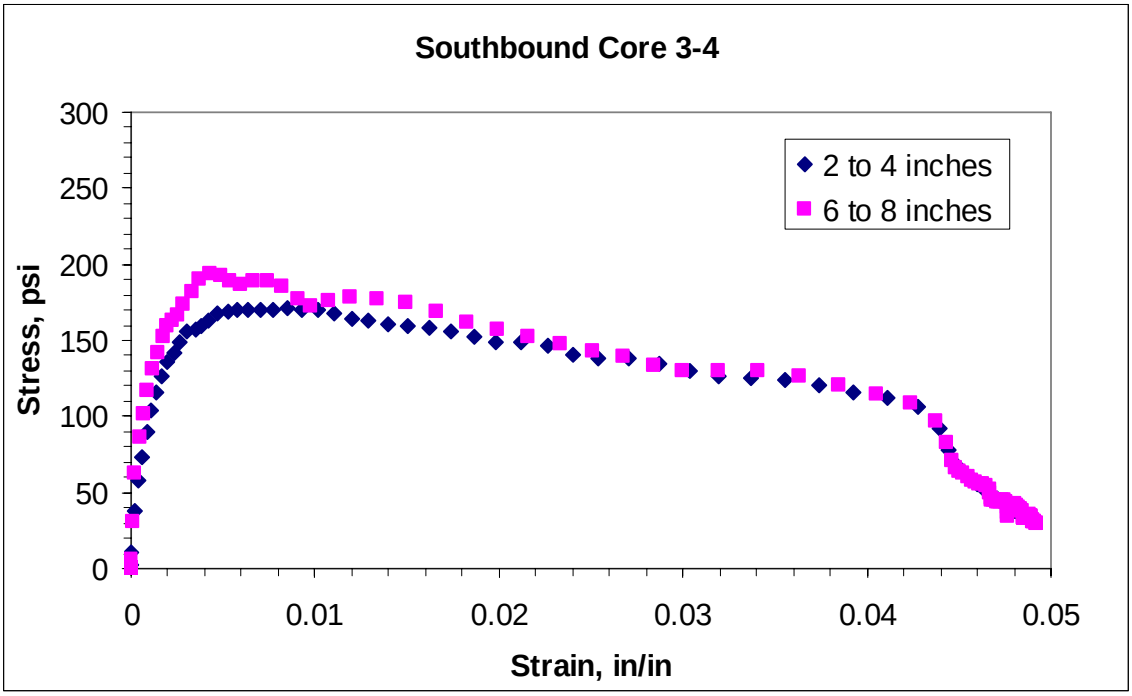
Southbound Core 3-4
Stress, psi
300
250
200
150
100
50
0
0
0.01
0.02
0.03
0.04
0.05
Strain, in/in
2 to 4 inches
6 to 8 inches

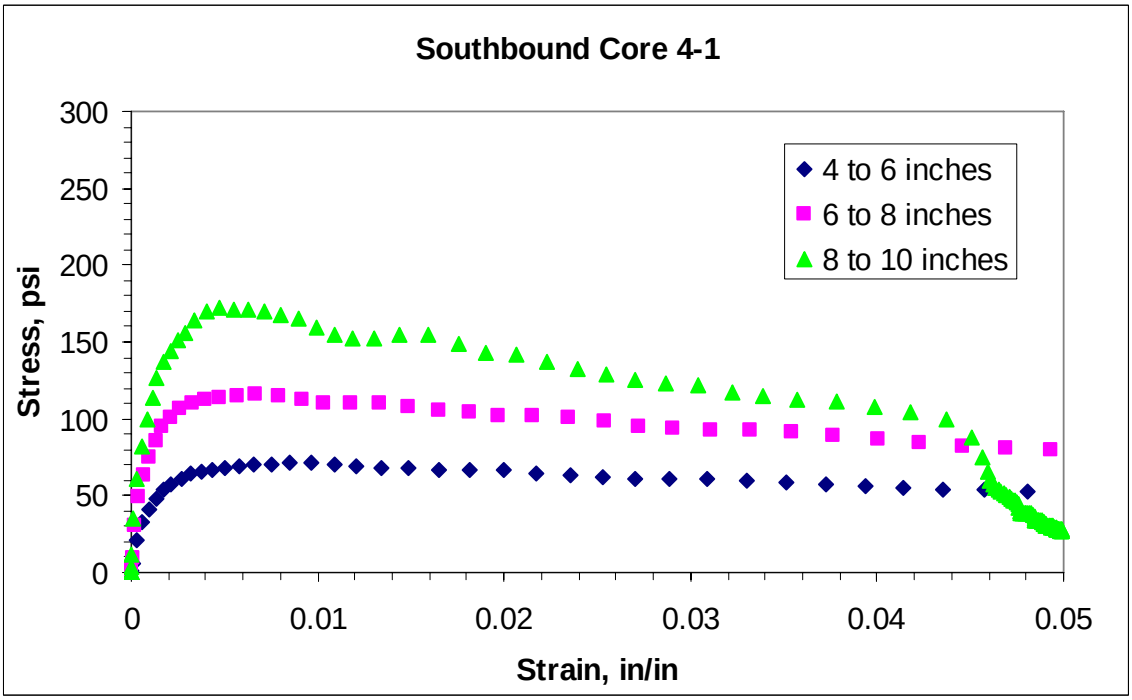
Southbound Core 4-1
Stress, psi
300
250
200
150
100
50
0
0
0.01
0.02
0.03
0.04
0.05
Strain, in/in
4 to 6 inches
6 to 8 inches
8 to 10 inches

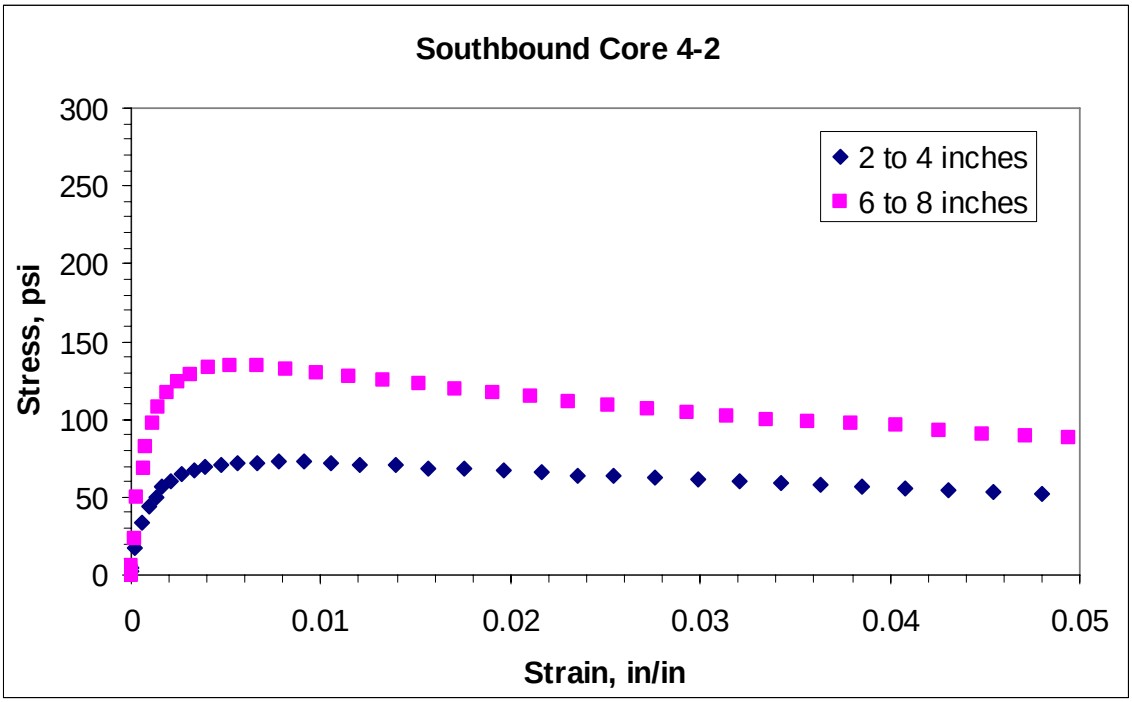
Southbound Core 4-2
Stress, psi
300
250
200
150
100
50
0
0
0.01
0.02
0.03
0.04
0.05
Strain, in/in
2 to 4 inches
6 to 8 inches

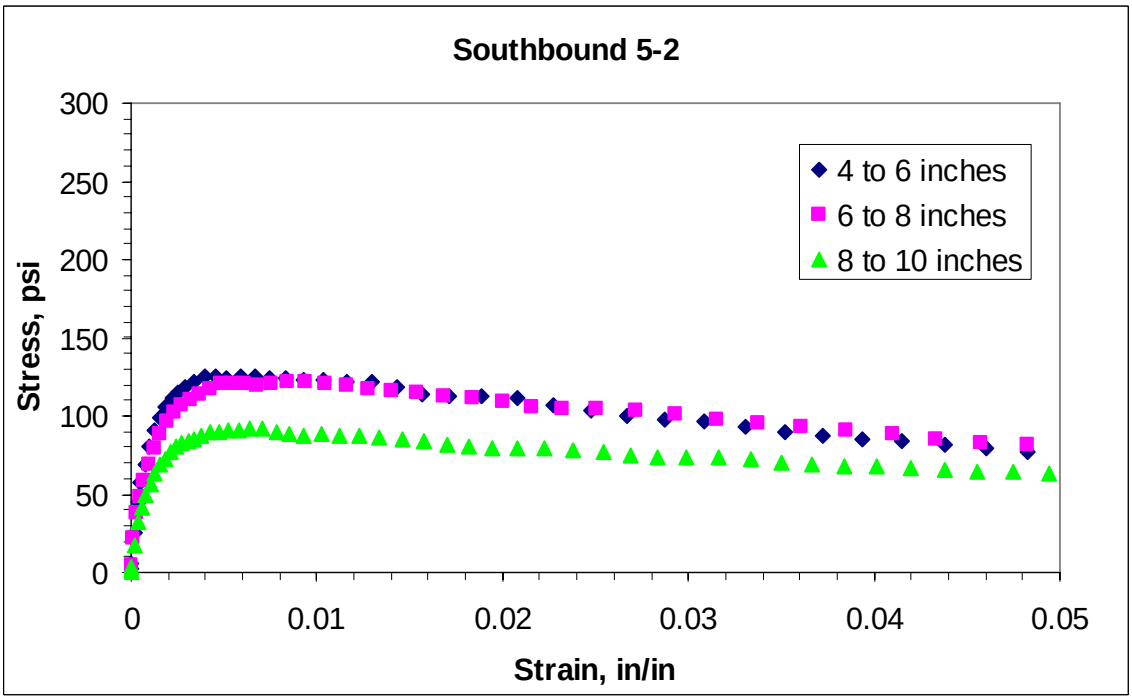
Southbound 5-2
Stress, psi
300
250
200
150
100
50
0
0
0.01
0.02
0.03
0.04
0.05
Strain, in/in
4 to 6 inches
6 to 8 inches
8 to 10 inches

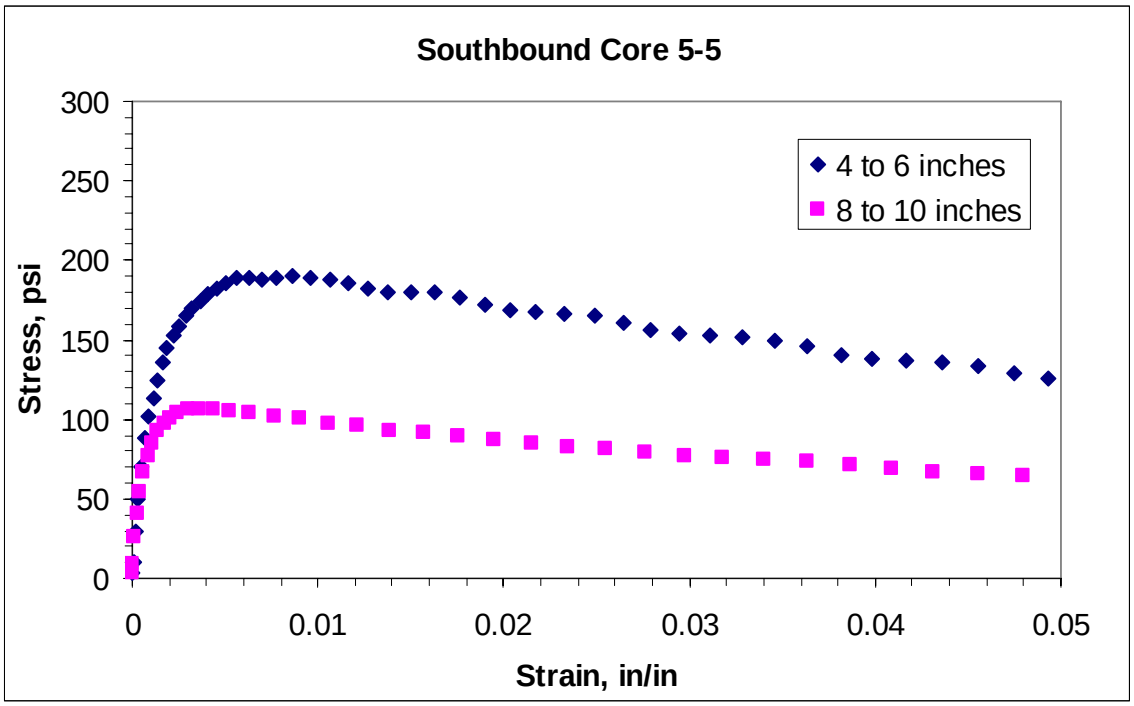
Southbound Core 5-5
Stress, psi
300
250
200
150
100
50
0
0
0.01
0.02
0.03
0.04
0.05
Strain, in/in
4 to 6 inches
8 to 10 inches